POTENTIAL USE OF ANEUSTAT FOR IMPROVEMENT OF DOCETAXEL-BASED THERAPY OF ADVANCED PROSTATE CANCER

by

Sifeng Qu

M.Sc., Shandong University, 2011

M.D., Shandong University, 2008

A THESIS SUBMITTED IN PARTIAL FULFILLMENT OF

THE REQUIREMENTS FOR THE DEGREE OF

DOCTOR OF PHILOSOPHY

in

THE FACULTY OF GRADUATE AND POSTDOCTORAL STUDIES

(Interdisciplinary Oncology)

THE UNIVERSITY OF BRITISH COLUMBIA

(Vancouver)

November 2017

Abstract

Metastatic prostate cancer (mPCa) is currently incurable. Docetaxel-based chemotherapy, used as first-line treatment for advanced PCa, is marginally effective. As PCa is a heterogeneous disease, use of therapeutics targeting multiple pathways may improve its treatment outcome. Aneustat is first-of-a-class of multivalent immuno-oncology drug candidates; a Phase-I trial has shown it is well-tolerated by patients and has immunomodulatory activity. The main goal of this PhD project is to determine whether Aneustat can be used to improve docetaxel-based therapy of advanced PCa.

In vitro, Aneustat markedly inhibited human metastatic C4-2 PCa cell proliferation/migration in a dose-dependent manner and, combined with docetaxel, showed synergistic growth inhibition. *In vivo*, a combination of Aneustat and docetaxel synergistically enhanced anticancer activity in a clinically relevant, patient-derived xenograft (PDX) metastatic PCa model without inducing major host toxicity (inhibition of tumor growth, lung micro-metastasis, kidney invasion). Gene expression analysis of microarray data obtained from xenografts, using Ingenuity Pathway Analysis (IPA) and Oncomine software, indicated that Aneustat+docetaxel, as distinct from the single drugs, targeted multiple pathways and cancer-driving genes. Aneustat alone significantly inhibited growth of human LNCaP cells/xenografts; glucose consumption, lactic acid secretion and glycolysis-related gene expressions of LNCaP cells were markedly reduced, indicating it inhibited aerobic glycolysis. Treatment of LNCaP xenografts and first-generation PCa PDX with Aneustat led to marked changes in host immune cell levels (mouse/human), i.e. a higher ratio of $CD8^+$ T/Treg cells, higher Natural Killer (NK) cell numbers, lower Treg cell and MDSC numbers – changes favoring the host anticancer immune response.

This study shows that combined use of Aneustat and docetaxel can lead to marked, synergistically increased anticancer activity, both *in vitro* and *in vivo*. As indicated by IPA and Oncomine analyses, this is due to the combination-induced expansion of the targeting of pathways and cancer-driving genes. Furthermore, as found with first-generation PDX PCa model, Aneustat has immunomodulatory properties, likely stemming from its inhibition of aerobic glycolysis, that may lead to stimulation of the anticancer immune response in immunocompetent hosts. Since a clinically relevant PDX metastatic PCa model was used in this study, treatment with Aneustat+docetaxel is likely valuable for clinical management of advanced PCa.

Lay Summary

When prostate cancer becomes metastatic (spreads within the body), it becomes incurable. Chemotherapy based on the drug, docetaxel, is the first-choice treatment for patients with metastatic prostate cancer who do not respond to medical castration. Unfortunately, it only marginally prolongs patients' lives. In this project it was examined whether the efficacy of docetaxel-based chemotherapy could be improved by combining docetaxel with Aneustat, a herbal preparation exhibiting multi-targeted anticancer activities and well-tolerated toxicity. Using a clinically relevant model, consisting of immunodeficient mice bearing patient-derived prostate cancers, it was found that the anticancer activity of docetaxel+Aneustat was markedly higher than that obtained with docetaxel alone, leading to potent inhibition of tumor growth and metastasis - importantly, without major host toxicity. In addition, evidence was found that Aneustat could boost the anticancer immune response of the host. As such, treatment with Aneustat+docetaxel is likely valuable for improved clinical management of metastatic prostate cancer.

Preface

Tumor tissues were obtained from patients through a protocol approved by the Clinical Research Ethics Board of the University of British Columbia (UBC) and the BC Cancer Agency (BCCA). All patients signed a consent form approved by the Ethics Board (UBC Ethics Board #: H04-60131 and H12-03428). Animal care and experimental procedures were carried out in accordance with the guidelines of the Canadian Council on Animal Care (CCAC) under the approval of the Animal Care Committee of the University of British Columbia.

Most sections of Chapter 2 have been published in: Qu S, Wang K, Xue H, Wang YW, Wu R, Liu C, Gao AC, Gout PW, Collins CC, Wang Y. Enhanced anticancer activity of a combination of docetaxel and Aneustat (OMN54) in a patient-derived, advanced prostate cancer tissue xenograft model. Mol Oncol. 2014 Mar;8(2):311-22. As the lead investigator, I conducted experiments, analyzed data, interpreted the results and wrote the basic draft. K Wang was involved in producing the microarray data and assisted with the microarray data analysis. H Xue and YW Wang carried out the experiments using a xenograft model. R Wu assisted me with H&E and IHC staining. C Liu and AC Gao provided the results of the Western Blotting experiments. CC Collins was involved in reviewing the article. PW Gout provided critical insight and revised the write-up. YZ Wang supervised the study and was involved throughout the project with regard to concept formation and manuscript design.

A part of Chapter 2 and whole sections of Chapter 3 have been submitted for publication with the following authors: Qu S, Ci X, Xue H, Dong X, Hao J, Lin D, Clermont PL, Wu R, Collins CC, Gout PW, Wang Y. Treatment with docetaxel in combination with Aneustat leads to potent inhibition of metastasis in a patient-derived xenograft model of advanced prostate cancer. I was the lead investigator of this study and responsible for conducting experiments, analyzing

data, interpreting the results and writing the first draft. X Ci and J Hao assisted with the FOXM1 overexpression experiment. H Xue performed the experiments with the xenograft model. X Dong conducted the lung micro-metastasis analysis. D Lin assisted with the kidney tissue invasion analysis. R Wu assisted with H&E and IHC staining. PL Clermont provided suggestions and revised the manuscript. CC Collins was involved in writing the manuscript. PW Gout assisted with the data interpretation and finalized the write-up. YZ Wang supervised the study and was involved throughout the project with regard to concept formation and manuscript design.

A section of Chapter 4 has been submitted for publication. Qu S, Xue H, Dong X, Lin D, Wu R, Collins CC, Gleave ME, Gout PW, Wang Y. Aneustat (OMN54) has aerobic glycolysis-inhibitory activity and also immunomodulatory activity as indicated by a first-generation PDX prostate cancer model. I was the lead investigator of this study and conducted experiments, analyzed data, interpreted the results and wrote the first draft. H Xue set up and supervised experiments using xenograft models. X Dong and D Lin provided professional insight on IHC analysis. R Wu assisted with H&E and IHC staining. CC Collins and ME Gleave reviewed the manuscript. PW Gout finalized the write-up. YZ Wang supervised the study and was involved throughout the project with regard to concept formation and manuscript design.

Table of Contents

List of Tables

List of Figures

List of Abbreviations

ADT: Androgen Deprivation Therapy

AR: Androgen Receptor

ATCC: American Type Culture Collection

AURKB: Aurora Kinase B

BCL2: B-cell Lymphoma 2-encoded Protein

BPH: Benign Prostatic Hyperplasia

CCNB1: Cyclin B1

CD8: Cluster of Differentiation 8

CDC25C: Cell Division Cycle 25C

CENPA: Centromere Protein A

CENPE: Centromere Protein E

CENPF: Centromere Protein F

CI: Combination Index

CRPC: Castration-resistant Prostate Cancer

DRE: Digital Rectal Examination

DRI: Dose Reduction Index

ECM: Extracellular Matrix

EIT: Epithelial Immune Cell-like Transition

EMT: Epithelial-mesenchymal Transition

FBS: Fetal bovine serum

FDA: Food and Drug Administration

FFPE: Formalin-fixed Paraffin-embedded

FOXM1: Forkhead Box M1

FOXP3: Forkhead Box P3

GAPDH: Glyceraldehyde-3-phosphate Dehydrogenase

GEO: Gene Expression Omnibus

GLUT1: Glucose Transporter 1

GVHD: Graft Versus Host Disease

H&E: Hematoxylin and Eosin

HPRT1: Hypoxanthine Phosphoribosyltransferase 1

IHC: Immunohistochemistry

IPA: Ingenuity Pathway Analysis

LDHA: Lactate Dehydrogenase A

LHRH: Luteinizing Hormone-releasing Hormone

MCT4: Monocarboxylate Transporter 4

MDSCs: Myeloid-derived Suppressive Cells

NCI: National Cancer Institute of the United States

NCR1: Natural Cytotoxicity Triggering Receptor 1

NEPC: Neuroendocrine Prostate Cancer

NK Cells: Natural Killer Cells

NOD-SCID: Non-obese Diabetic/severe Combined Immuno-deficient

NSG: NOD-SCID IL2Rgamma (null)

qRT-PCR: Quantitative Real-time Polymerase Chain Reaction

PBMCs: Peripheral Blood Mononuclear Cells

PBS: Phosphate Buffered Saline

PCa: Prostate Cancer

PCA3: Prostate Cancer Antigen 3

PDX: Patient-derived Xenograft

PI3K: Phosphatidylinositide 3-kinases

PIN: Prostatic Intraepithelial Neoplasia

PLK1: Polo Like Kinase 1

PSA: Prostate-specific Antigen

PTEN: Phosphatase and Tensin Homolog

PTTG1: Pituitary Tumor-transforming 1

RPMI: Roswell Park Memorial Institute

SDS: Sodium Dodecyl Sulfate

SRC: Subrenal Capsule

STMN1: Stathmin 1

TAM: Tumor-associated Macrophage

TRAMP: Transgenic Adenocarcinoma of Mouse Prostate

Tregs: Regulatory T cells

TNF-α: Tumor Necrosis Factor Alpha

UGE: Urogenital Sinus Epithelium

UGM: Urogenital Sinus Mesenchyme

UGS: Urogenital Sinus

Acknowledgements

The journey of my PhD study is one of the most significant experiences in my life. The PhD degree marks the beginning of my career.

First and foremost, I would like to express my deepest gratitude to my supervisor, Dr. Yuzhuo Wang. It is my fortune to have the opportunity to pursue my PhD with his guidance and support throughout the years. As an academic supervisor, Dr. Wang has taught me how to become a scientist. Critical thinking, sharp insight and sparkling ideas - all of these are needed to become a true and successful scientist. Also, I want to extend my deepest appreciation to the members of my supervisory committee, i.e. Drs Marianne Sadar, Colin Collins and Christopher Ong, for providing invaluable advice and suggestions throughout my project.

I would like to thank all of the past and present members of the Wang lab for their support and help. I give special thanks to Dr. Peter W. Gout for his support and encouragement throughout my PhD study. Dr. Gout is a mentor and a friend. His wisdom and thoroughness in science will guide me in my future career. I would like to thank Dr. Hui Xue for providing me with excellent training in studies involving use of mice, and Drs Fang Zhang and Dong Lin for valuable scientific advice and suggestions for my project. Thanks to Dr. Akira Watahiki, Dr. Francesco Crea and Dr. Pier-Luc Clermont: each of you showed me the beauty of science from various aspects. I really thank everyone in the Wang lab for providing a warm family atmosphere and supporting me. I am also thankful to all the members of the British Columbia Cancer Research Centre and the Vancouver Prostate Centre that I worked with. It was a pleasure to learn from each of them. Furthermore, I thank Omnitura Therapeutics Inc., for providing Aneustat and hence giving me a great opportunity to contribute to prostate cancer treatment. The China Scholarship Council is thanked for sponsoring my PhD study.

Finally, I have my special thanks to my dearest parents, who love me and supported me throughout my life. I am your pride, and will always be.

To My Parents

For their continued support

Chapter 1: Introduction

1.1 Prostate Cancer

1.1.1 Overview

Prostate cancer is the most commonly diagnosed, non-cutaneous cancer and one of the leading causes of cancer death in North American men [1]. The Canadian Cancer Society estimated that, in 2016, more than 21,600 men in Canada would be diagnosed with prostate cancer, representing 21% of all new cancer cases in Canadian men that year. In addition, 4,000 men would die from the disease, representing 10% of all cancer deaths in Canadian men. Approximately 1 in 8 Canadian men are expected to develop prostate cancer during their lifetime, and 1 in 27 of them would likely die from this disease.

More than 95% of prostate cancers are adenocarcinomas that originate from prostatic epithelial cells [2]. Most commonly, prostate cancer is found within the luminal epithelium of the peripheral zone [3]. If the disease is localized at the time of diagnosis, the 5-year survival is approximately 100%. In contrast, when distant metastases have occurred, the 5-year survival drops to approximately 28% [4]. However, about 20% to 30% of patients with localized disease will develop metastasis, even when they have been treated with definitive local therapies [5]. Once prostate cancer develops into metastatic disease, it becomes incurable with severe complications and a poor prognosis [6, 7].

Prostate cancer is a heterogeneous disease, since multiple distinct foci of carcinoma and prostatic intraepithelial neoplasia (PIN) with various degrees of cellular dysplasia tissue disorganization and genetic alterations can be found in a single prostate [8, 9]. Early-stage prostate cancer depends on androgen for growth and survival and responds to androgen ablation therapy [10]. Eventually, however, the disease progresses into castration-resistant prostate cancer

(CRPC) [11]. According to its androgen receptor (AR) status, CRPC is categorized as AR-positive CRPC and AR-negative CRPC, such as neuroendocrine prostate cancer (NEPC) [12]. CRPC is at present incurable and lethal to cancer patients [11, 13].

1.1.2 The Prostate

The prostate is the largest accessory sex gland in the male reproductive system. In human adults, the prostate is approximately the size of a walnut, weighing between 7 - 16 grams [14]. It is located below the base of the bladder and immediately in front of the bowel, surrounding the neck region of the urethra. The main function of the prostate is to secrete an alkaline fluid which nourishes and protects the sperm [15]. Adult prostatic epithelium consists mainly of luminal and basal cells, i.e. a continuous layer of cuboidal basal cells covered by a layer of columnar luminal cells which express the androgen receptor (AR) and prostate-specific antigen (PSA) [16].

The normal prostate is divided into three distinct anatomical zones: the central zone, the transition zone, and the peripheral zone (Fig. 1.1) [17]. The peripheral zone (70% of the prostate) is the largest region and is also the most common site in the prostate for developing prostatic carcinomas. The central zone, which comprises 25% of the prostate, has a relatively lower incidence of carcinomas and other diseases. Although the transition zone is the smallest region of the prostate, benign prostatic hyperplasia (BPH) mainly arises from this region [17].

The prostate originates from the endodermal urogenital sinus (UGS), which also gives rise to the prostatic urethra and bulbourethral glands in males, the lower vagina and urethra in females, and the bladder in both males and females [18, 19]. Androgen mediates the interaction between the urogenital sinus epithelium (UGE) and the urogenital sinus mesenchyme (UGM) to form the prostate [19-21]. During human prostate development, prostatic buds show up at about 10 weeks of fetal development. The solid prostate buds grow into the surrounding mesoderm.

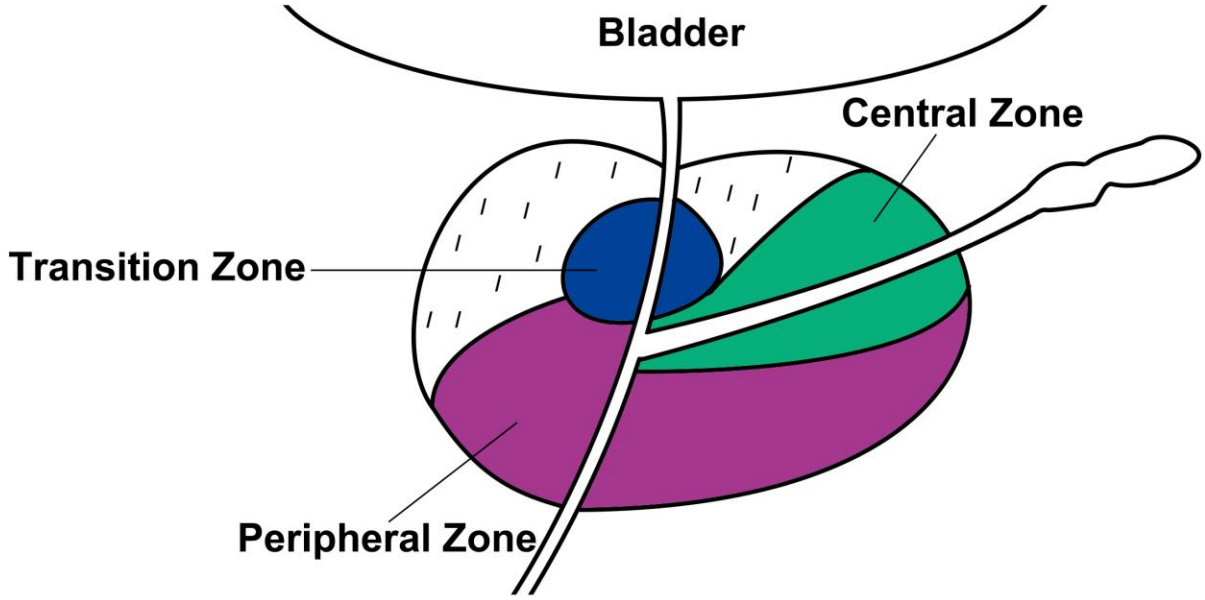

Figure 1.1 The anatomy of human prostate.

The prostate is located below the bladder. The normal human prostate is divided into three anatomical zones, i.e. the central zone, the transition zone, and the peripheral zone.

The canalization of solid buds starts from the proximal ductal region near the urethra to the distal end. During prostate development, androgen is required to establish secretory epithelial cell morphology and secretory function [15, 22, 23]. By the end of the 15th week of gestation, secretory prostatic epithelial cells are functional and PSA is produced by these cells. During embryonic development, the maturation of the prostate gland goes on when androgen levels are high. But prostate maturation stops at a quiescent state between birth and puberty. Prostate maturation and growth continue during puberty in response to increased androgen levels [16]. As such, androgen is essential for prostate development and maintenance. In adulthood, androgen receptors are expressed by the luminal epithelial cells, and the full secretory phenotype is established. Androgen deprivation can induce apoptosis of the prostatic epithelial cells and lead to a loss of nearly 90% of these cells within 3 weeks [24].

1.1.3 Risk Factors

Epidemiological studies of prostate cancer have found the potent risk factors for prostate cancer to be age, race/ethnicity, and family history [25]. Prostate cancer is an age-related disease; age-specific incidence rates reveal that the likelihood of developing prostate cancer rises sharply after age 50 [26]. In terms of race/ethnicity, the incidence of prostate cancer in Asian males is usually lower than in African American and Caucasian men, whereas African American men are more likely to develop prostate cancer than Caucasian men [27, 28]. However, the incidence of prostate cancer for Asian men living in Western countries is much higher than for Asian men living in their Asian countries of birth [27]. This indicates that environmental influences, such as diet and lifestyle, could be other risk factors for prostate cancer [25]. Finally, family history is another important risk factor for prostate cancer; a man with a positive family history has a 2-3 times higher chance of developing the disease [27]. Aside from these risk factors, there are other

potential risk factors that can increase the probability of developing prostate cancer, including hormone profiles, concomitant medical conditions, and occupational exposures (such as, pesticides, lacquers, binding agents, pigments and solvents) [25, 29, 30].

1.1.4 Diagnosis and Staging of Prostate Cancers

Studies of autopsies show that approximately 29% of men between the ages of 30-39 have microscopic evidence of prostate cancer, with the incidence increasing to 65% by age 70 [31]. Histopathological assessments of tissues can indicate the presence of malignancies and their degree of aggressiveness. The Gleason Classification system is a commonly used grading system, based on histologic patterns and extent of cell differentiation, to reveal how different prostate cancer tissue is from benign prostate tissue; as such it can be used as a powerful prognostic predictor of prostate cancer [32]. The Gleason *grade* ranges from 1 to 5, i.e. from well-differentiated (Grade 1) to poorly differentiated (Grade 5) tumors. The Gleason *score* is the sum of the two most prominent histological grades: the primary and secondary grade patterns. The primary pattern is the dominant pattern in an area, whereas the secondary pattern is the second most common pattern [33]. Gleason scores range from 2 to 10; a score of 2 indicates a well-differentiated tumor, while a score of 10 is a poorly differentiated tumor. In 2013, scientists from the Johns Hopkins Hospital proposed a new grading system. This new system includes five distinct Grade Groups: (i) Gleason score $\leqslant 6$, (ii) Gleason scores $3+4=7$, (iii) Gleason scores $4+3=7$, (iv) Gleason scores $4+4=8$, and (v) Gleason scores 9 and 10. At biopsy, the 5-year biochemical recurrence-free survivals for the 5 Grade Groups were 96, 88, 63, 48, and 26 %, respectively [34]. Prostate cancer patients with Gleason score 7 (4 + 3) are in higher risk than those with Gleason score 7 (3 + 4) [35]. Lastly, the clinical status of prostate cancer is also characterized by a tumor–node–metastasis (TNM) system. T1 and T2 represent cancers confined

to the prostate, and T3 and T4 represent cancers that have spread elsewhere. N0 indicates no regional lymph node metastasis, and N1 indicates metastases in regional lymph node(s). M0 represents no distant metastasis; M1 represents metastasis to distant organs (beyond regional lymph nodes) [36].

Prostate cancers are commonly discovered during a digital rectal examination (DRE) or by a serum prostate-specific antigen (PSA) test [37, 38]. Of these two methods, PSA screening is more sensitive than DRE [37], but has disadvantages as discussed below. Combined use of PSA and DRE is a more sensitive method for early detection [37], with prostate biopsy as the gold standard for prostate cancer diagnosis [39]. Therefore, men with a PSA level between 4.0 and 10 ng/mL should undergo a prostate biopsy even with a negative DRE [38].

Since the serum PSA test was introduced as a diagnostic marker into clinical practice in 1987 [40], and later approved by the FDA as a biomarker for prostate cancer diagnosis, it has been widely adopted. However, there is controversy over the efficacy and reliability of PSA screening. It is associated with a high false-positive rate (as demonstrated by tissue biopsy) and hence psychological harm [41]. In addition, PSA screening cannot differentiate lethal from nonlethal disease [42]. It may lead to over-diagnosis and over-treatment for patients with non-life threatening prostate cancer causing unnecessary harm to the patients [43, 44]. In view of these disadvantages of PSA tests, new diagnostic prostate cancer biomarkers have emerged based on novel molecular technologies, such as microarrays and whole-genome sequencing.

Prostate cancer antigen 3 (PCA3) is a gene that expresses a long noncoding RNA [45, 46]. PCA3 is only expressed in human prostate tissue and highly overexpressed in 95% of prostate cancers [45, 47]. RNA expression of PCA3, measured in urine samples after DRE, can be used as a prostate cancer diagnostic biomarker with a sensitivity of 53 - 69% and specificity of 71 - 83%

[48]. Use of PCA3 (Progensa by Gen Probe, Inc.) was approved by the FDA in 2012 for prostate cancer diagnosis [48].

TMPRSS2-ETS gene fusions are most frequently observed genetic alterations in prostate cancer. The ETS family numbers, ERG and ETV1,4,5, have been demonstrated to show genomic rearrangements leading to gene fusion with TMPRSS2 [49]. Among these aberrations, TMPRSS2-ERG gene fusion is the most common one in prostate cancer. It is specific for prostate cancer and not detectable in benign prostate tissue and benign prostatic hyperplasia (BPH) [50, 51]. The frequency of TMPRSS2-ERG gene fusion in primary prostate cancers is approximately ≥50% [52, 53]. However, the frequency of TMPRSS2-ERG gene fusion in CRPC patients varies from 37% to 80% based on various patient cohorts [54-56]. As well, TMPRSS2-ETV gene fusions account for less than 10% of prostate cancer samples [51]. As such, the TMPRSS2-ETS gene fusions provide diagnostic value for prostate cancer [57]. However, their prognostic value is controversial as indicated by various reports [48, 58].

“Liquid biopsy” based on analysis of circulating tumor cells (CTCs) and circulating cell-free tumor DNA (ctDNA) in the blood of patients has emerged as a promising non-invasive prostate cancer diagnostic method [59]. While the majority of research in this area has focused on blood-based liquid biopsy [60, 61], studies have shown that other body fluids, such as urine [62], saliva [63, 64], and cerebral spinal fluid [65, 66], may also be used for liquid biopsy. CTCs can be isolated from the blood of cancer patients as single cells or in cell clusters. Elevated numbers of CTCs are most commonly found in metastatic prostate cancer patients [67]. CTCs are not only useful as diagnostic biomarkers, but also have prognostic value [68]. As such, the CellSearch® test has been approved by the FDA for isolation and enumeration of CTCs from the peripheral blood, serving as an independent prognostic biomarker of survival of patients with

prostate, breast and colorectal cancers [69]. In addition to the information obtained through analysis of CTCs, the molecular profiles gathered from ctDNA can provide additional value for cancer diagnosis, response to treatment prognosis, and cancer monitoring [59, 61, 70]. The concentration of ctDNA in peripheral blood has been shown to correlate with tumor size and disease progression. A median concentration of ctDNA of patients with advanced prostate cancer is about 100-1,000 copies per 5 ml of plasma [60]. The application of ctDNA can be used to detect both specific genetic changes and all possible aberrations in DNA using targeted and whole exome/genome sequencing [70].

In addition, other commercially available prostate cancer biomarkers or tests have recently been developed. The Prostate Core Mitomic Test (Mitomics) is an RT-PCR test to distinguish benign from malignant prostate tissues by detecting large-scale mitochondrial DNA deletions in formalin-fixed paraffin-embedded (FFPE) biopsy samples [71]. Prolaris (Myriad Genetic Laboratories) is a gene test used to measure the cell cycle progression signature of 46 genes (31 cell cycle genes and 15 house-keepers) using FFPE material (biopsies or resected tumors) to predict prostate cancer progression and disease mortality [72]. Such commercial biomarkers or tests may be useful for improving diagnosis of prostate cancer and guidance for its treatment. Validations are needed to confirm their reliability, reproducibility and clinical utility with large cohorts from multiple centers.

1.1.5 Cancer Metastasis

1.1.5.1 The Metastatic Process

Metastasis is the spread of cancers from the place where they first formed to another part of the body [73]; it is the central step that makes most cancers incurable [74]. Metastasis is responsible for 90% of cancer deaths [75, 76], and is defined as one of the hallmarks of cancer [77]. The two

major routes of cancer metastasis are hematogenous spread (dissemination via blood vessels) and lymphogenous spread (dissemination via lymphatic systems). Other ways of cancer metastasis include local tissue invasion and direct seeding into body cavities [78, 79].

Metastasis is a multi-step process involving a series of complex biological events. Each of the steps can affect the time required for metastasis to occur, and failure of any of the steps can abolish the entire metastatic event [80, 81]. Metastasis begins with local tissue invasion, which involves changes in cancer cell adhesion to neighboring cells and to the extracellular matrix (ECM), and proteolytic degradation of the surrounding tissue leading to cancer cells penetrating the surrounding tissue [82, 83]. Matrix metalloproteinases (MMPs), especially MMP2 and MMP9, play an important role in cancer progression by degrading the ECM and stimulating epithelial-mesenchymal transition (EMT), which lead to cancer cell invasion [84-86]. EMT is a complex process by which epithelial cells acquire mesenchymal, fibroblast-like properties and reduced cell-cell adhesion, resulting in increased motility of the cancer cells [87]. Remarkable changes of EMT are the loss of an epithelial surface marker, namely E-cadherin, and the acquisition of mesenchymal markers, such as vimentin and N-cadherin [88]. Various transcription factors, such as SNAIL, SLUG and TWIST, contribute to activation of the EMT process [88].

The next step in metastasis involves entry of the cancer cells into the blood vessels, a process called intravasation. The bloodstream is a rough environment for circulating cancer cells, and for successful extravasation of the cancer cells to occur, they must survive immune attacks and destruction from velocity-induced shear forces [82, 83, 89]. One of the survival mechanisms of cancer cells in the bloodstream comes from the protection by platelets [90]. Thus cancer cell-platelet aggregations can provide shields for the cancer cells against attacks by immune cells in

the bloodstream. In addition, platelets can also protect cancer cells from high shear forces in the blood [90, 91]. Furthermore, platelets can facilitate the adhesion of cancer cells to the vascular endothelium and their subsequent extravasation [92, 93]. On their own, cancer cells may protect themselves from immune cell action by expressing acquired immunosuppressive activity that allows them to "communicate" with immune cells and evade immune surveillance. It has been proposed that acquisition of immunosuppressive properties by epithelial cancer cells can be obtained via a process termed ‘Epithelial Immune Cell-like Transition’ (EIT) [94].

Finally, to form metastatic colonies, extravasated cancer cells must survive in a microenvironment that usually markedly differs from the primary tumor site [82, 83, 89]. A large number of cancer cells die after arrival in distant organs [95, 96]. To survive an incompatible microenvironment at the metastatic site, cancer cells may establish a pre-metastatic niche before initiating the metastatic processes [97]. To overcome the harsh new environment, cancer cells may enter a quiescent state as single cells or micro-metastasis. The quiescence may last from months to years. Once the growth pathways are activated, latent cancer cells enter a fast growth stage, leading to the formation of macro-metastases and an overt lesion [96].

Studies show that cancer metastasis does not occur by chance; certain cancer cells (the “seed”) possess an affinity to certain organs (the “soil”). Therefore, metastatic events develop only when the seed and the soil are compatible [98]. It has been well-established that various types of cancer demonstrate organ-specific metastases [99], and numerous theories have been proposed to explain organ-specific metastasis. One theory proposes that tumor cells spread equally via the blood and lymphatic systems to all the organs, but only form colonies in organs with suitable growth factors. Another theory suggests that cancer metastasis results from adhesion molecules expressed by endothelial cells in the blood vessels of target organs. Lastly, a

"chemoattraction" theory outlines the spread of organ-specific attractive molecules into the circulating system, which leads circulating cancer cells to penetrate the blood vessels and enter the specific organs [100]. More evidence is needed to elucidate the mechanisms underlying organ-specific metastasis.

1.1.5.2 Prostate Cancer Metastasis

Bones are the most common sites of cancer metastasis and prostate cancer is one of the most common types of cancer to develop bone metastases, with an incidence of about 68% [98]. The incidence is even higher for advanced prostate cancer (>80%). As such, bone metastasis is associated with high morbidity: the 5-year patient survival rate is less than 30% and the median survival is approximately 40 months for metastatic prostate cancer patients [101].

When cancer cells arrive in the bone, they adapt to their new microenvironment and then usually enter a dormant state. Upon external stimulation, prostate cancer cells develop into micro-metastases. This is followed by a period of rapid growth, as cancer cells establish macro-metastases *in situ* [102]. Particularly in the case of prostate cancer, bone metastases can lead to numerous complications, including hypercalcemia of malignancy, bone marrow failure/ leukoerythroblastic anemia, and more commonly, skeletal-related events (SREs) [103]. SREs are defined as pathological fractures, spinal cord compression, and bone pain; SREs are associated with an increased risk of death, increased health care costs, and a reduced quality of life [103, 104]. As such, treatment regimens that can potentially delay or reduce prostate cancer metastasis would subsequently reduce the occurrence of SREs and benefit cancer patients [105].

Metastatic prostate cancer in bone has been shown to induce osteoblastic lesions [106]. Emerging evidence indicates that the development bone metastases of prostate cancer requires not only osteoblastic activity but also osteoclastic activity [107]. The bone-specific metastasis of

prostate cancer is very likely regulated by chemoattractant factors, such as CXCL12 and RANKL [108-110]. It has been shown that prostate cancer cells expressing CXCR4 migrate to bone marrow expressing CXCL12 [111, 112]. Using a mouse model it was found that prostate cancer bone metastasis could be reduced by neutralizing CXCR4 using anti-CXCR4 antibodies [113]. RANKL, and its receptor RANK, also appear to play important roles in prostate cancer metastasis. RANKL is expressed by osteoblasts while RANK is expressed on osteoclast precursor cells. Activation of RANK/RANKL can lead to osteoclast formation, which is inhibited by osteoprotegerin (OPG) binding to RANKL [114, 115]. RANK, however, is also expressed by prostate cancer cells, and the RANKL produced by osteoblasts shows chemoattractant activity, inducing bone metastasis of RANK-expressing cancer cells [116]. The expression levels of RANKL and RANK are positively correlated with prostate cancer grade and metastatic events [117, 118].

A variety of signaling pathways are thought to play important roles in prostate cancer metastasis, including the Wnt/β-catenin signaling pathway. Following activation of signaling pathway, it can induce stabilization of the transcriptional co-activator β-catenin and its translocation to the nucleus leading to activation of target genes [119]. *Twist* and *Slug* are target genes of the Wnt/β-catenin pathway; their activation can inhibit E-cadherin gene expression leading to promotion of prostate cancer metastasis [119, 120]. Recently, a key role of the FOXM1-CENPF pathway in the metastatic progression of prostate cancer has been highlighted. The FOXM1 transcription factor was shown to have an essential role in prostate cancer growth and metastasis [121, 122]. As well, analysis of gene expression profiles of both human and mouse prostate tumors indicated that FOXM1 and CENPF (a protein that associates with the centromere-kinetochore complex) are synergistic master regulators of prostate cancer metastasis;

co-expression of FOXM1 and CENPF is a robust prognostic indicator of metastasis and poor patient survival [123]. Recent evidence indicates that prostate cancer metastasis is promoted by dysregulation of the FOXM1-CENPF axis, i.e. with loss of functions of miRNAs leading to over-expression of FOXM1 and CENPF [124].

1.2 Prostate Cancer Treatment

1.2.1 Treatment Options

Treatment options for prostate cancer are mainly based on prognostic factors: initial PSA level, clinical TNM stage, and Gleason score. Other factors that are also considered are baseline urinary function, comorbidities, and age [125]. Active surveillance is suitable for patients with localized prostate cancer with pre-treatment clinical stage T1c or T2 tumours, serum PSA levels of <10 ng/ml, and biopsy Gleason scores of 6 or less. To monitor tumour progression during surveillance, patients are recommended to take serum PSA tests, digital rectal examinations, and surveillance biopsies [126, 127]. Surgery and radiation therapy are common options for treating localized prostate cancer [125], and can be curative [128]. However, many patients will likely experience local recurrence and progression to metastasis [128, 129]. Since prostate cancer growth is generally androgen-dependent, androgen ablation therapy (ADT) of locally advanced, recurrent, or metastatic prostate cancer is quite effective during the first 1 to 3 years of the disease. Either through medical or surgical castration, ADT aims for a serum testosterone level lower than 20 ng/dl to maximize therapeutic efficacy [130, 131]. Medical castration involves administering luteinizing hormone-releasing hormone (LHRH) agonists or antagonists [130]. However, within 18-24 months cancers will frequently develop into a more aggressive, androgen ablation therapy-resistant phenotype termed “castration-resistant prostate cancer” (CRPC) [132]. CRPC typically manifests itself alongside rising serum prostate-specific antigen (PSA) levels

[133]. It has been well established that PSA expression is regulated by androgen receptor (AR) [134]; as well, there is increasing evidence that AR plays an important role in the development of CRPC [135, 136]. Currently, the standard first line therapy for metastatic CRPC is systemic docetaxel plus prednisone chemotherapy, which was approved in 2004 [137].

After docetaxel, several new drugs have been approved by the U.S. Food & Drug Administration (FDA) for prostate cancer treatment. For example, Abiraterone Acetate inhibits androgen synthesis by selective inhibition of the enzyme CYP17, a critical enzyme in testosterone synthesis [138]. As demonstrated by Phase III clinical trials, it can be used for treatment of both chemotherapy-naïve and post-docetaxel treatment patients with metastatic CRPC [139-141]. Enzalutamide is a second-generation antiandrogen which binds strongly to the AR with a higher affinity than earlier generation anti-androgens, inhibiting AR nuclear translocation [142]; Enzalutamide can also impair AR-DNA binding, leading to inhibition of AR-mediated transcription [143]. Evidence from Phase III clinical trials has shown that Enzalutamide may be used for treatment of both chemotherapy-naïve and post-docetaxel treatment mCRPC patients [144, 145]. However, cross-resistance has been observed between Abiraterone Acetate and Enzalutamide [146, 147].

Cabazitaxel is a novel tubulin-binding taxane with poor affinity for P-glycoprotein compared to Docetaxel [148]. Although Cabazitaxel and Docetaxel belong to the same family, the TROPIC trial has shown that Cabazitaxel was effective after Docetaxel failure. As such, Cabazitaxel is used as post-docetaxel treatment [149, 150]. In addition, Cabazitaxel was found to show anti-prostate cancer activity in patients after Abiraterone or Enzalutamide therapy [151]. Sipuleucel-T is an autologous cellular immunotherapeutic and the first therapeutic vaccine for CRPC treatment approved by the FDA, based on the D9901, D9902A and IMPACT Phase III

trials [152, 153]. Sipuleucel-T contains a patient's peripheral blood mononuclear cells, including antigen-presenting cells (APCs), which are activated ex vivo and then injected back into the patient to induce an immune response [154].

There are also a small number of drugs used for treatment of patients with metastatic prostate cancer. Zoledronic acid, a third generation nitrogen-containing bisphosphonate, is used for treatment of CRPC patients with bone metastases. ADT-induced bone loss has been shown to increase the risk of fracture [155]. Bisphosphonates can suppress recruitment and activity of osteoclast to sites of bone resorption [156]. In addition, it was shown that bisphosphonates could inhibit prostate cancer invasion and cancer cell adhesion to the bone [157]. Treatment with Zoledronic acid was shown to reduce skeletal-related events (e.g., pathologic bone fracture) [158]. Denosumab, a monoclonal antibody specific for RANKL, targets the RANKL-RANK axis during prostate cancer bone metastasis [115, 159]. Denosumab can inhibit activation of RANK on the surface of osteoclasts by binding to RANKL which leads to inhibition of osteoclast function. As such, treatment with Denosumab may decrease bone resorption and reduce cancer-induced bone damage [160]. In Phase III clinical trials, it was found that treatment with Denosumab can significantly increase bone metastasis-free time of prostate cancer patients [161]. Radium-223, an alpha particle-emitting radiopharmaceutical, is recommended for treatment of prostate cancer patients with pain due to bone metastases, but with no known visceral metastasis [139, 162]. Radium-223 mimics calcium to form complexes with hydroxyapatite, particularly in areas with high osteoblastic turnover, i.e. metastatic prostate cancer cells surrounded by osteoblasts [163]. Alpha particles generated by decay of Radium-223 can induce double-strand DNA breaks, leading to cancer cell death. The short tissue-penetration range of alpha particles, however, limits the disruption of the surrounding healthy bone tissue [164]. Treatment with

Radium-223 has been shown to benefit metastatic prostate cancer patients by increasing the overall patient survival time and reducing the number of skeletal-related events [4].

1.2.2 Docetaxel-based Chemotherapy

1.2.2.1 Clinical Applications and Molecular Actions of Docetaxel

Docetaxel is a semi-synthetic, second generation taxane derived from the bark of the European yew tree, Taxus baccata [165]. Docetaxel is approved by the FDA for treatment of metastatic castration-resistant prostate cancer (mCRPC), breast cancer, non-small cell lung cancer, gastric adenocarcinoma and squamous cell carcinoma of the head and neck cancer. Based on a Phase III clinical trial-TAX327 study, docetaxel-based chemotherapy was approved in 2004 as a first line treatment for mCRPC patients. The recommended dosage of docetaxel is 75mg/m^2 (1 hour intravenous infusion) every three weeks, combined with 5mg of prednisone twice daily for 10 cycles. In a retrospective study, it was shown that patients who received docetaxel plus prednisone had limited longer progression-free survival time than those who received docetaxel alone [166]. This is likely due to the inhibitory effect of corticosteroids on adrenal androgen secretion and growth of prostate cancer cells by modulating the levels of cellular growth factors, such as down-regulation of IL-6 [167]. Recently, three independent Phase III clinical trials have shown that docetaxel-based chemotherapy plus androgen deprivation therapy (ADT) of metastatic, androgen-sensitive prostate cancer patients can improve patient overall survival compared to use of ADT alone [168, 169]. These trials indicate potential clinical use of docetaxel-based chemotherapy for treatment of early stages of prostate cancer in addition to metastatic CRPC.

The anticancer activity of docetaxel is based on interference with microtubule dynamics essential for mitotic and interphase cellular functions. Docetaxel has a high affinity for tubulin

which promotes the assembly of stable microtubules and inhibits their disassembly. This leads to a decrease in free tubulin, needed for microtubule formation, and results in inhibition of mitosis [137]. Furthermore, it has been shown that docetaxel can induce cell apoptosis by affecting the expression and phosphorylation of Bcl-2 family proteins [170]. In addition, it has been reported that docetaxel can not only down-regulate AR expression [171], but also inhibit microtubule-dependent AR nuclear translocation [172, 173].

Although docetaxel targets prostate cancer via various mechanisms, and treatment with docetaxel-based chemotherapy has led to prolonged overall patient survival, the patient response to treatment with docetaxel is lower than expected. In the TAX327 clinical trial, the PSA response (defined as a reduction in serum PSA levels of at least 50%) and tumor response of patients treated with standard docetaxel-based treatment were about 45% and 12%, respectively [174]. In the S9916 Phase III clinical trial, a 50% PSA response and 17% tumor response were observed in patients treated with docetaxel and estramustine [175]. In the CALGB-90401 Phase III clinical trial, mCRPC patients treated with standard docetaxel-based therapy showed a 57.9% PSA response and a 35.5% tumor response [176]. Recently, another Phase III clinical trial, conducted by Prof. Pirkko-Liisa Kellokumpu-Lehtinen, showed that treatment of mCRPC patients with 3-weekly docetaxel-based chemotherapy led to a PSA response of about 42% and a tumor response of about 22% [177].

In addition to the relatively low patient response, docetaxel resistance was found to develop in patients who initially responded to the drug. The development of docetaxel resistance may be caused by various conditions/factors [178, 179]: **i) Therapy resistance related to abnormal tumor vasculature.** Administration of an anticancer drug to a solid tumor usually takes place via the bloodstream. As the drug reaches the tumor via the blood, it still must cross

the extracellular matrix to enter the cancer cells. Tumor blood vessels are disorganized and have a chaotic blood flow. This can lead to impaired delivery of the drug to the various parts of the tumor and ultimately therapy resistance [180]. The abnormal tumor vasculature also leads to hypoxic regions in the tumor and to hypoxia-induced development of drug resistance [181]. Impaired drug delivery, and hence therapy resistance, can also be induced by increased interstitial fluid pressure caused by leaky vasculature coupled to impaired lymphatic drainage [182]. **ii) Altered intracellular docetaxel levels.** ATP-binding cassette transporters (ABC transporters) are members of a transporter family to pump docetaxel from the intracellular space to the extracellular space, leading to reduced amounts of drug inside the cancer cells. Docetaxel has a high affinity for P-glycoprotein, a member of the ABC transporter family. It has been shown that cancer cells that synthesize P-glycoprotein become resistant to docetaxel [183]. Over-expression of other ABC transporters, such as ABCB4 and ABCC1, also promotes docetaxel resistance in cancer cells [184]. **iii) Microtubule alterations.** Alterations in microtubule structure and/or function represent another mechanism of docetaxel resistance development. The changes of microtubule structure may be caused by β-tubulin gene mutations which affect docetaxel binding, increased total cellular β-tubulin content, altered expression of β-tubulin isotypes (e.g. βIII-tubulin) and led to post-translational β-tubulin modifications. Functional changes that may promote docetaxel resistance include alternative binding of docetaxel to β tubulin, changes in expression of microtubule-destabilizing phosphoproteins, elevated expression of kinesins and activation of the TXR1/thrombospondin pathway [185]. **iv) Impaired apoptotic pathway and activation of other pathways.** Changes in gene expression affecting the apoptotic pathway can form additional mechanisms of docetaxel resistance development. During treatment of prostate cancers with docetaxel, up-regulation of Bcl-2 decreases the efficacy of docetaxel by

impairing apoptosis [186]. In addition, other changes, such as *p53* mutation, Src tyrosine kinase inactivation, activation of PI3K/AKT pathway and NF-κB pathway, can lead to docetaxel resistance [179].

1.2.2.2 Docetaxel-based Combinations

In the TAX 327 randomized, Phase III clinical trial, docetaxel-based chemotherapy was shown to improve the overall survival of mCRPC patients, compared to the previous standard regime of mitoxantrone plus prednisone [174]. However, there were only marginal improvements in the overall patient survival. Since then, numerous clinical trials have focused on improving the efficacy of docetaxel by combining it, as a pivot drug, with a variety of other anticancer agents, including tyrosine kinase inhibitors (e.g., Dasatinib [187]), antiangiogenic agents (e.g., Bevacizumab [176]), bone-targeted agents (e.g., Zoledronic acid [188] and Atrasentan [189]), anti-apoptosis inhibitors (e.g., Custirsen [190]), vitamin D analogs (e.g., Calcitriol [191]), and other therapeutics such as Estramustine [175]. Although some of the Phase I/II clinical trials have shown positive data, Phase III clinical trials with docetaxel-based combinations have failed to demonstrate improvements in overall survival of mCRPC patients compared to the standard docetaxel-based treatment [192-194]. Therefore, the development of effective drugs and/or novel therapeutic regimens is critical for improving disease management and patient survival time.

Several criteria used in the design of the above docetaxel-based combinations need particular attention. First, some of the docetaxel-based combinations entered Phase III trials without having successfully reached the research goals in Phase II trials. Moreover, some of the drug combinations used were never tested in Phase II clinical trials before entering Phase III trials. Second, appropriate end points in clinical trials should be drug specific, e.g., PSA response rate as an end point for AR-targeting drugs. Third, early-phase studies should seek to confirm

that the drug in question reaches its target, engages and inhibits its target and that target inhibition produces a clinical effect [193].

1.3 Tumor-Immune System Interactions

1.3.1 Local Immune Response

The tumor microenvironment is the cellular environment in which the cancer cells exist. It includes surrounding blood vessels, immune cells, fibroblasts, bone marrow-derived inflammatory cells, lymphocytes, signaling molecules and the extracellular matrix. There is continuous interaction between the cancer cells and immune components of the tumor micro-environment affecting the growth and heterogeneity of the cancer cells. Various types of immune cells are recruited into the tumor microenvironment; this induces a dynamic process of local immune responses. Many studies have been conducted to examine the relationship between local immune responses and cancer progression [195]. It is now well-accepted that the immune system has a dual role in the development of cancer. It acts both as a tumour suppressor and promoter, by inducing cancer cell death and establishing an optimal microenvironment that facilitates cancer progression [196-198], respectively. This latter role is known as immunoediting [199-201]. Three stages of cancer immunoediting have been proposed: elimination, equilibrium, and escape [199, 202].

During the elimination phase, both innate and adaptive immune responses are involved, which leads to the elimination of cancer cells via various mechanisms [199]. If all the cancer cells are destroyed, the elimination phase represents an endpoint of immunoediting. However, if cancer cells remain, interactions between the immune system and the remaining cancer cells results in the equilibrium phase. This way, the immune system can limit tumor outgrowth and cancer cells can remain in a dormant state for many years, as has been demonstrated in

experimental models [203]. Eventually, cancer cells escape the immune control and flourish within the immunologically intact environment [199]. This ability to evade immunological destruction has been characterized as one of the hallmarks of cancer [77].

It has been proposed that cancer cells can escape immune destruction through various mechanisms. For example, by acquiring immunosuppressive properties via a trans-differentiation process termed epithelial immune cell-like transition (EIT) [94], or by inducing a local immunosuppressive microenvironment [204]. The latter is likely a major cause of immune evasion [195]. Immune genes/proteins that can be expressed by epithelial cancers include a variety of cytokines/receptors, immune transcription factors, and Ig motifs in cell surface molecules. By acquiring an ability to express immune genes/proteins, cancer cells can "communicate" with immune cells leading to (i) suppression of anticancer immune activity in their microenvironment and (ii) facilitation of the malignant progression of the disease [94]. To maintain a tumor-promoting microenvironment, immunosuppressive cells are recruited, including regulatory T cells (Treg), regulatory B cells (Breg), myeloid derived suppressor cells (MDSC), tumor-associated macrophages (TAM), and regulatory dendritic cells (DCreg) [205-209]. This leads to the suppression of the cytotoxic activity of antitumor immune cells such as natural killer (NK) cells and cytotoxic $CD8^+$ T cells [210-212].

1.3.2 Lactic Acid Induced Local Immune Suppression

Reprogrammed energy metabolism is commonly associated with deregulated proliferation of cancer cells, and is an emerging cancer hallmark [77, 213, 214]. In contrast to normal cells, cancer cells in general rely on energy generation via aerobic glycolysis (transformation of glucose to lactic acid), regardless of whether hypoxia is present; it is also known as the 'Warburg effect' [215, 216]. Prostate cancers, as distinct from other cancers, have relatively low glycolytic

activity, rendering ^{18}F-deoxyglucose positron emission tomography (FDG-PET) for glucose uptake measurement less effective [217]. However, metabolic heterogeneity, including aerobic glycolysis, is observed in primary, treatment-naïve prostate cancer [218]. Furthermore, there is evidence indicating that the aerobic glycolysis pathway of prostate cancer is more active as the disease progresses [219, 220]. In addition, prostate cancer cells can also generate energy from non-glucose-dependent pathways, such as glutaminolysis [216, 221, 222]. Secretion by the cancer cells of lactic acid, which is the product of both pathways, results in an acidic tumor microenvironment, with pH levels as low as 6.0-6.5, in contrast to pH levels of ~7.5 of the normal cell microenvironment [223-226].

The acidic tumor microenvironment that is produced by increased lactic acid secretion by cancer cells is a major cause of local immunosuppression [227, 228]. The cancer-generated lactic acid can affect the functions and levels of intratumoral immune cells. The anticancer immune response, as mainly mediated by cytotoxic $CD8^+$ T cells, has been shown to be dependent on components of the microenvironment such as helper cells and cytokines. However, it is also influenced by the surrounding acidity, as an acidic pH can markedly impair the proliferation and function of the cytotoxic $CD8^+$ T cells. Thus, lactic acid was found to inhibit the proliferation and cytotoxic activity of such T cells by 95% and 50%, respectively. In addition, the cytotoxic function of $CD8^+$ T cells could be restored by their transfer to lactic acid-free medium [229]. Recent studies also indicate that the activity of NK cells is inhibited by tumor-generated lactate. The cytotoxicity of NK cells was significantly decreased when cultured in the presence of lactate with down-regulation of the NK activation receptor, NKp46 [230]. Furthermore, abundant evidence has indicated that lactic acid can induce and promote the differentiation of regulatory T cells (Tregs), myeloid-derived suppressor cells (MDSCs), tolerogenic dendritic cells and M2

macrophages, which facilitate cancer progression [230-234]. As such, cancer-generated lactic acid inhibits the anticancer immune response, but activates immunosuppressive action, leading to immunosuppression in the tumor microenvironment.

As indicated above, targeting aerobic glycolysis to reduce lactic acid secretion by cancer cells would likely provide an attractive method to counteract cancer-induced immunosuppression. Using nude mice bearing subcutaneous PC3 human prostate cancer xenografts, it was shown that targeting MCT4 (the lactate transporter that transfers lactate from the cytoplasm to the extracellular space) led to inhibition of the growth of the xenografts; furthermore, increased numbers of intratumoral NK cells and $CD3^+$ T cells were observed around blood vessels [235]. Two other independent *in vivo* studies showed that specific targeting of lactate dehydrogenase-A (LDHA; the enzyme involved in the conversion of pyruvate to lactate) led to inhibition of tumor growth. Furthermore, the cytotoxic activity of $CD8^+$ T cells and NK cells was enhanced and the intratumoral levels of $CD8^+$ T cells and NK cells were higher in treated tumor tissues than in untreated tissues. As well, the numbers of intratumoral Tregs and MDSCs were significantly lower in the treatment group [230, 236]. Taken together, these findings indicate that reduction of cancer-generated lactic acid secretion obtained by targeting the aerobic glycolysis pathway can restore the host anticancer immune response, a promising observation for cancer treatment.

1.4 Patient-derived Xenograft (PDX) Models

1.4.1 Lessons Learned from Past Clinical Trials

In the last decades, 85% of new anticancer drug candidates failed during early stages of clinical trials, despite promising anticancer activity indicated by preclinical tests. Even among candidates that had successfully passed Phase III clinical trials, less than 50% were approved for clinical use [237]. Particularly for potential anticancer drugs, there was a large discrepancy between the

efficacies found for candidate drugs in clinical trials, versus those found during preclinical studies. As a result, only ~5% of anticancer drug candidates (that had successfully met the requirements of preclinical *in vivo* efficacy screening tests) showed significant effectiveness in clinical trials and were approved by the FDA for use in the clinic [238, 239]. These findings strongly indicated that the preclinical screening and assessments of drug candidates being used were hampered by a lack of clinically relevant experimental *in vivo* cancer models. Consequently, in early 2016, the NCI made an important decision to replace the traditional NCI-60 cell lines (a panel of 60 human cancer cell lines, which has been in use for more than 25 years) with patient-derived xenograft (PDX) human cancer models for drug screening [240].

1.4.2 Mouse Models for Prostate Cancer Research

Mouse models of cancer have played an essential role in understanding the biology and mechanisms of cancer initiation and progression, as well as provided new insight into the tumor microenvironment. As experimental tools, mouse cancer models also provide high value for drug screening in personalized cancer therapy and novel drug development, including mechanistic studies and drug efficacy tests. Based on particular research purposes, various mouse models can be applied to answer specific questions.

i) Genetically Engineered Mouse Models

Genetically engineered mouse models that could better recapitulate genetic alterations in human prostate cancer have been widely used in prostate cancer research. These models have been shown to have gained or lost functions of oncogenes, tumor suppressor genes, growth factors, cell-cycle regulators, pro- and anti-apoptotic genes. They have provided powerful tools for studying the biological effects and molecular actions of specific genes in cancers.

The transgenic adenocarcinoma of mouse prostate (TRAMP) model is widely used in research of prostate cancer characterized by rapid cancer progression. The TRAMP model has a C57BL/6 mouse background and expresses SV40 large-T and small-t antigens regulated by the prostate-specific rat probasin promoter [241]. PINs can be seen as early as 10 weeks of age and nearly 100% cancer penetrance is evident by 24 weeks of age [242, 243]. The TRAMP model shows a castration-resistant phenotype, since castration of the mice at 12 weeks of age did not affect cancer progression. Recently, this model has been claimed to develop neuroendocrine-like prostate cancer [244]. The LADY model shows pathological similarity to the TRAMP model, but is less aggressive than the TRAMP model [245]. The probasin promoter was used to drive the SV40 large-T antigen in the LADY mouse model for prostate cancer development [246]. PINs are observed by 10 weeks of age and cancer by 20 weeks of age. Similarly, the LADY model also shows neuroendocrine features [247, 248]. In addition, cancer metastasis can be observed in both TRAMP and LADY models [249, 250].

The PTEN-deficient mouse model represents another commonly used mouse model in prostate cancer studies. Loss-of-function in PTEN is found in about 35% of primary prostate cancers and 63% of metastatic disease. With conditional deletion of Pten in mouse prostate epithelium, the $Pten^{flox/flox}$ mice develop hyperplastic disease by 4 weeks of age, PIN at 6 weeks and prostate adenocarcinoma at 9-29 weeks. Metastatic disease is observed after 12-29 weeks [251]. Loss of PTEN is associated with activated PI3K/AKT signaling [252, 253], enhanced glycolytic activity [253] and docetaxel-resistant phenotype [254, 255]. Thus, an appropriate mouse model can be chosen based on specific characteristics. However, there are still many differences between human and mouse in prostate biology, tumorigenesis, cancer progression and metastasis development [256].

ii) Cancer Cell Line-derived Mouse Models

They include immunodeficient mice (e.g., nude and SCID mice) bearing (i) subcutaneous human prostate cancer cell line xenografts by injection of cultured human prostate cancer cells (e.g., LNCaP, C4-2, PC3 and DU145) or (ii) allografts by injection of mouse prostate cancer cells (e.g., TRAMP C-2 and RM1). This type of mouse model is valuable for basic research, but has limitations with regard to clinical relevance, likely due to the loss of cancer heterogeneity, absence of tissue architecture observed in patient samples, lack of original tumor microenvironment in clinical samples [257]. As such, these limitations restrict the use of the cell line-derived mouse model.

iii) Cancer Tissue-derived Mouse Models

To overcome the limitations of cell line-derived mouse models, fresh, unprocessed patient cancer tissue specimens are implanted into immunodeficient mice (e.g., NOD-SCID mice). Such xenografts can maintain cellular heterogeneity, tissue architecture and the original cancer microenvironment. However, successful grafting of patient cancer tissues is dependent on the graft site used.

There are three major graft sites for PDX models: the subcutaneous, orthotopic, and subrenal capsule (SRC) sites. The subcutaneous xenograft is most frequently used, due to the straightforward process of implantation of the tissue and ability to non-invasively monitor the developing tumor. However, a drawback of subcutaneous grafting is its low take rate, which is mainly due to lack of vascularization at the graft site [258]. By contrast, the orthotopic graft site is considered the ideal graft site for evaluating the metastatic ability of prostate cancer tissue, as it should theoretically provide an environment highly similar to that of the original cancer. However, aside from the challenging surgical procedure, the orthotopic site has a very limited

xenograft carrying capacity, which severely restricts its use for establishing transplantable xenografts [257]. Both subcutaneous and orthotopic xenografts have been mostly successful with highly advanced cancers, which represents a small subsect of the total cancer population [257]. The advantages of SRC xenografts will be discussed in detail below.

iv) Humanized Mouse Models

With the advancement of cancer immunotherapies, there is a critical need for mouse models that can be used for cancer immunology studies. Humanized mice, which are immunodeficient mice (such as NOD-SCID mice and NSG mice) that have been reconstituted with various components of a human immune system, are established to provide powerful tools for research. There are three major ways to establish human immune systems in the immunodeficient mice: transplantation of peripheral blood mononuclear cells (PBMCs), human-derived hematopoietic stem cells ($CD34^+$ stem cells) and fetal tissues [259].

PBMCs can be isolated from blood of healthy donors and injected into mice either intravenously or via a combination of intravenous and intraperitoneal administrations [260]. The advantage of engrafting PBMCs is the relatively ease of obtaining these cells and engrafting them into the mice. Human $CD34^+$ stem cells can be isolated from cord blood, bone marrow, peripheral blood, and fetal liver. Isolation is usually performed by Ficoll separation, followed by incubation with human CD34 magnetic selection beads [259]. It was shown that there is no statistical difference in reconstitution capacity of $CD34^+$ cells transplanted via the intrafemoral, intrahepatic, or intravenous route in adult mice [261]. However, the intrahepatic route is recommended when using neonatal mice [262], since the liver of neonatal mice is the main hematopoietic organ at birth [263]. The third method using fetal tissues is also called the bone-liver-thymus (BLT) model. In this method, fetal liver and thymus tissue are implanted under

subrenal capsules with co-transplantation of autologous $CD34^+$ cells into the mouse host. The fetal tissues usually engraft well in the mouse liver and develop a functional humanized organoid.

The great advantage of a humanized mouse model is that it provides a platform for studying human immune cells and human cancer in a mouse model. However, there are some limitations that reduce the wide application of this type of mouse model. First, it involves a complex technique which needs sophisticated work experience. Second, it is time consuming to establish the immune system in the mouse host, especially for the $CD34^+$ cell and BLT models. Third, a host developing xenogeneic graft versus host disease (GVHD) could markedly affect the results of the studies. Furthermore, the percentage distribution of T cells, B cells and myeloid cells is different in mice compared to humans. In addition, the established adaptive immune system in the mouse host is naïve and human T cells are 'educated' on the mouse thymus epithelium and exhibit mouse T-cell restrictions [259].

1.4.3 High Fidelity Subrenal Capsule PDX Cancer Models

Due to the high vascularization of the kidney, one of the major advantages of the SRC graft site is its ability to provide an abundant blood supply. Even before xenograft vascularization, the graft is able to receive a consistent supply of nutrients, hormones, growth factors, and oxygen [264-267]. In addition, the SRC site has the ability to accommodate a range of xenograft tissues, of varying sizes and origins [268]. By comparing the take rates of both benign and malignant human prostate tissues in the subcutaneous, orthotopic, and SRC sites of immunodeficient mice, we have found the SRC site to show the highest take rate [269]. This finding has been confirmed by others [270, 271]. Over the past few years, we have established a panel of transplantable patient-derived prostate cancer tissue lines, known as the Living Tumor Laboratory (LTL) series (www.livingtumorlab.com). These PDX cancer models were produced from intact primary and

metastatic clinical specimens implanted at the subrenal capsule of immunodeficient mice (e.g., NOD-SCID, NSG mice) [257, 272-274].

We have demonstrated that subrenal capsule PDX cancer models show the highest fidelity and most accurately recapitulate clinical biological and molecular heterogeneity. These PDX xenografts retain the histopathology, clinical marker expression, genome architecture, and global gene expression of their original parent tumors. Moreover, the aggressiveness of the subsequent tumors is consistent with patient observations; responses to androgen withdrawal also correlate with tumor subtype. As we have demonstrated, prolonged exposure of androgen-sensitive prostatic adenocarcinoma xenografts to castration led to the development of castration-resistant prostate cancer, including the first-in-field model of complete transdifferentiation from adenocarcinoma into lethal neuroendocrine prostate cancer (NEPC) [272-274].

As such, subrenal capsule PDX cancer models have a wide range of potential applications. These models can be used for basic prostate cancer research, since they cover major histopathologic and molecular subtypes of prostate cancer, capturing cancer heterogeneity observed in the clinic. As well, they can be used for studying cancer-stroma interactions to investigate the tumor microenvironment [275]. As recommended by the NCI, and as we have demonstrated, PDX cancer models are powerful tools for translational research, such as efficacy screening of potential and approved anticancer drugs and novel therapeutic approaches. Furthermore, the PDX models may be used for evidence-based personalized cancer therapy [273]. More importantly, the subrenal capsule PDX model provides a unique opportunity and platform for us to fully develop the use of first-generation PDX models.

1.4.4 First-Generation PDX Cancer Models

A first-generation PDX cancer model consists of an immunodeficient mouse carrying a first implantation of fresh patient cancer tissue specimen that will not be further transplanted, thus representing an initial human-to-mouse generation. So far, first-generation PDX models have not been well characterized nor widely applied; while they may harbor great potential value for cancer research, further studies are needed. However, compared to later generation PDX models, first-generation PDX models have an important advantage. They show better retention of tumor microenvironment components of the patient tumor such as human stroma and non-cancerous immune cells that play important roles in the anticancer and pro-cancer activity of the human immune system and are absent in later generation xenografts. This makes first-generation PDX models attractive for limited cancer immunological studies such as screening of compounds for immunomodulatory activity. As well, first-generation PDX models may have value for personalized cancer therapy, allowing therapy to be tailored to the unique properties of each individual patient's cancer [273].

1.5 Aneustat

1.5.1 Herbal Medicine in Cancer Treatment

For many centuries, herbal medicine has been used for cancer treatment. It has been shown that extracts from herbs can have anticancer activity both *in vitro* and *in vivo* [276-278], and can reduce host toxicity when used in combination with chemotherapeutics [279]. The anticancer activity of extracts from herbs can be based on inhibition of the cell cycle [280], induction of apoptosis [281], inhibition of cancer metastasis [282], and modulation of the host immune response [283]. A number of anticancer herbal drugs have been obtained from natural sources in various ways [284]. Among these drugs, vinblastine and vincristine are vinca alkaloids isolated

from the plant Catharantus rosea for a number of types of cancer, such as leukemia, lymphoma and testicular cancer [285-287]. Docetaxel, a semi-synthetic taxane derived from the bark of the European yew tree, Taxus baccata [288], is widely used for treatment of e.g., prostate cancer, breast cancer and non-small cell lung cancer [289].

Ganoderma Lucidum is a herb that has been used in traditional Chinese medicine for over thousands of years to improve health and promote longevity [290]. One of the major functions of Ganoderma Lucidum, is its modulatory effect on the immune system [291]. Extracts of Ganoderma Lucidum have been widely used for cancer treatment and reported to lead to cell cycle arrest [292], inhibition of angiogenesis [293], and immunomodulatory activity favoring host immunity [294, 295].

Salvia Miltiorrhiza has been used for treatment of coronary artery disease and cerebrovascular diseases with minimal side effects for over a thousand years [296]. In addition, extracts of Salvia Miltiorrhiza have been shown to have anti-inflammatory and anticancer activities [297], with potency to sensitize cancer cells to chemo drugs by inhibition of the function of P-glycoprotein (P-gp), an ATP-binding cassette transporter mediating the efflux of drugs out of cancer cells [298].

Scutellaria Barbata, a mint plant with a mildly bitter taste, is commonly used as an anti-inflammatory and antitumor agent [299]. Extractions of Scutellaria Barbata have been shown to have various anticancer activities, such as anti-angiogenic activity by down-regulating VEGF [300], induction of cancer cell apoptosis and inhibition of cell proliferation [301, 302], inhibition of HIF-1α expression [303], antioxidant activity [304], and down-regulation of regulatory T cells in tumor tissue [305]. Bezielle (BZL101), extracts of Scutellaria Barbata, has been shown to be well tolerated by patients [306, 307]. The potential mechanisms of Bezielle include inhibition of

glycolysis [308, 309], inhibition of oxidative phosphorylation [309], and induction of DNA damage [308].

1.5.2 Aneustat

Aneustat (OMN54) is a first-in-class immuno-oncology drug candidate targeting multiple pathways (National Cancer Institute Drug Dictionary), developed by Omnitura Therapeutics Inc., USA. It is a mixture formulated with phytochemicals from three plants, Ganoderma lucidum, Salvia miltiorrhiza, and Scutellaria barbata. Aneustat was designed with biological considerations of the heterogeneous characteristics of cancer cells. Aneustat has been reported to exhibit anticancer, anti-inflammatory, and immunomodulatory activity [310]. Studies have shown that treatment with Aneustat can significantly inhibit growth of DU145 human prostate cancer xenografts and induce apoptosis in chemo-resistant AB79 human small cell lung cancer xenografts in mice. In addition, Aneustat has been reported to be effective in inhibiting multiple targets and pathways involved in tumor growth [310].

As mentioned in the introduction of the Aneustat patent (US 20160143970 A1), a number of therapeutically active chemical components are present in Aneustat, including Ganoderic acid A, Tanshinone IIA, Scutellarein, and Apigenin. Each of these components has been reported to have anticancer activities acting via various mechanisms. Ganoderic acid A has been shown to inhibit cell proliferation of cancers, such as lymphoma [311], meningioma [312], breast cancer [313] and prostate cancer [314]. In addition, Ganoderic acid A has modest inhibitory activity against 5α-reductase, an enzyme that catalyzes the formation of 5α-dihydrotestosterone (DHT) from testosterone [315]. Furthermore, Ganoderic acid A can enhance anticancer immune responses by reducing the number of MDSCs and elevating the number of cytotoxic $CD8^+$ T cells in C57BL/6 mice bearing mouse EL4 lymphoma [311]. Tanshinone IIA has been shown to

induce mitochondria-dependent apoptosis in LNCaP and PC3 prostate cancer cells [316] and inhibit AR and PSA expression in LNCaP cells [317]. Importantly, it was shown that Tanshinone IIA can inhibit the activities of CYP3A4 [318, 319], the key enzyme involved in docetaxel metabolism [320]. Scutellarein has also been shown to induce cancer cell apoptosis by activation of mitochondria-dependent apoptosis [321] and to suppress cancer metastasis by inhibiting the activation of the NF-κB signaling pathway [322]. Apigenin has been reported to reduce prostate cancer cell survival and migration by targeting the PI3K/Akt signaling pathway [323] and to promote cell cycle arrest and apoptosis in pancreatic cancer cells through the p53 pathway [324]. Also, Apigenin can lead to reduction of glucose uptake by downregulating GLUT1 expression in human pancreatic cancer cells [325].

Furthermore, a Phase I Clinical Trial in Canada (NCTId: NCT01555242) has shown Aneustat to be well tolerated by patients, with a recommended dose of 2.5 g orally twice daily. The half-life of Aneustat is approximately 1-2 hours, with no evidence of drug accumulation. Finally, treatment with Aneustat was found to lead to decreased levels of immune suppression markers in patients (e.g., TGF-β), which indicates reduced suppression of the host anticancer immune response [326].

1.6 Objectives and Hypotheses

The current first-line treatment for advanced metastatic prostate cancer is docetaxel-based chemotherapy, which is unfortunately only marginally effective. Prostate cancer has the ability to circumvent therapy, as it is a heterogeneous disease and consists of treatment-resistant subpopulations in addition to treatment-sensitive subpopulations; in addition it has an ability, based on plasticity, to evade therapy by switching from a targeted pathway to a non-targeted one. As such, one potential approach to treat this disease is to simultaneously target multiple

pathways. To this end, Dr. Elledge [327] has proposed 'Orthogonal Cancer Therapies' for elimination of such cancers, i.e. use of combinatorial therapies that are aimed at different targets and do not interfere with each other. However, up to this date, no Phase III clinical trials of combinations of docetaxel with a variety of other anticancer agents have demonstrated improvements in survival of patients with metastatic CRPC. Aneustat is a mixture of compounds with multiple targets [310]. The Aneustat components have been reported to have anticancer activities targeting different mechanisms that cancer cells rely on for growth. Aneustat fulfills the criteria of the ideal 'Orthogonal Cancer Therapies'. As such, it may be prudent to use docetaxel in combination with Aneustat on the off chance that the combination of docetaxel with one of the Aneustat components will have increased anticancer activity.

As such, the main **objectives** of the present project are (i) to determine whether docetaxel-based therapies can be improved by combining docetaxel with Aneustat and (ii) to determine whether Aneustat shows immunomodulatory activities. My working **hypotheses** are whether Aneustat is able to (i) boost the anticancer activity of docetaxel, since preliminary studies have shown that Aneustat exhibits anti-prostate cancer and anti-metastatic activity; and (ii) enhance anticancer activity by boosting the local host immune response, as Aneustat has been reported to exhibit immunomodulatory activity. Accordingly, I have the following **Specific Aims**.

Specific Aim 1: To determine the effects of docetaxel and Aneustat, as single agents and in combination, on prostate cancer growth *in vitro* and *in vivo*.

Specific Aim 2: To determine the effects of docetaxel and Aneustat, as single agents and in combination, on tissue invasion and metastasis of prostate cancer cells *in vivo*, with the aim to elucidate the underlying mechanisms of potential anti-metastatic action of the drugs.

Specific Aim 3: To determine the effect of Aneustat on the host anticancer immune response, by using first generation PDX models to elucidate potential local immunomodulatory mechanisms of Aneustat.

Chapter 2: Enhanced Anticancer Activity of a Combination of Docetaxel and Aneustat in a PDX Prostate Cancer Model

2.1 Introduction

Prostate cancer is the most commonly diagnosed non-cutaneous cancer and one of the leading causes of cancer death for North American men [1]. When the malignancy is confined to the prostate, surgery and radiation therapy can be curative. However, many patients will develop local recurrence of the cancer and its progression to distant metastasis [129]. As prostate cancer growth in general is androgen-dependent, androgen deprivation therapy (ADT) of locally advanced, recurrent or metastatic prostate cancer is usually quite effective in the first few years. However, cancers frequently develop within 18-24 months into a more aggressive, presently incurable, androgen ablation-resistant phenotype, called "castration-resistant prostate cancer" (CRPC) [132]. Emergence of CRPC typically manifests itself by an increase in serum prostate-specific antigen (PSA) levels [328]. It is well established that the regulation of PSA gene expression is mediated by the androgen receptor (AR), and increasing evidence suggests that the AR plays an important role in the development of CRPC [135, 136]. Furthermore, there is an emerging role in the carcinogenesis and progression of prostate cancer for the PI3K/AKT pathway [329, 330], reported to be involved in cell migration, tissue invasion and therapy resistance of various types of cancer [331, 332].

The current standard first-line treatment for highly advanced metastatic prostate cancer consists of systemic docetaxel plus prednisone chemotherapy adopted in 2004 [137]. Docetaxel is a semi-synthetic, second-generation taxane derived from the bark of the European yew tree, Taxus baccata [165]. Its main mode of anticancer action is based on interference with

microtubule dynamics, i.e. inhibition of disassembly of microtubules [333], leading to inhibition of the progression of cells through the cell cycle [334, 335]. Furthermore, docetaxel can induce cancer cell apoptosis by altering the expression and phosphorylation of members of the Bcl-2 family of proteins [170, 336]. However, treatment with docetaxel plus prednisone is not curative, is associated with severe side effects and improves the overall survival of patients only marginally when compared to the previous mitoxantrone plus prednisone standard regimen [174].

New therapeutics have been developed, including Abiraterone acetate, a CYP17 inhibitor [138]; Enzalutamide (formerly known as MDV3100), an AR inhibitor [142]; Cabazitaxel, a novel tubulin-binding taxane [149]; Sipuleucel-T, an autologous cellular immunotherapeutic [154]; and Radium-223, an alpha particle-emitting radiopharmaceutical [337], which have been approved by the US Food and Drug Administration (FDA) for treatment of metastatic CRPC patients [338, 339]. Various agents, demonstrating additive or synergistic effects in preclinical studies, have also been used in combination with docetaxel. Unfortunately, the overall patient survival has so far not been extended compared to that obtained with the docetaxel plus prednisone standard regimen [192-194]. Clearly, development of more effective drugs and novel therapeutic approaches are of critical importance for improving disease management and survival of metastatic prostate cancer patients.

Aneustat (OMN54) is an immuno-oncology drug candidate targeting multiple pathways (National Cancer Institute Drug Dictionary), developed by Omnitura Therapeutics Inc., USA. Recently, it was found that Aneustat was well tolerated by patients in a Phase-I Clinical Trial in Canada (NCTId: NCT01555242) [326]. Furthermore, treatment with Aneustat was reported to markedly inhibit the growth of DU145 xenografts [310]. In the present study it was found that the combination of docetaxel and Aneustat can markedly and synergistically enhance anticancer

activity in a patient-derived, metastatic prostate cancer tissue xenograft model [272]. Gene expression microarray analysis indicated that the combined use of docetaxel and Aneustat led to expanded anticancer activity, in particular to targeting of pathways and cancer hallmarks that was not achieved when the drugs were used as single agents.

2.2 Materials and Methods

2.2.1 Materials

Chemicals, solvents and solutions were obtained from Sigma-Aldrich, Oakville, ON, Canada, unless otherwise indicated. Aneustat was supplied by Omnitura Therapeutics Inc. (Henderson, NV) and docetaxel was purchased from Sanofi-Aventis Canada Inc. (Laval, Quebec, Canada).

2.2.2 Cell Culture

Human C4-2 androgen-independent prostate cancer cells, i.e. metastatic, PTEN-deficient cells derived from the LNCaP cell line (Sobel and Sadar, 2005; Wu et al., 1998), were obtained from the American Type Culture Collection (ATCC; Manassas, VA). They were maintained as monolayer cultures in RPMI-1640 medium (HyClone, GE Healthcare Life Sciences; Mississauga, Ontario, Canada) supplemented with fetal bovine serum (10%), at 37 °C in a humidified incubator with a 5% CO_2 atmosphere.

2.2.3 *In vitro* Drug Efficacy Determination

C4-2 single cell suspensions were seeded into 6-well culture plates (starting concentration ~2.5 × 10^5 cells/well) and incubated at 37 °C in 5% CO_2 for 24h. Docetaxel and Aneustat (dissolved in DMSO + ethanol) were then added to the cultures as single drugs at a range of concentrations for a further 48h incubation to assess the effects of the drugs on cell numbers; DMSO + ethanol was used as a vehicle control. Cell cultures were trypsinized to obtain single cell suspensions and

then counted using a TC20 Automated Cell Counter (Bio-Rad) and cell viability was determined by Trypan blue exclusion. The IC50s of C4-2 cells treated with docetaxel and Aneustat for 48h were estimated using GraphPad Prism 5 (La Jolla, CA). To determine the dosage of docetaxel and Aneustat in the combination, a fixed ratio of docetaxel and Aneustat (approximating $IC50_{docetaxel}/IC50_{Aneustat}$) was applied, as a way to manage the dosage of a combination [340]. Similarly, the IC50 of treatment with the combination for 48h were obtained. Using CalcuSyn software (Biosoft, Cambridge, UK), the combination index (CI) was assessed to determine an additive effect (CI = 1), synergism (CI < 1), or antagonism (CI > 1) for the drug combinations. Synergism is defined as an effect of two drugs that is greater than the sum of the effects of the single drugs, while antagonism is defined as an effect of two drugs that is smaller than the sum of the effects of the single drugs. The dose reduction index (DRI) is a measurement of how many folds the dose of each drug in a synergistic combination may be reduced at a certain effect level, compared to the doses of the individual drugs [341, 342].

2.2.4 Animals

Non-obese diabetic severe combined immunodeficiency (NOD-SCID) mice (males; 6-8 weeks old; body weight, 23-25 g), bred in the BC Cancer Research Centre ARC animal facility, were housed in sterile micro-isolator cages under specific pathogen-free conditions. Food and water were sterilized prior to use. Temperature (20-21°C) and humidity (50-60%) were controlled. Daily light cycles were 12 hours light and 12 hours dark. Cages were completely changed once or twice a week. Animals were handled under sterile conditions. The maximum tolerated dose of Aneustat was determined using conventional methodology. Animal care and experiments were carried out in accordance with the guidelines of the Canadian Council on Animal Care.

2.2.5 Patient-derived Prostate Cancer Xenograft Model and Treatment

The LTL-313H transplantable, PTEN-deficient, metastatic and PSA-secreting, patient-derived prostate cancer tissue line [272] (generation 13) was maintained as grafts under the renal capsules of male NOD-SCID mice supplemented with testosterone as previously described [343]. For experiments, tumors were harvested 10 weeks after grafting and pieces of tumor tissue ($2.5\times2.5\times1.25$ mm^3) were grafted under the renal capsules of testosterone-supplemented male mice (4 groups; 6 mice/group; 4 grafts/mouse). The grafts had a 100% engraftment rate with an average tumor volume doubling time of 13-15 days. Increases in the plasma PSA levels of the mice were used as a measure of tumor growth. After about 6 weeks, when levels of ~13 ng PSA/ml plasma had been reached, i.e. equivalent to tumor volumes of 30-50 mm^3, the mice were randomly distributed into 6 groups and treated with docetaxel (i.p.; Q7d/3) and Aneustat (orally; Q1d×5/3) using the following schedule: (a) vehicle control (Tween 80 in saline solution), (b) docetaxel (5 mg/kg), (c) Aneustat (1652 mg/kg), and (d) docetaxel (5 mg/kg) + Aneustat (1652 mg/kg). After 3 weeks, the mice were euthanized, tumor volumes measured using calipers, and tissue sections prepared for histopathological analysis (see below). Tumor growth of treated animals relative to untreated animals was used as a measure of antitumor activity, i.e. T/C = (treated tumor volume $_{3wks}$ – treated tumor volume $_{0wks}$) : (control tumor volume $_{3wks}$ – control tumor volume $_{0wks}$) × 100%, with T/C>0 indicating tumor growth and T/C<0 indicating tumor shrinkage. Tumor growth inhibition = 100% -T/C.

2.2.6 Immunohistochemical Staining

Preparation of paraffin-embedded tissue sections and immunohistochemical analyses were carried out as previously described [344]. The anti-Cleaved Caspase 3 (Asp175) (5A1E) (#9664, 1:50, rabbit anti-human; Cell Signaling Technology, Danvers, MA) was used for

immunohistochemical staining. All sections used for immunohistochemistry were lightly counterstained with 5% (w/v) Harris hematoxylin. Five fields of each slide were randomly chosen and images taken (×400), using an AxioCam HR CCD mounted on an Axioplan 2 microscope and Axiovision 3.1 software (Carl Zeiss, Canada). Positively stained cells and the total number of cells in each image were counted and the percentage of positive cells was calculated.

2.2.7 Real-Time PCR Analysis

Total RNA was extracted using Trizol reagent (Invitrogen, Carlsbad, CA) according to the manufacturer's instructions. RNA (1 µg) extract was treated with DNase and reverse transcribed with random primers and Im-Prom II Reverse transcriptase (Promega, Madison, WI). The cDNA was subjected to quantitative real-time RT-PCR using specific primers for AR and β-actin. [AR forward: 5'-CCTGGCTTCCGCAACTTACAC, AR reverse: 3'-GGACTTGTGCATGCGGTACTCA, β-actin forward: 5'-CCCAGCCATGTACGTTGCTA, β-actin reverse: 3'-AGGGCATACCCCTCGTAGATG]. It was performed in 25 µl reaction mixtures using SYBR Green IQ supermix (Bio-Rad, Hercules, CA) according to the manufacturer's instructions. Expression levels of AR were normalized to β-actin. The experiment was performed three times in duplicate.

2.2.8 Western Blotting

Whole cell and tissue protein extracts were resolved on SDS–PAGE using procedures previously reported [345, 346]. Proteins were then transferred to nitrocellulose membrane. After blocking for 1 hour at room temperature in 5% milk in PBS/0.1% Tween-20, membranes were incubated overnight at 4°C with the appropriate primary antibodies. Following incubation with secondary antibody, immunoreactive proteins were visualized with an enhanced chemiluminescence

detection system (Amersham Pharmacia Biotech, Buckinghamshire, England). [AR (441) (sc-7305, mouse monoclonal antibody, Santa Cruz Biotechnology, Santa Cruz, CA); p-AKT1/2/3 (ser 473)-R (sc-7985-R, rabbit polyclonal antibody, Santa Cruz Biotechnology, Santa Cruz, CA); AKT (#9272, rabbit polyclonal antibody, Cell Signaling Technology); Bcl-2 (human specific) (#2872, rabbit polyclonal antibody, Cell Signaling Technology); Tubulin (T5168, Monoclonal Anti-α-Tubulin antibody, Sigma-Aldrich, St. Louis, MO)]. Tubulin was used to monitor the amounts of samples applied. The density of the bands was quantified using ImageJ software (National Institutes of Health, Bethesda, MD, USA)

2.2.9 Microarray Analysis to Establish Gene Expression Profiles

Total RNA was extracted from xenograft tissues using a mirVana™ miRNA Isolation Kit (Life Technologies, Burlington, ON, Canada) according to the manufacturer's instructions. The quality of the RNA was assessed with an Agilent 2100 bioanalyzer (Agilent, Santa Clara, CA); batches with an RNA integrity number value $\geqslant$ 8.0 were considered acceptable for microarray analysis. Samples were prepared following Agilent's One-Color Microarray-Based Gene Expression Analysis Low Input Quick Amp Labeling v6.0 (Agilent). An input of 100 ng of total RNA was used to generate cyanine-3-labeled cRNA. Samples were hybridized on Agilent SurePrint G3 Human GE 8x60K Microarray v2 (Design ID 039494). Then, arrays were scanned with the Agilent DNA Microarray Scanner at a 3 μm scan resolution and the data processed with Agilent Feature Extraction 11.0.1.1. Processed green signal was quantile normalized with Agilent GeneSpring 12.0. RNA quality control and microarray analysis were carried out by the Laboratory for Advanced Genome Analysis at the Vancouver Prostate Centre, Vancouver, Canada. All microarray profiling analyses were done in duplicate. The microarray gene

expression data have been deposited in NCBI's Gene Expression Omnibus (GEO, www.ncbi.nlm.nih.gov/geo/) under accession number GSE48667.

2.2.10 Microarray Data Analysis

Microarray probe expression data were filtered for improved quality prior to downstream analysis. Specifically, probes without corresponding gene annotations and probes without detectable expression levels (less than 4 in log2 scale) were removed. Genes of treated tissues were considered differentially expressed relative to corresponding genes in non-treated, control tissues if their probes showed $\geqslant$ 2-fold difference. Pathway enrichment analysis was performed on such differentially expressed genes using Ingenuity Pathway Analysis software (IPA; Ingenuity Systems, Inc., Redwood City, CA). Statistical over-representation of canonical pathways in the drug-response-expression signatures was calculated using the Fischer's Exact Test [347], and pathways with a p-value<0.05 were considered significant. Differentially expressed genes in "docetaxel+Aneustat"-treated tissues, compared to controls, were linked to mechanism-based therapeutic targets, and the linkages of genes and functions were verified in the literature.

2.2.11 Statistics

Statistical analyses of gene expression data were performed as described above. The Student's t-test was carried out to compare means between two groups. One-way ANOVA was used to compare means of more than two groups. Results were considered statistically significant when $p<0.05$ and are expressed as means ± SEM.

2.3 Results

2.3.1 Synergistic Inhibition by Docetaxel+Aneustat of Human C4-2 Prostate Cancer Cell Proliferation

C4-2 prostate cancer cell proliferation was inhibited, in a dose dependent manner, by treatment with docetaxel and Aneustat used as single drugs. Using GraphPad Prism 5 to calculate the IC50s of the drugs used for a 48h period, an IC50 of 8.7 nM was found for docetaxel and an IC50 of 162.4 μg/ml for Aneustat (Fig. 2.1A, B). With a fixed ratio of docetaxel:Aneustat (approximating $IC50_{docetaxel}/IC50_{Aneustat}$), a series of concentrations of docetaxel plus Aneustat was administrated to C4-2 cell cultures for a 48 h incubation (Fig. 2.1C). The IC50 of this combination was docetaxel 5 nM and Aneustat 100 μg/ml (Fig. 2.1C). As calculated via CalcuSyn software, the combination index (CI) of docetaxel+Aneustat at the IC50 is <1 (0.78; Fig. 2.1C), indicating that the combination of the drugs has a synergistic effect. The dose reduction index (DRI) of the combined use of docetaxel and Aneustat at IC50 indicates that the dose of docetaxel may be reduced 2.4 times and the dose of Aneustat may be reduced 2.6 times (Fig. 2.1C), to lower the toxicity of each individual drug while maintaining efficacy of the combination.

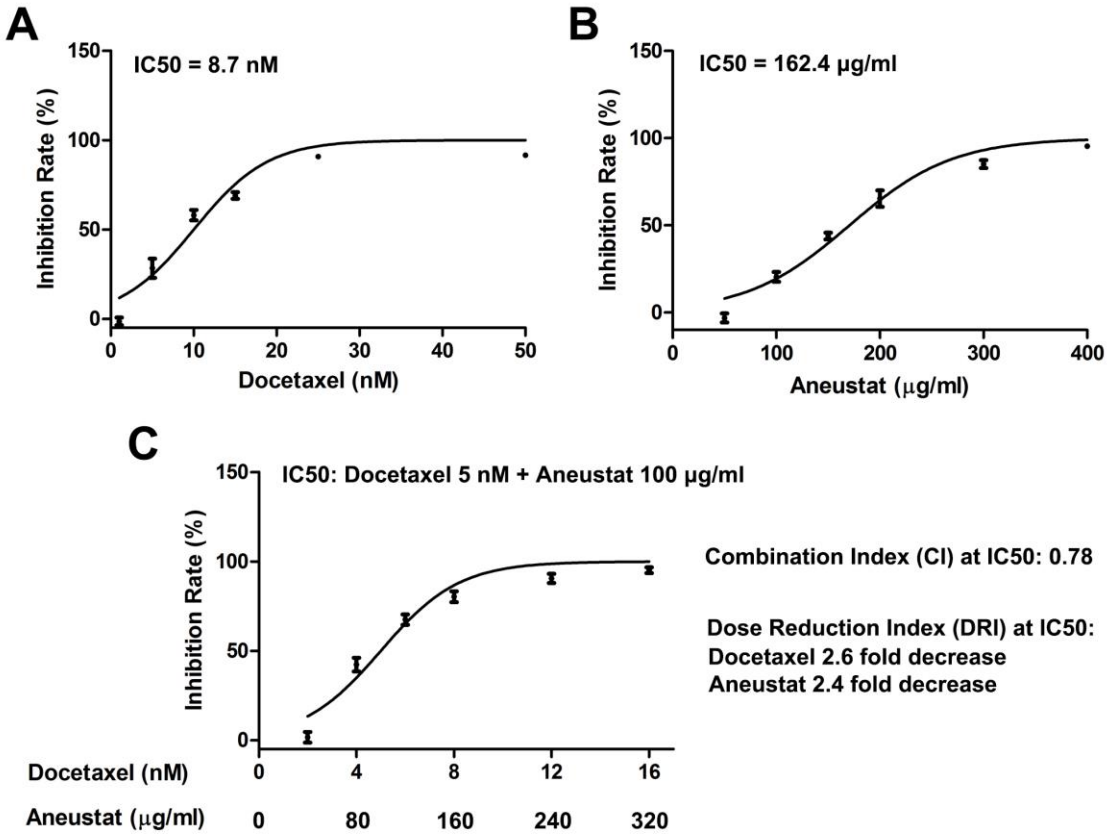

Figure 2.1 The combination of docetaxel and Aneustat synergistically inhibits C4-2 cell proliferation.

Effect of treatment with docetaxel, Aneustat, and the combination of docetaxel and Aneustat, on the growth of C4-2 prostate cancer cell cultures. Cells were cultured for 48h with docetaxel (A), Aneustat (B) and the combination (C) at various concentrations. The IC50 of each treatment was determined using GraphPad Prism 5. The combination index (CI) was determined using CalcuSyn software (CI = 1, additive effect; CI < 1, synergism; CI > 1, antagonism). Percentage growth inhibition is relative to control. The dose reduction index (DRI) of the combined use of docetaxel and Aneustat at IC50 was calculated on the basis of the doses of the individual drugs when used alone at IC50. The experiment was performed in triplicate.

2.3.2 Effect of Docetaxel+Aneustat on Growth of LTL-313H Prostate Cancer Xenografts: Synergistic Growth Inhibition

In preliminary experiments it was found that the maximum tolerated dose of orally administered Aneustat (used in combination with docetaxel) was 1652 mg/kg body weight for NOD-SCID mice at Q1d×5/3.

Groups of NOD-SCID mice bearing LTL-313H xenografts with an average tumor volume of about 32 mm^3 (as indicated by plasma PSA levels) were treated for 3 weeks with docetaxel and Aneustat as single agents and with a combination of the two drugs, using Aneustat (1652 mg/kg body weight) and a sub-therapeutic dosage of docetaxel (5 mg/kg body weight) (Fig. 2.2). The final average tumor volume in the control group was 133 ± 21 mm^3 (mean ± SEM). Treatment of the mice with Aneustat (1652 mg/kg), inhibited tumor growth by 30% (p=0.09), and treatment with docetaxel (5 mg/kg) inhibited tumor growth by 51% (p<0.01). However, Aneustat (1652 mg/kg) significantly increased the growth-inhibitory effect obtained with 5 mg/kg docetaxel to 106% (p<0.001). The combination of docetaxel and Aneustat caused complete growth inhibition coupled to significant tumor volume shrinkage with a T/C value of -6.1% (Fig. 2.2). The data indicate that Aneustat enhanced the anticancer *in vivo* effect of docetaxel in a synergistic fashion. No major change in appearance and behavior of the animals was observed during the experiments, nor significant organ damage at the endpoint, indicating that the treatments were quite well tolerated by the mice bearing LTL-313H xenografts.

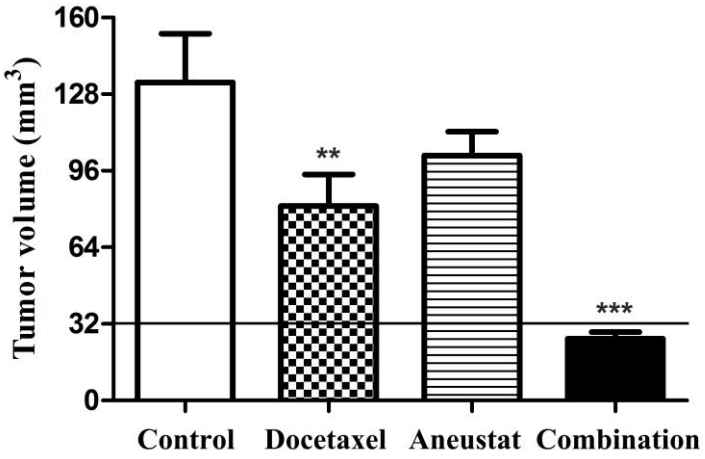

Figure 2.2 Effects of a 3-week treatment with docetaxel, Aneustat, and a combination of the two drugs, on the growth of LTL-313H prostate cancer xenografts.

The average volume of the xenografts at the start of treatment was approximately 32 mm^3 (indicated by the horizontal line). Control (DMSO); docetaxel (5 mg/kg; i.p. Q7d/3); Aneustat (1652 mg/kg; Q1d × 5/3); Combination of docetaxel (5 mg/kg) + Aneustat (1652 mg/kg). Each group of mice contained 24 xenografts. Data are presented as tumor volume (mean ± SEM). ** indicates $p < 0.01$; *** indicates $p < 0.001$.

2.3.3 Treatment with Docetaxel+Aneustat Leads to Increased Apoptosis in LTL-313H Xenografts

Histopathological analysis of H&E-stained tumor tissue sections (Fig. 2.3A-D) showed regular mitotic activity in the control tumors as well as sporadic areas of local necrosis, presumably due to the fast growth of the tumors. The tumors treated with docetaxel or Aneustat as single agents showed elevated numbers of cells arrested in the early phase of mitosis. In contrast, the tumors treated with the combination of docetaxel and Aneustat exhibited the highest amounts of stroma and necrosis areas; few cells could be seen in mitosis.

Caspase 3 expression, used as an indicator of cell apoptotic activity (Fig. 2.3E-H), indicated that docetaxel and Aneustat alone only slightly increased apoptosis; in contrast, the combined use of docetaxel and Aneustat substantially enhanced caspase-dependent apoptosis relative to the control (207%) and to apoptosis induced by docetaxel alone (117%) (Fig. 2.3M; $p<0.001$). Ki67 is widely used as a cell proliferation marker [348]. As shown in Fig. 2.3 I-L and N, combined use of docetaxel and Aneustat led to a dramatically low cell proliferation rate (1.64%). The high apoptotic rate and low proliferation rate induced by the combination of docetaxel and Aneustat contributed to the inhibition of tumor growth.

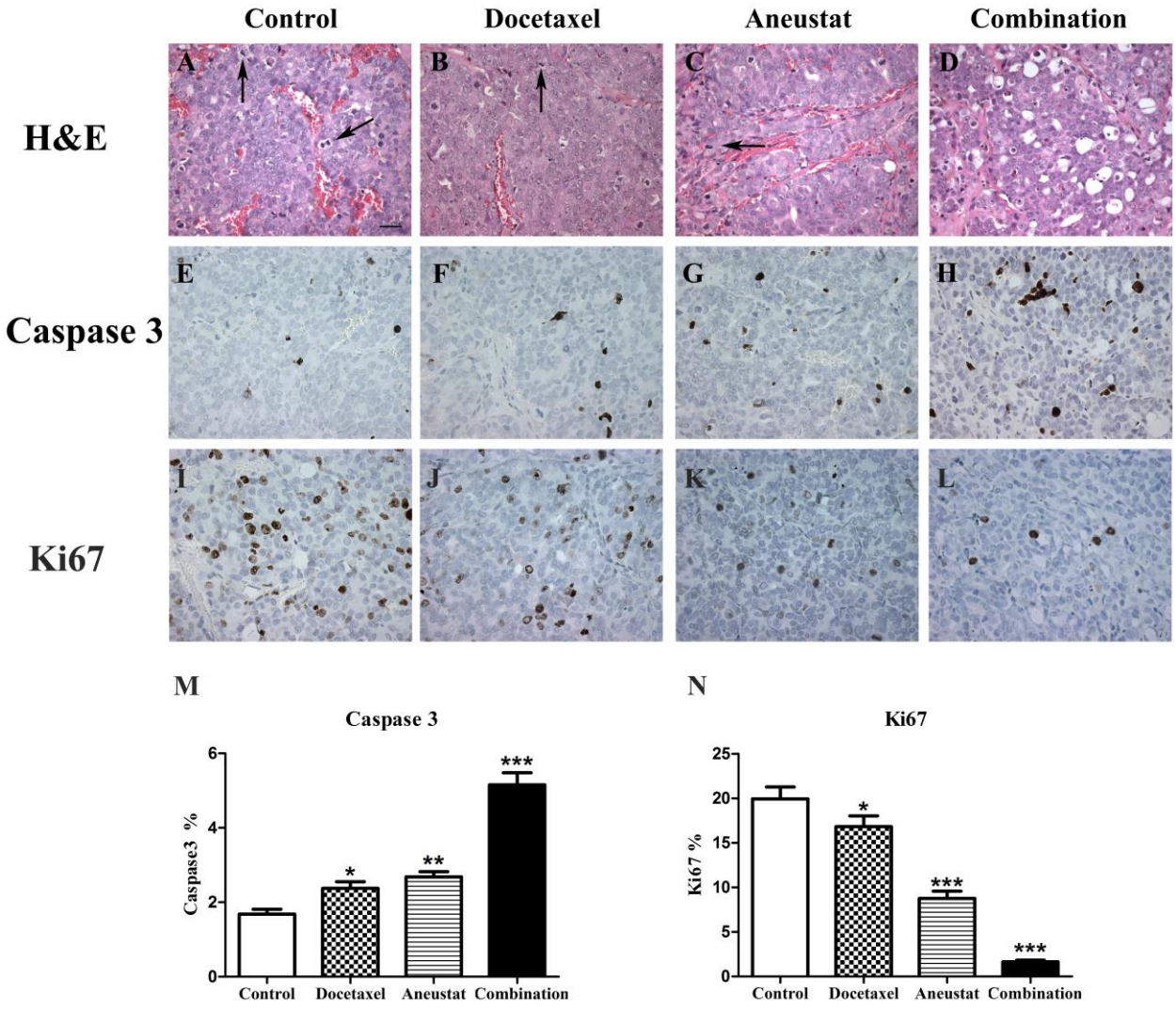

Figure 2.3 Apoptotic and proliferative effects of a 3-week treatment of LTL-313H xenografts with Aneustat and docetaxel used as single agents and in combination.

Apoptosis and proliferation in LTL-313H xenografts, induced by treatment with docetaxel and Aneustat as single drugs and in combination, were revealed by caspase 3 and Ki67 expressions. A-D: tissue sections stained with H&E, black arrows point at mitotic figures; E-H: tissue sections stained for caspase 3; I-L: tissue sections stained for Ki67; magnification ×400. M-N: Relative caspase 3 and Ki67 expressions (means ± SEM). * indicates $p < 0.05$; ** indicates $p < 0.01$; *** indicates $p < 0.001$. Scale bar: 20 μm.

2.3.4 Effects of Aneustat and Docetaxel+Aneustat on AR Expression and AKT Phosphorylation

Since AR and AKT signaling play critical roles in the malignant progression of prostate cancer [349, 350], the effects of docetaxel and Aneustat were investigated on the expressions of AR and AKT. As shown in Fig. 2.4A, AR mRNA expression in C4-2 cells was markedly inhibited by treatment with Aneustat ($\geqslant$100 μg/ml). Densitometric analysis using ImageJ software of Western blot bands (Fig. 2.4B) showed that Aneustat caused decreases of 53, 76 and 86% in the AR expression of C4-2 cells, compared with controls, at dosages of 50, 100 and 200 μg/ml, respectively. Similarly, Aneustat inhibited the phosphorylation of AKT by 63% and 89% at dosages of 100 and 200 μg/ml, respectively, as distinct from the amount of AKT (Fig. 2.4B). A marked effect of Aneustat on expression of Bcl-2, an anti-apoptotic protein that plays a role in the PI3K/AKT pathway, was found only at a concentration of 200 μg/ml, i.e. 85% inhibition (Fig. 2.4B).

As shown by Western blot and densitometric analyses (Fig. 2.4C), treatment of LTL-313H xenografts with Aneustat alone (1652 mg/kg) did not affect AR expression, but slightly down-regulated AKT phosphorylation (23%). Treatment with docetaxel alone (5 mg/kg) down-regulated both AR expression and AKT phosphorylation by 33 and 44%, respectively. However, the combination of docetaxel (5 mg/kg) and Aneustat (1652 mg/kg) markedly inhibited both AR expression (77%) and AKT phosphorylation (69%) (without affecting the amount of AKT), indicative of synergistic action of the two drugs.

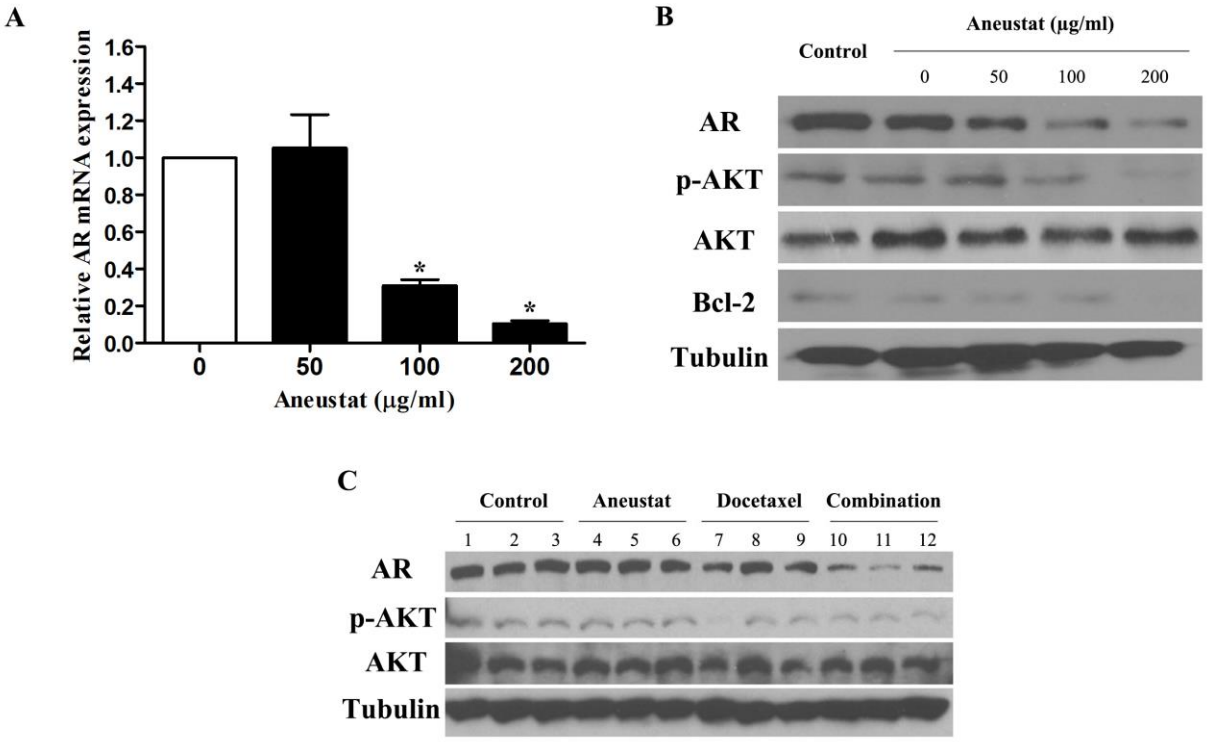

Figure 2.4 Effect of Aneustat and docetaxel on AR expression and AKT phosphorylation.

(A) Effect of a 24h treatment of C4-2 cell cultures with Aneustat on AR mRNA expression (by qPCR) and (B) on AR protein expression, AKT phosphorylation and amount of AKT. (C) Effect of a 3-week treatment of LTL-313H xenografts with Aneustat (1652 mg/kg), docetaxel (5 mg/kg) and a combination of docetaxel (5 mg/kg) and Aneustat (1652 mg/kg) on AR protein expression, AKT phosphorylation and amount of AKT.

2.3.5 Pathways Affected by Docetaxel, Aneustat and Docetaxel+Aneustat as Indicated by DNA Microarray Data Analysis

Gene expression microarray data were obtained from LTL-313H xenografts treated for 3 weeks with docetaxel (5 mg/kg), Aneustat (1652 mg/kg), docetaxel (5 mg/kg) + Aneustat (1652 mg/kg), and from untreated controls. Genes showing significant differential expression ($\geqslant$ 2-fold change) between untreated and treated xenografts were selected for pathway analysis using Ingenuity Pathway Analysis (IPA) software. The results indicate that both single drugs and combined drugs can act through inhibition or stimulation of various canonical pathways (Table 2.1). For example, docetaxel can inhibit cell cycling and promote apoptosis (by boosting p53 signaling), consistent with established observations [351]. Aneustat, used as a single drug, stimulates LXR/RXR activation and serotonin degradation, inhibits cell cycling and promotes apoptosis. Whereas the combination of 'docetaxel+Aneustat' can affect pathways induced by the drugs acting as single agents, such as inhibition of IGF-1 signaling by docetaxel, or stimulation of LXR/RXR activation by Aneustat, the drug combination can also act on pathways not noticeably influenced by the drugs on their own, such as the metabolic pathways of cholesterol biosynthesis, glycolysis I and gluconeogenesis I.

Canonical Pathway	Docetaxel	Aneustat	Combination
Mitotic roles of polo-like Kinase	-	-	↓
Cell cycle control of chromosomal replication	-	-	↓
ATM signaling	-	-	↓
Cholesterol biosynthesis	-	-	↓
Glycolysis I	-	-	↓
Gluconeogenesis I	-	-	↓
Cell Cycle: G1/S checkpoint regulation	↓	↓	↓
Mitochondrial dysfunction	↓	↓	↓
Cyclins and cell cycle regulation	↓	↓	↓
p53 signaling	↑	↑	↑
GADD45 signaling	↑	↑	↑
IGF-1 signaling	↓	-	↓
LXR/RXR activation	-	↑	↑
Serotonin degradation	-	↑	-
ILK signaling	↓	-	-

Table 2.1 Pathways stimulated (↑) or inhibited (↓) in LTL-313H xenografts by treatment with docetaxel (5 mg/kg), Aneustat (1652 mg/kg) and docetaxel + Aneustat as predicted by Ingenuity Pathway Analysis of DNA microarray data.

2.3.6 Treatment of LTL-313H Xenografts with Docetaxel+Aneustat Affects Genes Involved in Cancer Hallmarks

Genes showing significant differences in expression ($\geqslant$ 2-fold changes) in response to treatment of the xenografts with 'docetaxel+Aneustat' (compared to controls) were categorized based on their roles in hallmarks of cancer. Figure 2.5A shows that treatment with the combined drugs affected most major cancer hallmarks. Thus the drug combination down-regulated genes promoting cell proliferation, facilitating tissue invasion and metastasis, inducing angiogenesis and enhancing aerobic glycolysis; it up-regulated genes promoting cell apoptosis. Figure 2.5B shows a down-regulatory effect of the treatment with docetaxel+Aneustat on the expression of key genes involved in aerobic glycolysis, a major hallmark of cancer [352], indicating down-regulation of aerobic glycolysis activity in the treated xenografts. A list of 155 differentially expressed genes is presented in a published report [288].

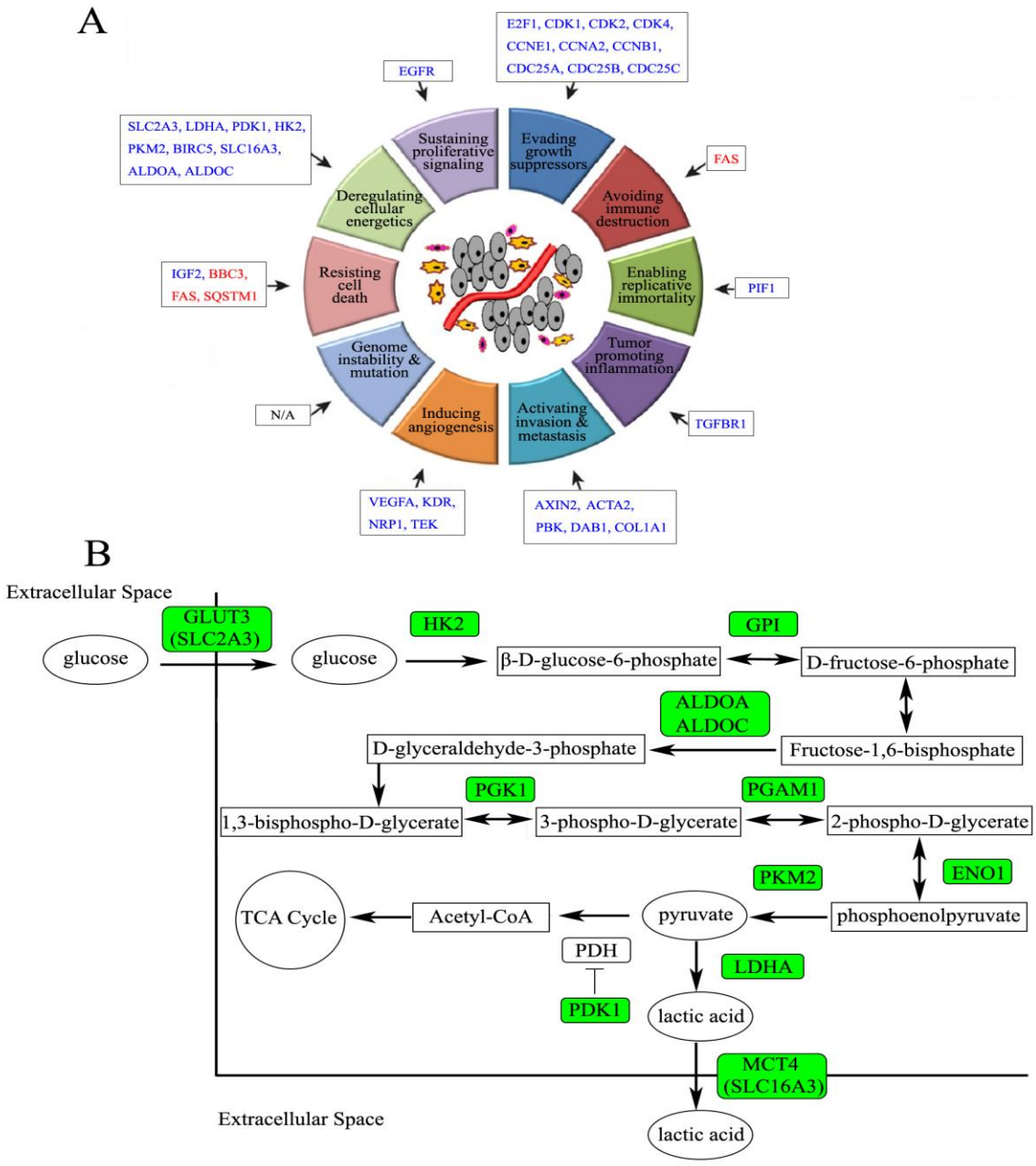

Figure 2.5 Effects of treatment of LTL-313H xenografts with docetaxel+Aneustat on expression of genes involved in cancer hallmarks.

Genes of treated xenografts were categorized based on changes in expression profiles as revealed via DNA microarray analysis. (A) Up-regulated (red) and down-regulated (blue) genes. (B) Down-regulated (green) glycolysis-associated genes.

2.4 Discussion

The present study was aimed at determining, in preclinical studies, whether the anticancer efficacy of docetaxel-based therapy could be enhanced by combining docetaxel with Aneustat (OMN54), a multivalent immuno-oncology drug candidate that successfully passed a Phase-I Clinical Trial (NCTId: NCT01555242). Although docetaxel-based therapy currently represents the best available treatment for highly advanced metastatic prostate cancer, it only marginally extends patients' lives [137, 174]. Consequently, therapy development efforts have focused on improvement of docetaxel's efficacy by combining it with a wide variety of anticancer agents used in clinical and preclinical studies. However, as recently pointed out [192-194], various Phase III clinical trials using docetaxel as a pivot in drug combinations for treatment of metastatic castration-resistant prostate cancer have so far failed to demonstrate an improvement in patient survival, in spite of indications by preclinical studies that the efficacy of docetaxel was enhanced by the drug combinations. Such a discrepancy between drug efficacies predicted by preclinical studies and encountered in the clinic was very common in the past decades. Thus only ~5% of anticancer drug candidates, which successfully passed required preclinical *in vivo* efficacy screening tests, had significant effectiveness in clinical trials and were approved for clinical usage by the FDA [238, 239]. It has become apparent that preclinical assessment of clinical efficacy of anticancer drugs is seriously hampered by the lack of clinically relevant, experimental *in vivo* cancer models. Subcutaneous cancer cell line xenograft models, commonly used for preclinical *in vivo* drug efficacy tests, do not adequately predict the efficacy of anticancer agents in the clinic [239, 353-355]. Consequently, in early 2016, the NCI decided to replace its NCI-60 Human Tumor Cell Lines Screen, a panel of 60 human cancer cell lines, with patient-derived xenografts (PDX) cancer tissue models for preclinical anticancer drug screening

[240]. To assess the effect of combining docetaxel with Aneustat, I therefore did not only make use of C4-2 cell cultures, but especially of NOD-SCID mice carrying xenografts of a transplantable LTL-313H prostate cancer tissue xenograft line. This metastatic, PTEN-deficient, PSA-secreting line was developed from a patient's primary prostatic adenocarcinoma [343], using subrenal capsule grafting technology that tends to preserve important properties of the original cancers, including histopathology, chromosomal aberrations, gene expression profiles and 3-dimensional architecture of the malignancy [269, 272, 344, 356, 357], thus rendering high clinical relevance to this prostate cancer model. The application of this model in the present study therefore increases the likelihood that the obtained results are clinically useful.

In contrast to the marked inhibitory effect of Aneustat alone on the replication of C4-2 cells *in vitro* (Fig. 2.1), treatment of LTL-313H xenografts with Aneustat alone during a 3-week period (Q1d×5/3) did not have a statistically significant growth-inhibitory effect (Fig. 2.2). However, the combination of Aneustat with docetaxel (used at 5 mg/kg body weight, a sub-therapeutic dosage), markedly increased the inhibition of the growth of the xenografts compared to the growth inhibition obtained with docetaxel alone (Fig. 2.2). The synergistic enhancement of anticancer activity by the combined use of docetaxel and Aneustat, a signature observed in C4-2 cells with CI < 1 (Fig. 2.1), is particularly evident from the complete inhibition of the growth of the LTL-313H xenografts and in particular from their shrinkage (T/C=-6.1%) (Fig. 2.2). Furthermore, the tumor shrinkage was associated with an increase in apoptotic activity and a decrease in cell proliferation (Fig. 2.3 M and N). In addition, the dose reduction index (DRI) of this combination at IC50 indicated that a more than 2 fold decrease of the dose of each individual drug (Fig. 2.1) would lead to reduction of toxicity in the combination treatment without loss of efficacy. Moreover, the combination of docetaxel and Aneustat was well tolerated by the

animals. Taken together, the data indicate that docetaxel-based treatment of advanced prostate cancer may be improved by using docetaxel in combination with Aneustat.

The mechanism by which the combination of docetaxel and Aneustat enhances the anticancer activity *in vivo* should be of major interest for potential improvement of docetaxel-based therapy of advanced prostate cancer. Its elucidation requires an understanding of the molecular actions of both drugs, in particular when they are used in combination. Docetaxel is well known for its inhibition of microtubule disassembly to cause growth arrest and induction of apoptosis [170, 333, 336], as also observed in the present study using LTL-313H prostate cancer xenografts (Figs 2.2, 2.3). These mechanisms of docetaxel action are confirmed in the gene expression profiling analysis of the docetaxel-treated xenografts (Table 2.1), indicating that the reductive effects of docetaxel on the xenografts are based on inhibition of cyclins and cell cycle regulation and also on stimulation of p53 signaling, a process that leads to apoptosis [358]. Furthermore, it has been reported that docetaxel can down-regulate AR expression in prostate cancer [171], an observation which was confirmed in the present study (Fig. 2.4C).

First in field, the present study indicates that Aneustat can induce apoptosis (Fig. 2.3), as well as inhibit AR expression, AKT phosphorylation and Bcl-2 expression (Fig. 2.4), processes that play important roles in the malignant progression of prostate cancer and its chemo-resistance [359-361]. The gene expression profiling of Aneustat-treated xenografts (Table 2.1) suggests stimulation of LXR/RXR activation as an action of Aneustat. This suggestion is supported by the finding that Aneustat led to reduction of AKT phosphorylation of C4-2 prostate cancer cells (Fig. 2B), as LXR activation has been reported to down-regulate phosphorylation of AKT in prostate cancer cells [362]. The gene expression analysis also suggests stimulation of serotonin degradation as another action of Aneustat (Table 2.1). Studies have shown that the proliferation

of prostate cancer cells can be interrupted by inhibiting the synthesis and metabolism of serotonin, a neurotransmitter that plays a role as a growth factor for prostate cancer cells [363, 364]. Additional experimental verification will be needed to establish these mechanistic properties of Aneustat. The pathway exploration may lead to expanded use of Aneustat in clinic.

Notably, treatment of the prostate cancer xenografts with the 'docetaxel+Aneustat' combination led to inhibition of critical cancer pathways that were not obviously affected by the individual drugs, such as cholesterol biosynthesis, glycolysis I and gluconeogenesis I (Table 2.1). Cholesterol has an emerging role in prostate cancer as a potential therapeutic target, as intracellular cholesterol has recently been found to promote prostate cancer progression through regulation of AKT signaling and as a substrate for *de novo* androgen synthesis [365, 366]. The inhibitions of glycolysis I and gluconeogenesis I are of special interest, since these two pathways have important roles in "reprogrammed energy metabolism", a key hallmark of cancer [77, 367]. Gene expression microarray profiling of the xenografts confirmed that the majority of the genes involved in the glycolysis pathway were indeed down-regulated by the treatment with docetaxel+Aneustat (Fig. 2.5B). Taken together, the data suggest that the increased anti-tumor activity of the combination of docetaxel and Aneustat is based on an expansion of anticancer activity, targeting multiple pathways and hallmarks of cancer, not attainable with the individual drugs. In addition, combined use of docetaxel and Aneustat will also act on the canonical pathways affected by the individual drugs, such as stimulation of p53 signaling leading to apoptosis, which is consistent with the results using caspase 3 staining (Fig. 2.3 H and M).

The effect of docetaxel+Aneustat on glycolysis is of major interest. Although in the present study the glycolysis pathway is not significantly affected by Aneustat alone as indicated by IPA analysis (Table 2.1), genes involved in the aerobic glycolysis pathway showed a trend to

be down-regulated by treatment with Aneustat. As recently reviewed by our laboratory [227], there is increasing evidence that cancer cells can suppress the host anticancer immune response by creating a relatively low pH (6.0-6.5) in their microenvironment via increased lactic acid secretion. The cancers are thought to achieve this via preferential use of aerobic glycolysis. Treatment targeting aerobic glycolysis could reduce cancer-generated lactic acid production/secretion and hence favor the host anticancer immune response. Since the combination of docetaxel and Aneustat showed more significant inhibition of glycolysis than Aneustat or docetaxel alone, it appears that treatment with docetaxel+Aneustat may not only affect cancers by direct drug-cancer cell interactions, but also indirectly, through promoting the local anticancer immune response in immunocompetent hosts.

It is generally accepted that cancers have an ability to circumvent therapy by switching from a targeted pathway to a different one [77]. The combination of docetaxel+Aneustat may also interfere with this process by targeting multiple aspects of cancer (Fig. 2.5, Table 2.1) and hence reduce the probability for the disease to evade a particular therapeutic approach by switching to other pathways.

AR and AKT signaling are important processes underlying prostate cancer growth [361]. Inhibition of both AR expression and AKT signaling is apparently required to obtain near-complete regression of PTEN-deficient prostate cancers [368, 369]. The LTL-313H prostate cancer tissue xenograft line used in this study is deficient in *PTEN* [370] and the finding that treatment of the xenografts with docetaxel+Aneustat, as distinct from the single agents, led to complete inhibition of tumor growth coupled to tumor shrinkage, is consistent with inhibition of both AR expression and AKT phosphorylation in xenografts obtained only in the case of the combined drug treatment (Fig. 2.4C).

In conclusion, the present study has shown, for the first time, that combined use of docetaxel and Aneustat in a PDX advanced prostate cancer model, i.e. LTL-313H, can lead to anticancer activity exceeding the sum of the anticancer activities of the individual drugs. This enhanced efficacy appears to be based on expanded anticancer activity, targeting multiple pathways and hallmarks of cancer. Since the LTL-313H prostate cancer model is considered clinically highly relevant, treatment with Aneustat+docetaxel may likely lead to improved clinical management of advanced prostate cancer.

Chapter 3: Inhibition of Metastasis by Docetaxel+Aneustat in a PDX Metastatic Prostate Cancer Model

3.1 Introduction

Prostate cancer is the most common, non-cutaneous malignancy in North American men and a major cause of cancer deaths [371]. At the time of prostate cancer diagnosis, the 5-year survival rate of patients with localized disease is almost 100%; in contrast, the 5-year survival rate of patients with metastatic disease is much lower, about 28% [4]. Metastasis is the most lethal attribute of cancer [75, 76] and is based on complex, successive biological steps of primary cancer cells, i.e. local tissue invasion, intravasation, survival in the circulation, extravasation and metastatic colonization, all essential steps in the metastatic process [89].

Metastatic prostate cancer is an incurable disease. For its treatment there are only a few drugs available with only limited efficacy. Docetaxel-based chemotherapy was approved in 2004 as a first line treatment for metastatic, castration-resistant prostate cancer, even though it only marginally improved patient survival [137, 174]. In the case of metastatic, but androgen-sensitive prostate cancer, Phase-III clinical trials demonstrated that treatment with docetaxel-based chemotherapy plus androgen deprivation therapy (ADT) could improve patient survival compared to use of ADT alone [168, 169]. However, the toxicity of this new regimen was of major concern [169, 372]. So far, a small number of pharmaceuticals have gone through Phase III clinical trials for treatment of metastatic prostate cancer. Zoledronic acid was shown to reduce skeletal-related events (e.g., pathologic bone fracture), but failed to prevent the development of metastasis [158]. Denosumab was found to increase bone metastasis-free time by 4.2 months but, unfortunately, did not improve patient overall survival [161]. Therapy using Radium-223 was

shown to benefit metastatic prostate cancer patients by reducing the number of skeletal-related events and increasing overall survival time [4]; however, its low cell permeability restricts its use for treating large volumes of soft tissue and visceral cancer [337]. In spite of these new developments there is at present no effective treatment for advanced prostate cancer. Consequently, there is an urgent need for new, more effective therapeutic approaches especially aimed at reducing/eliminating metastasis.

Aneustat is a multivalent immuno-oncology drug candidate, a mixture formulated with phytochemicals from three plants: Ganoderma lucidum, Salvia miltiorrhiza and Scutellaria barbata [326], developed by Omnitura Therapeutics Inc., USA. Recently, Aneustat was shown to be well tolerated by patients in a Phase-I Clinical Trial in Canada (NCTId: NCT01555242) [326]. As patient-derived xenograft (PDX) cancer models have recently been strongly promoted by the NCI for anticancer drug screening [240], the LTL-313H PDX metastatic prostate cancer model, a highly clinically relevant model [272] (www.livingtumorlab.com), was used to investigate Aneustat for anti-prostate cancer activity (as described in Chapter 2). It was found that a combination of Aneustat and docetaxel can lead to markedly higher cancer growth-inhibitory activity, without inducing major host toxicity [288]. Further analysis indicated that the combination of docetaxel and Aneustat could target multiple pathways and hallmarks of cancer that were not affected by the individual drugs [288].

In the present study, the LTL-313H subrenal capsule xenograft model was used to investigate the effects of docetaxel+Aneustat on prostate cancer metastasis and underlying molecular processes. It was found that treatment with docetaxel+Aneustat significantly inhibited lung micro-metastasis, kidney tissue invasion and, in particular, suppressed the expression of *FOXM1*, a gene generally considered to be a major promoter of cancer metastasis [121].

Furthermore, a novel use of the PDX model has been developed for an adjacent (kidney) tissue invasion assay.

3.2 Materials and Methods

3.2.1 Materials

Chemicals, solvents and solutions were purchased from Sigma-Aldrich, Oakville, ON, Canada, unless otherwise indicated. Aneustat was supplied by Omnitura Therapeutics Inc. (Henderson, NV); and docetaxel was purchased from Sanofi-Aventis Canada Inc. (Laval, Quebec, Canada).

3.2.2 Cell Culture

Human C4-2 metastatic, androgen-independent prostate cancer cells were obtained from the American Type Culture Collection (ATCC; Manassas, VA). They were maintained as monolayer cultures in RPMI-1640 medium (HyClone, GE Healthcare Life Sciences; Mississauga, Ontario, Canada) supplemented with fetal bovine serum (10%) at 37 °C in a humidified incubator with a 5% CO_2 atmosphere.

3.2.3 Wound-healing Assay

A wound-healing assay was performed following procedures previously reported [373]. Replicate C4-2 cell cultures were incubated for 48 h with vehicle control, docetaxel (5 nM), Aneustat (100 μg/ml) or a combination of docetaxel (5 nM) and Aneustat (100 μg/ml). After this treatment, each culture was trypsinized into a single cell suspension. Cells from each group were seeded into 12-well culture plates (~7.5×10^5 cells/well) and incubated at 37 °C in a 5% CO_2 atmosphere. Following cell attachment, the medium was replaced with serum-free medium. The next day, a "wound" was created with a pipette tip in the middle of a confluent cell monolayer. Cell debris was removed by washing with l×PBS (2-3 times) and images were taken at various

time points using a Zeiss AxioObserver.Z1 microscope (Carl Zeiss). The cell migration area was analyzed using ImageJ (National Institutes of Health, Bethesda, MD). The percentages of migration areas at various time points were normalized to time 0.

3.2.4 Histopathology and Immunohistochemistry

Preparation of paraffin-embedded tissue sections and immunohistochemical analyses were carried out as previously described [344]. For histopathology, routine hematoxylin and eosin (H&E) staining was used. The anti-human mitochondria antibody (MAB1273, Millipore) was used for identification of tissues of human origin. All sections used for immunohistochemistry were lightly counterstained with 5% (w/v) Harris hematoxylin (Leica Biosystems Inc.; Concord, Ontario, Canada).

3.2.5 Mouse Lung Micro-metastasis and Kidney Tissue Invasion in the LTL-313H Xenograft Model

As previously described [288], NOD-SCID mice carrying LTL-313H xenografts were treated for 3 weeks with vehicle control, docetaxel (5 mg/kg), Aneustat (1652 mg/kg), or the combination of docetaxel (5 mg/kg) and Aneustat (1652 mg/kg). Anti-human mitochondria antibody was used to identify human prostate cancer cells in mouse lung tissues. Groups of positively stained cells, with cell numbers >4, were considered lung micro-metastases. Five fields of each slide were randomly chosen and images taken (×400), using an AxioCam HR CCD mounted on an Axioplan 2 microscope and Axiovision 3.1 software (Carl Zeiss). The numbers of mouse lung micro-metastases were counted in each group and analyzed. As shown in Figure 3.1, host (mouse) kidney tissue invasion analysis was carried out as follows: i) images were taken using low power magnification; ii) normal mouse kidney tissue areas were identified within tissue sections under high power magnification (see arrows in Fig. 1) and a curve connecting the areas

was drawn to mark the original mouse kidney boundary; iii) any xenograft tissue observed beyond the curve was considered invading tumor tissue, and the proportion of invasive area was analyzed. Host toxicity was estimated as described in Chapter 2.

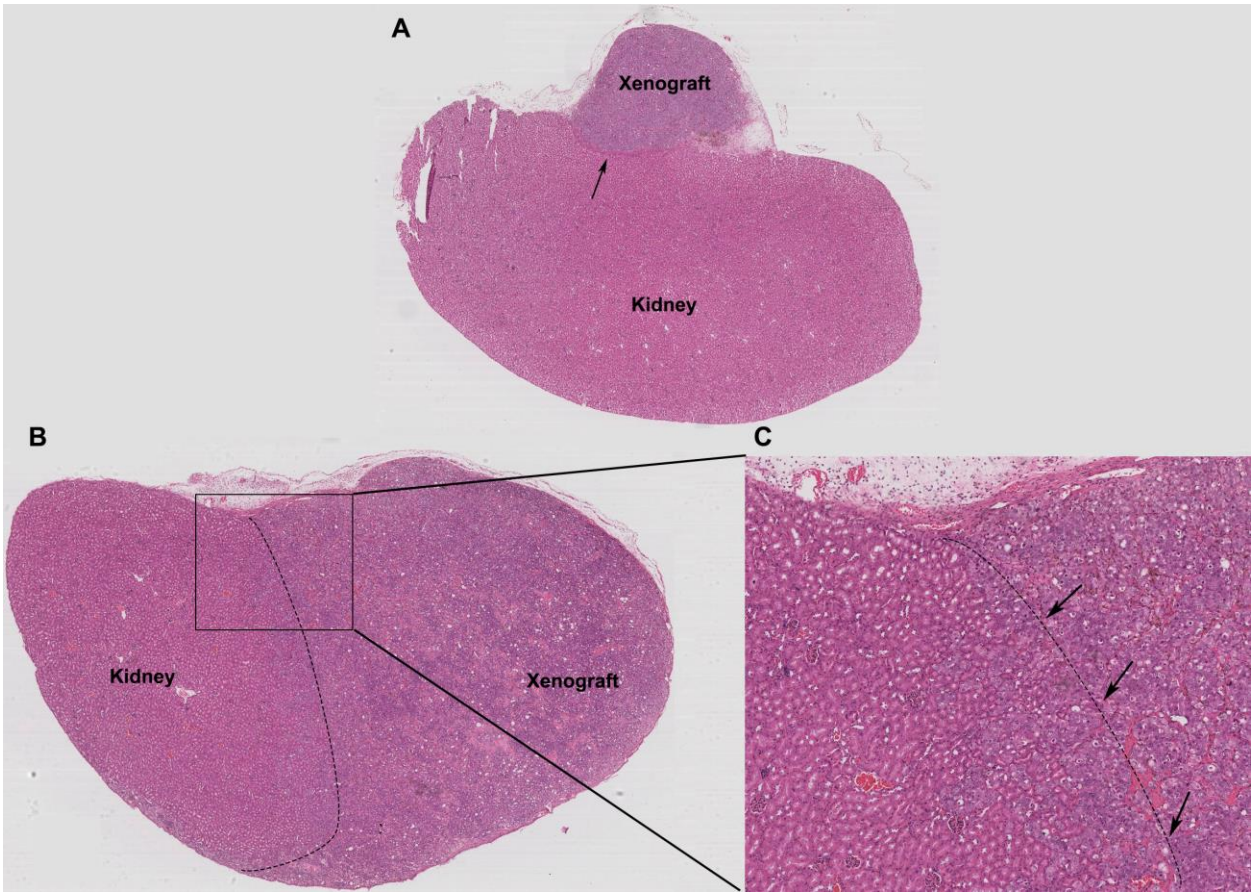

Figure 3.1 Section of host kidney engrafted with LTL-313H prostate cancer tissue.

Boundaries between kidney and xenograft: (A) Clear boundary as indicated by arrows. (B) Fuzzy boundary indicated by the curve between kidney tissue (left) and xenograft tissue (right); (C) Magnified section, arrows indicate kidney residue areas.

3.2.6 Microarray Data Analysis

Gene expression microarray data obtained in the previous study with LTL-313H prostate cancer xenografts [288] were used. 1757 genes were found which showed ≥2-fold changes in expression in response to treatment of the xenografts with docetaxel+Aneustat (compared to controls), i.e. 919 up-regulated genes and 838 down-regulated genes. To compare the gene expression profiles obtained from docetaxel+Aneustat-treated LTL-313H xenografts with those from clinical patients, up-regulated genes and down-regulated genes were uploaded onto the Oncomine database [374]. To investigate the molecular action of docetaxel+Aneustat, the 1757 genes with ≥2-fold expression changes were uploaded onto the Ingenuity Pathway Analysis (IPA) program, and upstream regulator analysis was used to identify potential cancer driver genes for this dataset [375].

3.2.7 Quantitative Real-Time PCR

Total RNA was extracted using the RNeasy Mini Kit (Qiagen Inc.) and cDNA was synthesized using the QuantiTect Reverse Transcription Kit (Qiagen Inc.) according to the manufacturer's instructions. Primers used were described in Table 3.1. qRT-PCR reactions using KAPA SYBR FAST Universal (Kapa Biosystems) were performed in triplicate in a ViiA 7 Real-Time PCR System (Applied Biosystems). Expression levels of genes were normalized to that of *GAPDH*.

Gene Name (Human)	Sequences (5’ to 3’)
FOXM1 F	GGAGGAAATGCCACACTTAGCG
FOXM1 R	TAGGACTTCTTGGGTCTTGGGGTG
AURKB F	AAGATTGCTGACTTCGGCTGGTCT
AURKB R	ATGCACCACAGATCCACCTTCTCA
CCNB1 F	GCAGCAGGAGCTTTTTGCTT
CCNB1 R	TACACCTTTGCCACAGCCTT
CDC25C F	ATGACAATGGAAACTTGGTGGAC
CDC25C R	GGAGCGATATAGGCCACTTCTG
CENPA F	ACGCCTATCTCCTCACCTT
CENPA R	TGGCTGAGCAGGAAAGAC
CENPE F	GATTCTGCCATACAAGGCTACAA
CENPE R	TGCCCTGGGTATAACTCCCAA
CENPF F	CGAAGAACAACCATGGCAACTCG
CENPF R	TTCTCGGAGGATGGTGCCTGAAT
PLK1 F	CACAGTGTCAATGCCTCCAA
PLK1 R	TTGCTGACCCAGAAGATGG
PTTG1 F	ACCCGTGTGGTTGCTAAGG
PTTG1 R	ACGTGGTGTTGAAACTTGAGAT

Table 3.1 qPCR primers used

Gene Name (Human)	Sequences (5’ to 3’)
STMN1 F	TCAGCCCTCGGTCAAAAGAAT
STMN1 R	TTCTCGTGCTCTCGTTTCTCA
GAPDH F	CACCAGGGCTGCTTTTAACTC
GAPDH R	GACAAGCTTCCCGTTCTCAG

Table 3.1 qPCR primers used (continued)

3.2.8 Western Blotting

Whole cell and tissue protein extracts were resolved on SDS-PAGE using procedures previously reported [288]. Proteins were then transferred to PVDF membranes. After blocking membranes for 1h at room temperature in 5% milk in TBS/0.1% Tween-20, they were incubated overnight at 4 °C with appropriate primary antibodies. Following incubation with the secondary antibody, immunoreactive proteins were visualized with a SuperSignal™ West Femto Maximum Sensitivity Substrate (Thermo Scientific). We used the following antibodies: anti-FOXM1 (#5436, rabbit monoclonal antibody, Cell Signaling Technology) and anti-actin (A2066, rabbit polyclonal antibody, Sigma). Actin was used as a loading control.

3.2.9 Overexpression of FOXM1 in C4-2 Prostate Cancer Cells

Since the isoform of FOXM1a is considered transcriptionally inactive [376, 377], lentiviruses expressing FOXM1b and FOXM1c were produced by transfecting the respective plasmids in 293T cells as described in a previous study [378]. Briefly, the pSin-FOXM1b and pSin-FOXM1c expression vectors were constructed by a PCR approach with templates of pCW57.1-FOXM1b and pCW57.1-FOXM1c [379] purchased from Addgene (Cambridge, MA), respectively. pSin-mCherry was used as a control. C4-2 cultures were infected with the viruses; puromycin in medium (1 μg/ml) was applied for a 96 h incubation to obtain infected cell populations for treatment with drugs and subsequent analysis.

3.2.10 Boyden Chamber Cell Migration Assay

C4-2 cells infected with lentiviruses (pSin-mCherry, pSin-FOXM1b and pSin-FOXM1c) were treated for 48 h with the combination of docetaxel (5 nM) and Aneustat (100 μg/ml) or vehicle control. Live cells (~1×10^5) from each group were then seeded into the Boyden Chamber insert (24-well plate; BD Bioscience). After an 18 h incubation at 37 °C in a 5% CO_2 incubator, cells

were fixed with 4% paraformaldehyde. Non-migrated cells on the upper surface of the membranes were removed and migrated cells on the lower surface of the membranes were stained with 0.1% crystal violet. Using a microscope, five pictures of each chamber were taken, and migrated cells were counted via Image J software.

3.2.11 Statistics

Statistical analyses of gene expression data were performed as described above. The Student's t-test was carried out to compare means between two groups. One-way ANOVA was used to compare means of more than two groups. Results were considered statistically significant when $p<0.05$ and are expressed as means ± SEM.

3.3 Results

3.3.1 Inhibition by Docetaxel+Aneustat of C4-2 Cell Migration *in vitro*

Replicate C4-2 prostate cancer cell cultures were incubated for 48 h with docetaxel (5 nM) and Aneustat (100 μg/ml) as single agents and with the combination of the drugs. Using the wound-healing assay, the migration areas of the C4-2 cells at various time points (0, 6, 12, 24, 36 and 48 h) were measured, and normalized to the wound area at time 0. As shown in Figure 3.2, the C4-2 cell motility in the wound-healing assay was significantly reduced ($p < 0.05$) (starting at 12 h) by treatment of the cells with docetaxel+Aneustat as distinct from the single agents.

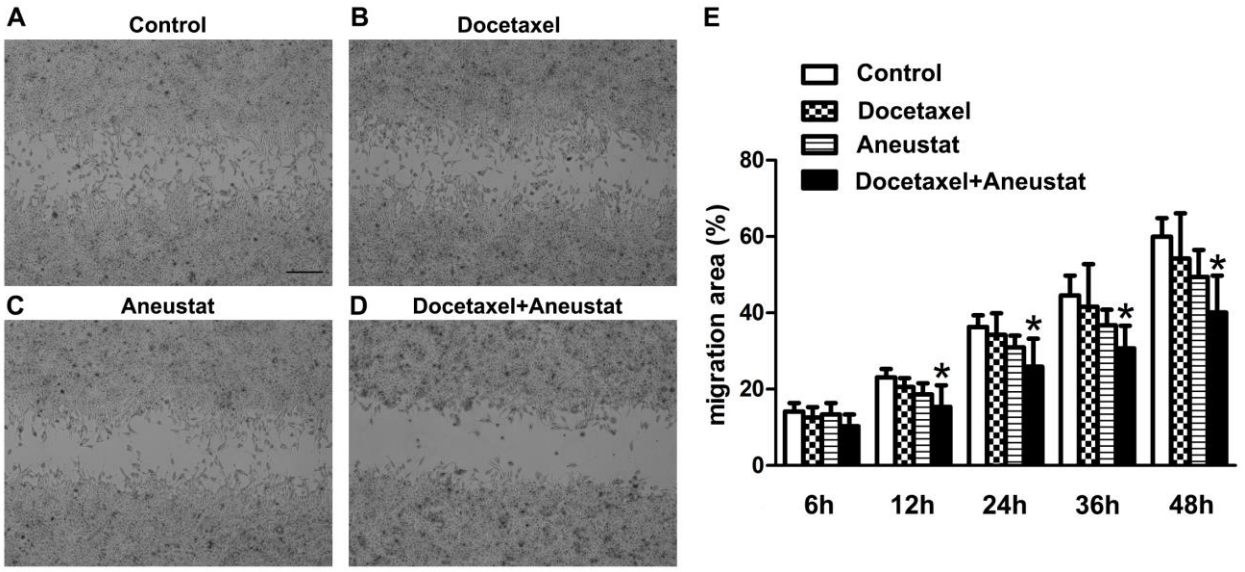

Figure 3.2 Effect of docetaxel+Aneustat on C4-2 cell migration.

C4-2 cells were incubated for 48h with docetaxel, Aneustat or the combination of docetaxel and Aneustat. The wound-healing assay was performed to determine the effect of treatment on cell migration. The images of cell migration into the wound area after a 48h incubation are shown as (A) control, (B) docetaxel, (C) Aneustat, and (D) the combination of docetaxel and Aneustat. (E) The percentage of cell-migrated wound areas is shown in the bar graph. The experiment was performed in triplicate. Asterisks indicate $p < 0.05$ relative to control. Scale bar: 100 μm.

3.3.2 Lung Micro-metastasis and Kidney Tissue Invasion by LTL-313H Prostate Cancer Cells Inhibited by Docetaxel+Aneustat

In a previous experiment, it was shown that a 3-week treatment of LTL-313H prostate cancer xenografts with a combination of docetaxel (5 mg/kg) and Aneustat (1652 mg/kg) synergistically and markedly inhibited the growth of the tumors, without development of major host toxicity [288]. It has repeatedly been demonstrated that cells of LTL-313H subrenal capsule xenografts can invade the mouse host kidney tissue and metastasize to the lungs [272, 343]. Metastasizing LTL-313H cells can be identified by positive staining for human mitochondria (via IHC using specific anti-human mitochondria antibody). In the present study it was found that, as shown in Figure 3.3, treatment with docetaxel, as distinct from Aneustat, markedly reduced the number of lung micro-metastasis (compared to controls). Furthermore, the combination of docetaxel and Aneustat led to a much higher reduction in lung micro-metastases relative to the control ($p < 0.001$). As well, it was found that treatment with docetaxel+Aneustat, in contrast to docetaxel or Aneustat alone, markedly inhibited the invasion of kidney tissue by the grafted cells (Fig. 3.4), as measured by invasion of the mouse kidney tissue (Fig. 3.1).

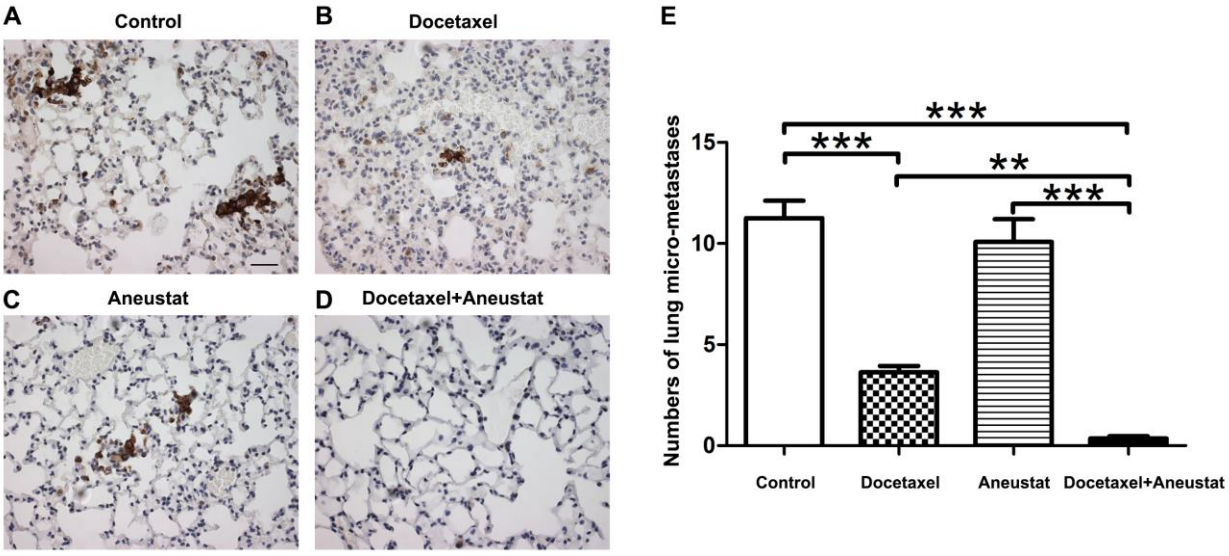

Figure 3.3 Effects of docetaxel, Aneustat and docetaxel+Aneustat on lung micro-metastases in representative sections of lung tissue from mice bearing LTL-313H tumors.

The effect of docetaxel, Aneustat and docetaxel+Aneustat on the number of mouse micro-metastases as identified by positive staining via specific, anti-human mitochondria antibody: (A) control, (B) docetaxel, (C) Aneustat and (D) the combination. (E) Numbers of mouse lung micro-metastases per 10 high power field, means ± SEM. ** indicates $p < 0.01$; *** indicates $p < 0.001$. Scale bar: 20 μm.

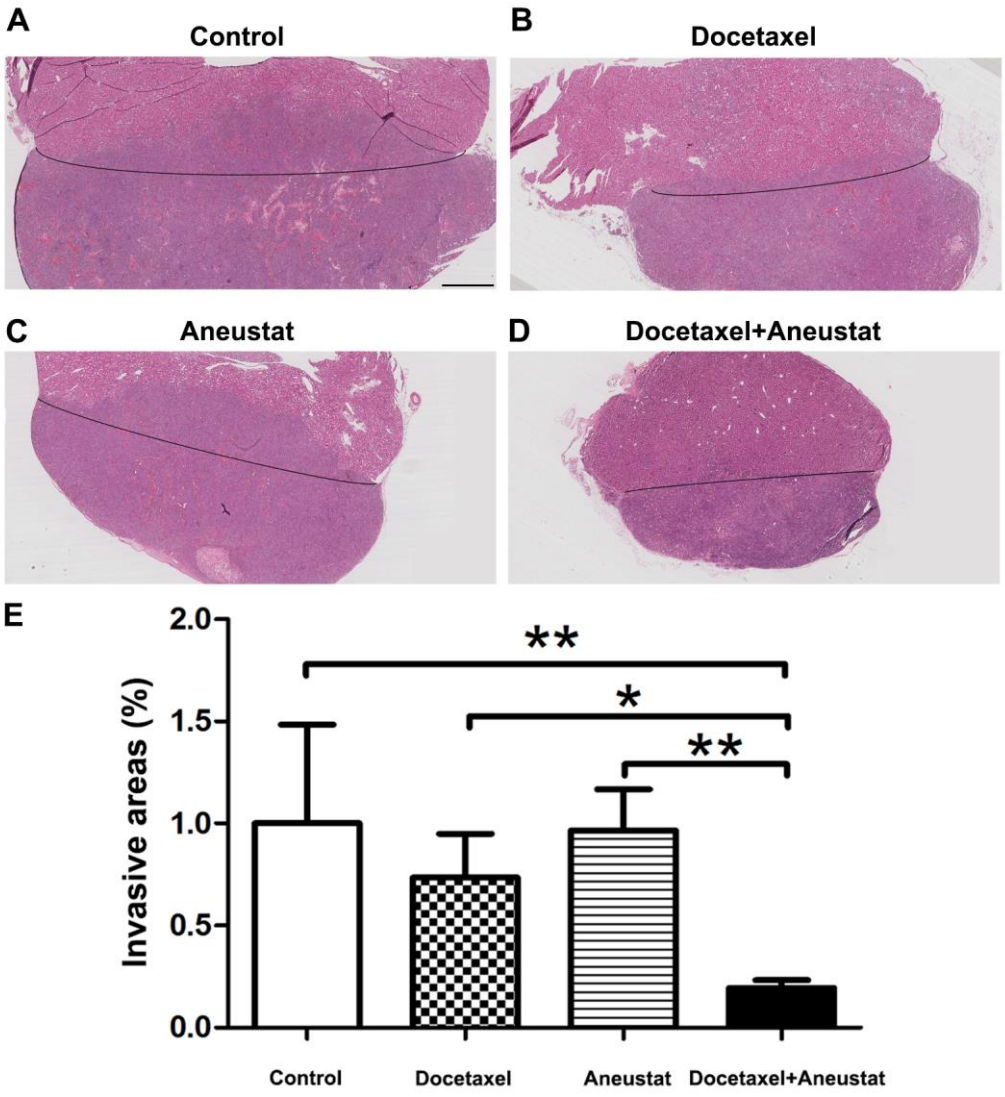

Figure 3.4 Effects of a 3-week treatment with docetaxel, Aneustat and docetaxel+Aneustat on host adjacent kidney tissue invasion by prostate cancer cells in the LTL-313H model.

Kidney tissues (upper sections) and xenograft tissues (lower sections) of the LTL-313H PDX prostate cancer model treated with (A) control, (B) docetaxel, (C) Aneustat and (D) the combination of docetaxel and Aneustat. The way to determine the boundary of xenograft tissue and kidney tissue is shown in Figure 3.1. (E) Infiltrated kidney areas (percentages). * indicates $p < 0.05$; ** indicates $p < 0.01$. Scale bar: 1 mm.

3.3.3 Gene Expression Profile of Docetaxel+Aneustat-treated LTL-313H Xenografts: Correlation with Gene Expression Profiles of Patients with Improved Outcome (Oncomine)

Two gene expression profiles were obtained from LTL-313H prostate cancer xenografts treated with docetaxel+Aneustat, involving (i) 838 down-regulated genes and (ii) 919 upregulated genes [i.e. genes showing significant changes in expression ($\geqslant$ 2-fold) in response to the treatment of the xenografts compared to vehicle control]. These gene profiles were then compared with gene expression profiles from prostate cancer patients (Oncomine database). It was found that the gene expression profiles obtained from the docetaxel+Aneustat-treated xenografts positively correlated with the expression profiles of (i) patients showing longer survival time or longer cancer recurrence time and (ii) patients carrying non-metastatic tumors (odds ratio > 2, p<1E-4) (Tables 3.2 and 3.3), i.e. changes indicative of improved clinical patient outcome. Taken together, the data indicate that treatment with docetaxel+Aneustat is associated with improved patient outcome.

Clinical Event	Clinical Cohort	*p* value	q value	Odds Ratio
Survival				
> 5 years	Setlur Prostate	8.53E-21	5.13E-19	3.9
> 5 years	Nakagawa Prostate	2.12E-10	7.72E-9	21.0
> 5 years	Nakagawa Prostate 2	1.18E-5	2.84E-4	10.3
Recurrence				
> 5 years	Taylor Prostate 3	5.28E-35	5.05E-33	11.1
> 5 years	Nakagawa Prostate	3.33E-9	1.12E-7	9.9
Metastasis				
	Taylor Prostate 3	1.12E-104	8.23E-102	9.4
	Varambally Prostate	7.45E-47	9.95E-45	4.0
	Grasso Prostate	1.10E-44	1.37E-42	3.9
	LaTulippe Prostate	6.28E-39	6.65E-37	7.1
	Vanaja Prostate	1.28E-34	1.21E-32	3.4
	Holzbeierlein Prostate	2.14E-14	9.86E-13	3.4

Table 3.2 Correlation between the down-regulated gene expression profile obtained with docetaxel+Aneustat-treated LTL-313H xenografts and gene expression profiles of prostate cancer patients with improved outcome as indicated by Oncomine analysis.

Clinical Event	Clinical Cohort	*p* value	q value	Odds Ratio
Recurrence				
> 5 years	Taylor Prostate 3	6.59E-7	6.82E-5	2.1
Metastasis				
	Tamura Prostate	2.71E-10	8.43E-8	2.8
	Taylor Prostate 3	3.83E-21	1.71E-17	3.5
	Yu Prostate	1.43E-5	8.73E-4	2.5
	Grasso Prostate	1.42E-11	6.19E-9	2.2
	LaTulippe Prostate	3.62E-8	5.94E-6	2.4

Table 3.3 Correlation between the up-regulated gene expression profile obtained with docetaxel+Aneustat-treated LTL-313H xenografts and gene expression profiles of prostate cancer patients with improved outcome as indicated by Oncomine analysis.

3.3.4 Suppression of FOXM1 Expression as a Potential Mechanism Underlying Treatment with Docetaxel+Aneustat

Following IPA analysis of the 1757 genes showing significant differential expression (⩾ 2-fold difference) between control and docetaxel+Aneustat-treated xenografts (see Chapter 2), 'Upstream Regulators' of the data were used to identify potential cancer driver genes affected by the combination of docetaxel and Aneustat. The top 10 genes (Upstream Regulators) identified are presented in Table 3.4. In particular, the *FOXM1* gene, important in the promotion of cancer metastasis [121], was substantially down-regulated by treatment with the combination with a fold change of -7.5. As well, IPA analysis was used to identify genes directly regulated by FOXM1 protein, i.e. *AURKB* [380], *CCNB1* [381], *CDC25C* [382, 383], *CENPA* [384], *CENPE* [382], *CENPF* [381], *PLK1* [385], *PTTG1* [386], and *STMN1* [387, 388]. It was found that the expression of these genes were also down-regulated as shown by the microarray data of docetaxel+Aneustat-treated LTL-313H xenografts compared to controls (Fig. 3.5A). To confirm down-regulation of FOXM1 by treatment with docetaxel+Aneustat, the expressions of *FOXM1* and *FOXM1*-target genes in LTL-313H xenografts and C4-2 cells treated with the drug combination were further analyzed. It was found that the mRNA and protein expressions of *FOXM1* were significantly down-regulated by treatment with the combination in both LTL-313H xenografts (Fig. 3.5B) and C4-2 cells (Fig. 3.6A). Furthermore, the expression levels of *FOXM1*-target genes were all significantly down-regulated in LTL-313H xenografts following treatment with the drug combination (Fig. 3.5C); similar results were obtained with C4-2 cells (Fig. 3.6B). Taken together, the results indicate that treatment with docetaxel+Aneustat markedly reduced the expression of *FOXM1*, a metastasis-promoting driver gene.

Upstream Regulator	Gene Expression Fold Change	Molecule Type	Predicted Activation State	Activation z-score	p-value of overlap
ERBB2	-1.0	kinase	Inhibited	-6.896	2.27E-34
MITF	-1.9	transcription regulator	Inhibited	-6.832	1.89E-28
CSF2	Not detectable	cytokine	Inhibited	-6.563	5.27E-28
RABL6	-1.7	other	Inhibited	-5.925	7.30E-30
FOXM1	-7.5	transcription regulator	Inhibited	-5.118	5.25E-27
PTGER2	Not detectable	g-protein coupled receptor	Inhibited	-5.059	1.13E-19
EP400	1.2	other	Inhibited	-4.663	2.70E-17
E2F3	-1.7	transcription regulator	Inhibited	-4.398	2.13E-13
MYC	1.4	transcription regulator	Inhibited	-4.343	5.31E-10
CCND1	-1.4	transcription regulator	Inhibited	-3.857	7.65E-31

Table 3.4 'Upstream regulators' predicted by IPA as potentially affected by docetaxel+Aneustat.

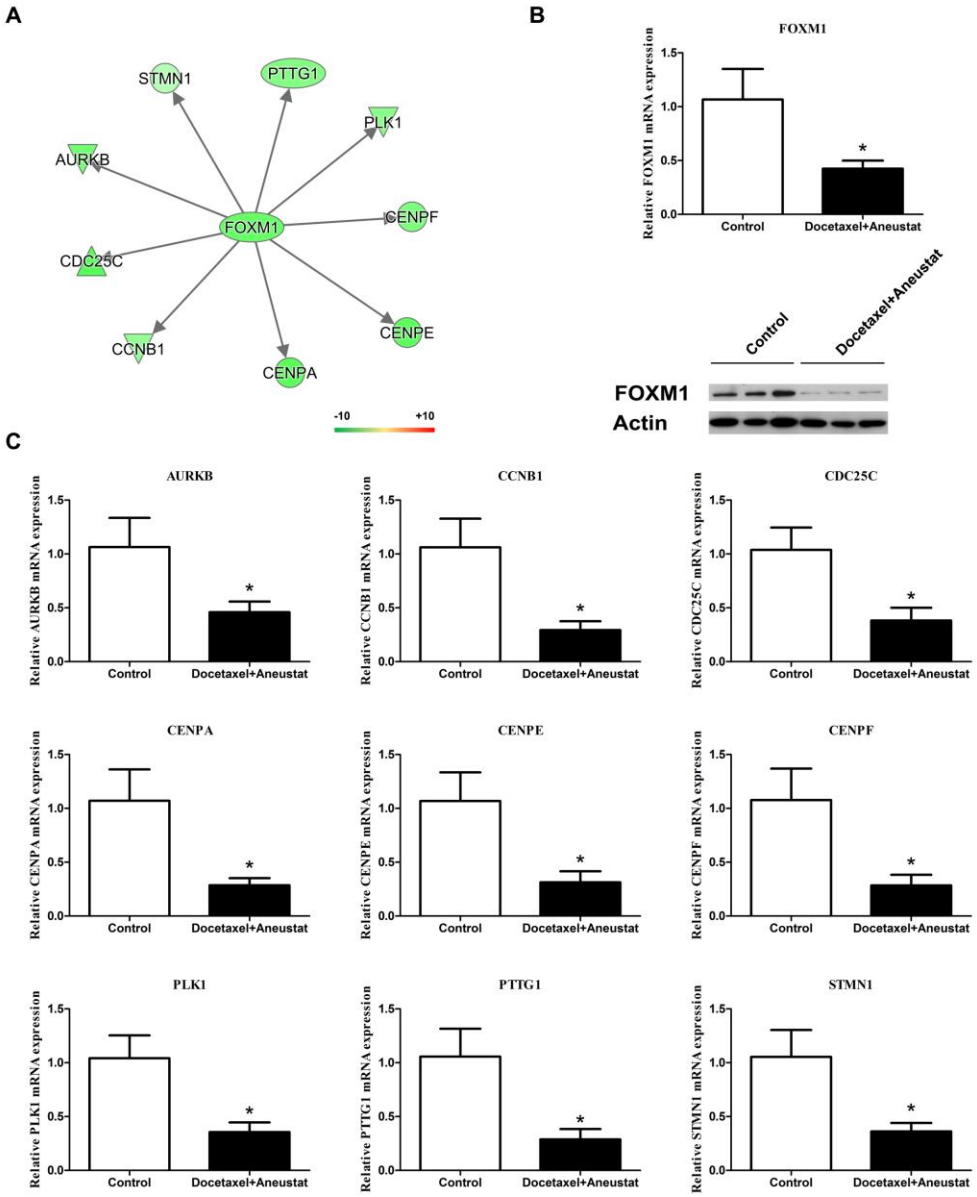

Figure 3.5 Effect of docetaxel+Aneustat on the expressions of *FOXM1* and *FOXM1*-target genes in LTL-313H xenografts.

(A) Genes transcriptionally regulated by FOXM1 protein as predicted by IPA; green color indicates down-regulation of genes based on microarray data obtained with docetaxel+Aneustat-treated LTL-313H xenografts. (B) mRNA and protein expression of *FOXM1* in LTL-313H xenografts, and (C) the mRNA levels of *FOXM1*-target genes. The experiment was performed in triplicate. * indicates $p < 0.05$.

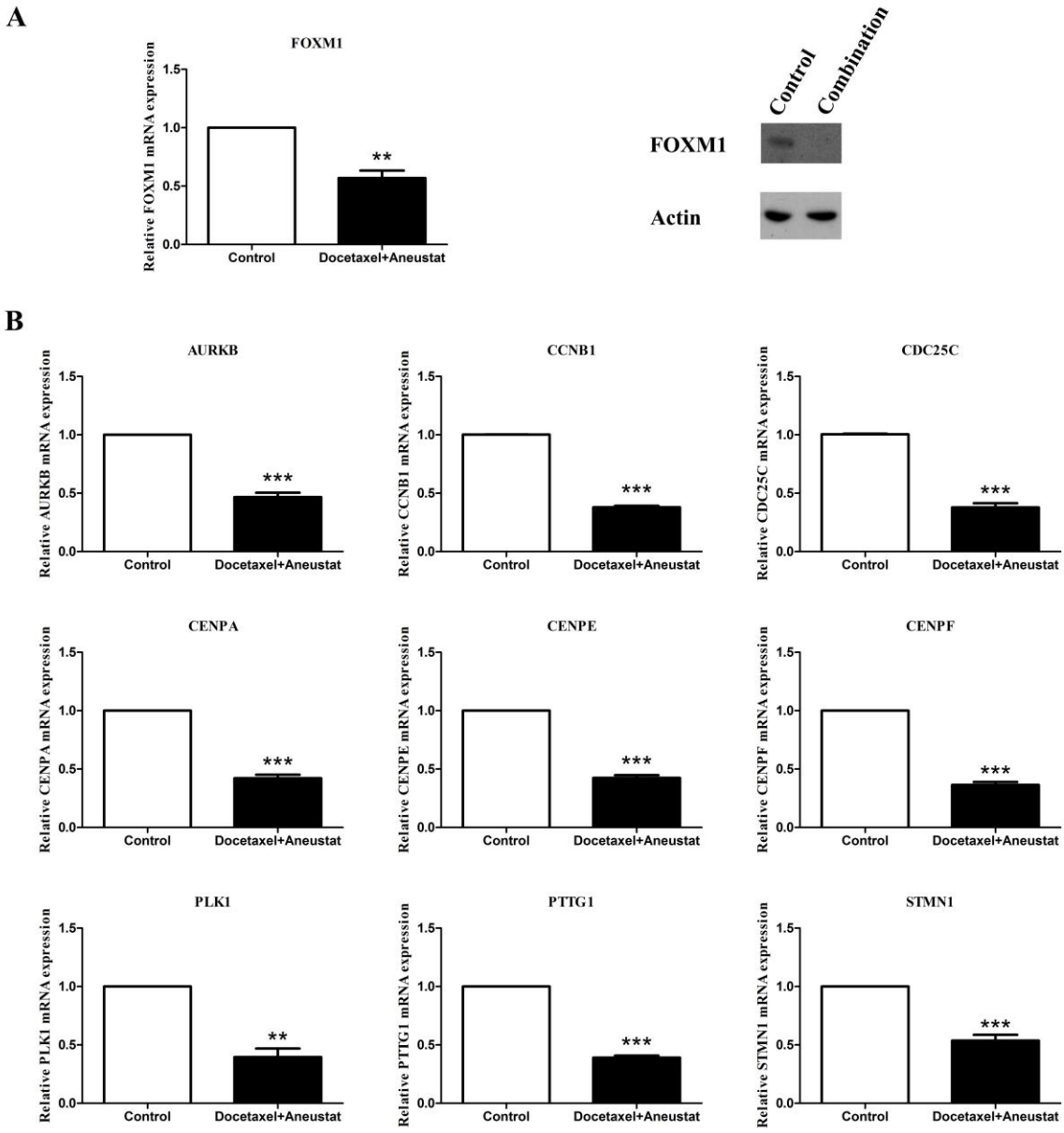

Figure 3.6 Effect of docetaxel+Aneustat on the expressions of *FOXM1* and *FOXM1*-target genes in C4-2 cells *in vitro*.

C4-2 cells were incubated with docetaxel+Aneustat or control for 48 h. (A) mRNA and protein expression of *FOXM1*, (B) the mRNA levels of *FOXM1*-target genes. The experiment was performed in triplicate. ** indicates $p < 0.01$; *** indicates $p < 0.001$.

3.3.5 *FOXM1* Overexpression Attenuates Docetaxel+Aneustat-induced Inhibition of C4-2 Cell Migration

As shown in Figure 3.7A, C4-2 cells infected by lentiviruses pSin-FOXM1b or pSin-FOXM1c overexpress *FOXM1*. Such C4-2 cells and vector control pSin-mCherry cells were treated for 48h with the combination of docetaxel (5 nM) and Aneustat (100 μg/ml) or with vehicle control. The Boyden Chamber cell migration assay was applied to determine the effects of the treatment with docetaxel+Aneustat on cell motility. The C4-2 cells that overexpressed *FOXM1b*/*FOXM1c*, and had been treated with docetaxel+Aneustat, showed higher migration ability compared to the pSin-mCherry control cells (Fig. 3.7B, C), indicating that overexpression of FOXM1 can reduce the inhibitory effect of docetaxel+Aneustat on cell motility.

Furthermore, treatment of the pSin-mCherry vector control cells with docetaxel+Aneustat led to reduction of the expression of the *FOXM1*-target genes. In contrast, all of the *FOXM1*-target genes showed higher expression when *FOXM1b* or *FOXM1c* were overexpressed (Fig. 3.8). Taken together, the results indicate that *FOXM1*, a gene encoding a key transcription factor, is a major cancer driver gene that is affected by treatment with docetaxel+Aneustat.

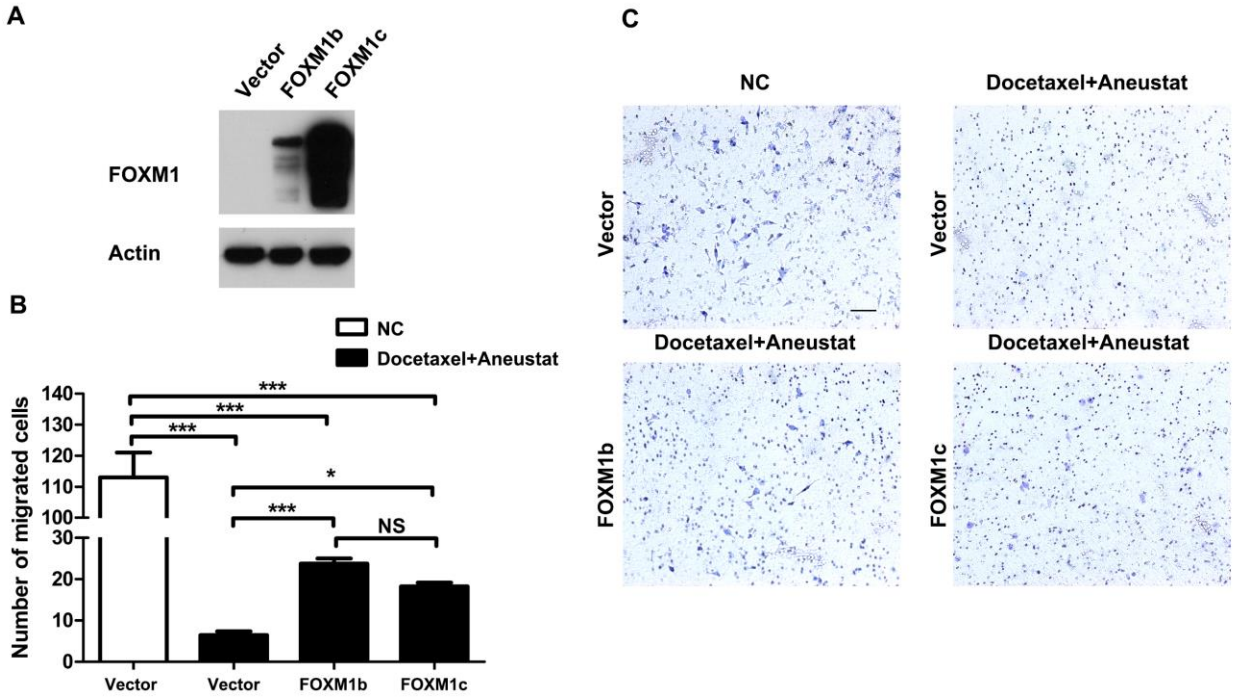

Figure 3.7 Effects of treatment with docetaxel+Aneustat on migration of *FOXM1* overexpressing C4-2 cells using the Boyden Chamber assay.

(A) C4-2 cells infected with pSin-FOXM1b and pSin-FOXM1c show overexpression of FOXM1b and FOXM1c protein. (B, C) Boyden Chamber cell migration assay of pSin-FOXM1b and pSin-FOXM1c C4-2 cells and pSin-mCherry control cells, treated and not-treated with docetaxel+Aneustat. The experiment was performed in triplicate. * indicates $p < 0.05$; *** indicates $p < 0.001$; NS indicates no statistical significance. Scale bar: 20 μm.

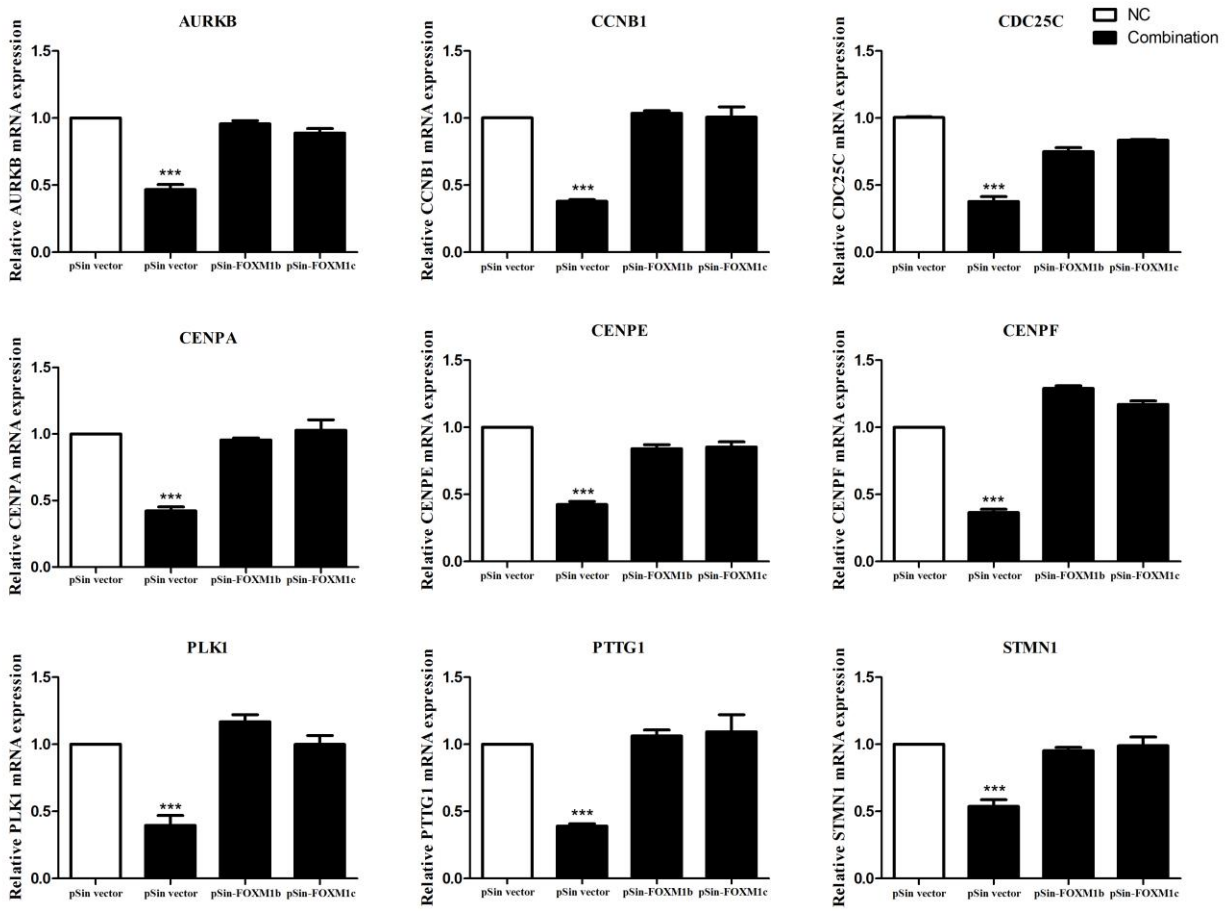

Figure 3.8 The effect of *FOXM1* overexpression on *FOXM1*-target gene mRNA levels in C4-2 cells as affected by treatment with docetaxel+Aneustat.

Effects of the treatment on mRNA expression of *FOXM1*-target genes in pSin-mCherry, pSin-FOXM1b and pSin-FOXM1c C4-2 cells. The experiment was performed in triplicate. *** indicates $p < 0.001$.

3.4 Discussion

Based on a previous study showing that combining docetaxel with Aneustat can lead to much higher prostate cancer growth-inhibitory activity than the combined activities of the individual drugs (see Chapter 2) [288], the present study explored the effect of this drug combination on cancer metastasis. The findings that docetaxel+Aneustat can potently inhibit lung micro-metastasis by prostate cancer cells in the LTL-313H model and also host kidney tissue invasion (Figs 3.3 and 3.4) are consistent with (i) the inhibition by docetaxel+Aneustat of C4-2 cell migration (Fig. 3.2), and (ii) the findings of the previous study indicating that docetaxel+Aneustat would affect a variety of cancer hallmarks, including 'tissue invasion and metastasis' [288]. As well, the inhibition by docetaxel+Aneustat of lung micro-metastasis and adjacent kidney tissue invasion in the LTL-313H PDX prostate cancer model (Figs 3.3 and 3.4) is in agreement with the prediction by Oncomine gene expression profile analysis in the present study that treatment with docetaxel+Aneustat is associated with improved patient outcome, as evidenced by longer survival time, longer disease relapse time and lack of metastasis development (Tables 3.2 and 3.3). As such, combined use of docetaxel and Aneustat appears to represent a promising new therapeutic strategy for metastatic prostate cancer, a disease whose prognosis is currently grim.

The findings in the present study, i.e. that treatment of the LTL-313H PDX prostate cancer model with docetaxel+Aneustat can markedly inhibit the expression of *FOXM1* and its target genes (Fig. 3.5), is consistent with the inhibition by docetaxel+Aneustat of lung micro-metastasis and adjacent kidney tissue invasion (Figs 3.3 and 3.4) as *FOXM1* is considered an important promoter of metastasis [121], as are its target genes such as *CENPA, PTTG1* and *STMN1* [384, 386, 389]. *FOXM1* and its target gene *CENPF*, in particular, have been identified

as synergistic drivers of prostate cancer [390], and overexpression of both *FOXM1* and *CENPF* harbors a robust poor prognostic value, indicative of poor patient survival and metastasis [123]. As well, overexpression of *FOXM1* in C4-2 cells led to both upregulation of *FOXM1*-target genes and reduction of the anti-migration activity of docetaxel+Aneustat (Figs 3.7 and 3.8), supporting the prediction by IPA that *FOXM1* is a cancer driver gene that is affected by docetaxel+Aneustat (Table 3.4).

As an upstream regulator, *FOXM1* has been shown to regulate a number of canonical pathways such as the 'Mitotic roles of polo-like Kinase' pathway as we reported previously [288], acting via PLK1 (Polo-like Kinase 1), a key factor in this pathway [391]. The marked down-regulation of PLK1 by docetaxel+Aneustat (Figs 3.5 and 3.6) is in agreement with that. It has also been reported that down-regulation of *FOXM1* expression can inhibit aerobic glycolysis of cancers [392], consistent with our report that the drug combination can affect glycolysis pathway [288]. Taken together, it appears that inhibition of expression of *FOXM1* and its target genes is one of the mechanisms underlying docetaxel+Aneustat-induced inhibition of prostate cancer tissue invasion and metastasis. Recently, it has been shown that FOXM1 could be an important target for therapy of Enzalutamide-resistant prostate cancer [393]. *In vivo* studies using compounds that inhibit expression of FOXM1, such as Monensin [393] and Plumbagin [394], did not show major host toxicity. However, more studies are needed to further investigate the effect of targeting FOXM1 on host toxicity. Thus, *FOXM1* provides a novel target for therapy of metastatic prostate cancer and patients with *FOXM1* dysregulation would likely benefit from treatment with combined use of docetaxel and Aneustat.

Subcutaneous mouse xenograft models of human cancer are in general not considered suitable for studies of local tissue invasion, an important characteristic of metastasis [395]. In the

present study, however, it was found, using an innovative histological approach (Fig. 3.1), that subrenal capsule PDX cancer models can be used for studying local invasion of host kidney tissue - an observation that could lead to wider application.

In conclusion, the present study shows, using a high fidelity subrenal capsule PDX metastatic prostate cancer model, that combined use of docetaxel and Aneustat, as distinct from the individual drugs, can markedly inhibit metastasis and local tissue invasion – apparently a result of suppression of expression of metastasis driver genes such as *FOXM1*. As such, combined use of docetaxel and Aneustat may provide a novel, more effective regimen for therapy of advanced, metastatic prostate cancer. In addition, it was found that subrenal capsule PDX models can be used for studies of local tissue invasiveness.

Chapter 4: Anticancer Activity and Immunomodulatory Properties of Aneustat

4.1 Introduction

It is now well recognized that the immune system has a dual role in cancer development and progression, as cancers characteristically contain a wide variety of tumor-infiltrating immune cells which can inhibit or promote cancer growth [197, 396]. On one hand, intratumoral $CD8^+$ T cells, NK cells and M1 macrophages, i.e. major effector cells of the host anticancer immune response, are aimed at eliminating cancer cells via various mechanisms [202, 396]. On the other hand, tumors also contain immunosuppressive cells, such as regulatory T cells (Tregs), myeloid-derived suppressive cells (MDSCs) and M2 macrophages, that can promote cancer development by suppressing the host anticancer immune response [202]. Unfortunately, as cancers progress, intratumoral cancer-induced immunosuppression becomes dominant [397]. Recent successes in cancer immunotherapy based on stimulation of the host anticancer immune response have underlined the importance of the latter in the fight against the disease [398].

There is compelling evidence that epithelial cancers can suppress the host anticancer immune response by various mechanisms [399]. Reprogrammed glucose metabolism, i.e. aerobic glycolysis, which is commonly used by cancer cells, leads to increased lactic acid secretion and a low, immune function-inhibiting pH in their microenvironment [227, 235]. The acidification of the tumor microenvironment can suppress the host anticancer immune response as it has been found to promote expansion of intratumoral numbers of Treg cells and MDSCs and reduce intratumoral levels of $CD8^+$ T cells and NK cells [230, 236], resulting in a lower ratio of intratumoral $CD8^+$ T cells to Treg cells as observed in patients [400]. Such a role of cancer-

generated lactic acid has been demonstrated using B16 mouse melanoma allografts in immunocompetent C57BL/6 and $Rag2^{-/-}$ mice. Thus a reduction of lactic acid secretion by the tumors, obtained by specific depletion of lactate dehydrogenase-A (LDHA), led to lower numbers of intratumoral MDSCs and higher numbers of intratumoral NK cells and $CD8^+$ T cells compared to controls [236]. As such, targeting aerobic glycolysis to reduce lactic acid secretion by cancer cells appears to be a useful strategy for restoring the host anticancer immune response [227, 235]. This would lead to a higher ratio of $CD8^+$ T cells to Treg cells, a higher number of NK cells and a lower number of MDSCs - a signature associated with improved patient outcome [401-404].

Aneustat is a multivalent immuno-oncology drug candidate developed by Omnitura Therapeutics Inc., USA. Recently, a Phase-I Clinical Trial (NCTId: NCT01555242) has shown that Aneustat was well tolerated by patients. Furthermore, treatment with Aneustat led to a decrease in the levels of immune suppression markers in patients (e.g., TGF-β) indicative of a reduction in the suppression of the host anticancer immune response [326]. As well, preliminary preclinical studies have indicated that Aneustat has anti-inflammatory and immunomodulatory activities [310]. We previously demonstrated, using a patient-derived prostate cancer xenograft model, that a combination of docetaxel and Aneustat led to much higher antitumor activity than the combined activities of the individual drugs, with indications that inhibition of aerobic glycolysis was involved [288].

In the present study, we investigated Aneustat with regard to effects on (i) aerobic glycolysis of LNCaP prostate cancer cells, a process underlying cancer-generated lactic acid-induced immunosuppression and (ii) immune system-related processes such as macrophage

differentiation and shifts in the levels of intratumoral host immune cells using LNCaP xenografts and first-generation patient-derived prostate cancer tissue xenografts.

4.2 Materials and Methods

4.2.1 Materials

Chemicals, solvents and solutions were obtained from Sigma-Aldrich, Oakville, ON, Canada, unless otherwise indicated. Aneustat was supplied by Omnitura Therapeutics Inc. (Henderson, NV).

4.2.2 Oncomine Analysis

Oncomine is a cancer transcriptomic database and web-based discovery platform [18]. Gene expression analyses of a single gene or a set of genes can be performed with this platform to predict the potential role of the gene(s) in a malignancy [405].

4.2.3 Cell Culture

Human LNCaP prostate cancer cells and mouse RAW264.7 macrophages were purchased from the American Type Culture Collection (ATCC; Manassas, VA). LNCaP cells and RAW264.7 macrophages were maintained as monolayer cultures in RPMI-1640 medium (GE Healthcare HyClone) and DMEM medium (GE Healthcare HyClone), respectively, supplemented with fetal bovine serum (FBS 10%; GE Healthcare HyClone), at 37°C in a humidified incubator with a 5% CO_2/air atmosphere. Cells were trypsinized to form a single cell suspension and counted using a TC20 Automated Cell Counter (Bio-Rad). Cell viability was determined by Trypan blue exclusion.

4.2.4 Treatment of LNCaP and RAW264.7 Cell Cultures with Aneustat

LNCaP and RAW264.7 single cell suspensions were seeded into 6-well culture plates (starting concentration ~2.5×10^5 cells/well for LNCaP cells and ~2×10^5 cells/well for RAW264.7 cells) and incubated at 37 °C in 5% CO_2/air for 18h. Aneustat (dissolved in DMSO + Ethanol) or vehicle control (DMSO + Ethanol) were then added to the cultures for a further 48h incubation to assess the effects of Aneustat.

4.2.5 Quantitative Real-Time PCR

Total RNA was isolated using the RNeasy Mini Kit (Qiagen Inc.) and cDNA was synthesized using the QuantiTect Reverse Transcription Kit (Qiagen Inc.) according to the manufacturer's instructions. Primers used were described in Table 4.1. qRT-PCR reactions using KAPA SYBR FAST Universal (Kapa Biosystems) were performed in triplicate in a ViiA 7 Real-Time PCR System (Applied Biosystems). Expression levels of genes were normalized to HRPT1.

Gene Name (Human)	Sequences (5’ to 3’)
SLC2A1 (GLUT1) F	CCTGCAGTTTGGCTACAACAC
SLC2A1 (GLUT1) R	CAGGATGCTCTCCCCATAGC
LDHA F	GGAAAGGCTGGGAGTTCACC
LDHA R	CTGGGTGCAGAGTCTTCAGAG
SLC16A3 (MCT4) F	ACCCACAAGTTCTCCAGTGC
SLC16A3 (MCT4) R	AGCAAAATCAGGGAGGAGGT
HRPT1 F	GGTCAGGCAGTATAATCCAAAG
HRPT1 R	CGATGTCAATAGGACTCCAGATG
ENO1 F	CCTGCCCTGGTTAGCAAGAA
ENO1 R	GGGACTGGCAGGATGACTTC
PDHA1 F	CGCTATGGAATGGGAACGTCTG
PDHA1 R	TCGTGTACGGTAACTGACTCC
PDK1 F	TTGAATACAAGGAGAGCTTTGGGGT
PDK1 R	AATCACACAGACGCCTAGCATTTT
PGAM1 F	GCTAATCCCAGTCGGTGCC
PGAM1 R	GTCCGGATCGCTCTCTTCTG
PGK1 F	GTGTTCCGCATTCTGCAAGCC
PGK1 R	TTGGGACAGCAGCCTTAATCC

Table 4.1 qPCR primer sequences used

Gene Name (Human)	Sequences (5’ to 3’)
ASCT2 F	CCGCTTCTTCAACTCCTTCAA
ASCT2 R	ACCCACATCCTCCATCTCCA
GLS F	TTCAGTCCCGATTTGTGGGG
GLS R	CACTCGGCTCTTTTCCAACA
GLS2 F	TGGATATGGAACAGAAAGACTATG
GLS2 R	AAGCAGTTTGACCACCTCCAGATG
GOT1 F	AGCTGTGCTTCTCGTCTTGC
GOT1 R	AGATTGCACACCTCCTACCC
GOT2 F	CAACACATCACCGACCAAAT
GOT2 R	CGGCCATCTTTTGTCATGTA
GPT F	CGCAGTGCAGGTGGATTACTAC
GPT R	GAAGGCGAAGCGGATCACGG
GPT2 F	GACCCCGACAACATCTACCTG
GPT2 R	TCATCACACCTGTCCGTGACT
PSAT1 F	ACAGGAGCTTGGTCAGCTAAG
PSAT1 R	CATGCACCGTCTCATTTGCG

Table 4.1 qPCR primer sequences used (continued)

Gene Name (Human)	**Sequences (5’ to 3’)**
GLUD1 F	CTGGCTTGGCATACACAATG
GLUD1 R	GCTGTTCTCAGGTCCAATCC
GLUD2 F	TCGTGGAGGACAAGTTGGTG
GLUD2 R	TTGCAGGGCTTGATGATCCG
Gene Name (Mouse)	**Sequences (5’ to 3’)**
Gapdh F	AATGTGTCCGTCGTGGATCT
Gapdh R	GCTTCACCACCTTCTTGATGT
Tnf F	TCTTCTCATTCCTGCTTGTGG
Tnf R	GGTCTGGGCCATAGAACTGA

Table 4.1 qPCR primer sequences used (continued)

4.2.6 Western Blotting

LNCaP cells were treated with vehicle control and Aneustat for 48h; whole cell protein extracts were resolved on SDS-PAGE using procedures previously reported [235]. Proteins were then transferred to PVDF membranes. After blocking for 1h at room temperature in 5% milk in TBS/0.1% Tween-20, membranes were incubated overnight at 4°C with appropriate primary antibodies. Following incubation with secondary antibody, immunoreactive proteins were visualized with a SuperSignal™ West Femto Maximum Sensitivity Substrate (Thermo Scientific). The following antibodies were used: anti-GLUT1 (ab115730, rabbit monoclonal antibody, Abcam); anti-LDHA (3582, rabbit monoclonal antibody, Cell Signaling Technology); anti-MCT4 (sc-50329, rabbit polyclonal antibody, Santa Cruz); anti-actin (A2066, rabbit polyclonal antibody, Sigma). Actin was used to monitor the amounts of samples applied.

4.2.7 Glucose Consumption and Lactate Secretion Determinations

LNCaP cells and RAW264.7 cells, treated for 48h with Aneustat or vehicle control, were assessed for glucose consumption and lactate secretion after another 8h incubation with fresh medium. Samples of the media were then taken and deproteinized with 10K Spin Columns (BioVision) prior to determination of glucose and lactate concentration using the Glucose Assay Kit and Lactate Assay Kit (BioVision) as previously described [235]. Final concentrations of glucose and lactate were determined by normalizing to the total number of live cells.

4.2.8 ELISA of TNF-α Secretion

RAW264.7 cells, treated for 48h with Aneustat or vehicle control, were used for TNF-α secretion assessment after another 8h incubation in fresh medium. Samples of the media were then taken and the TNF-α concentration was determined using Mouse TNF ELISA Set II (558534, BD)

following the manufacturer's instructions. The final concentration of secreted TNF-α was normalized to the total number of live cells.

4.2.9 Animals

Athymic nude mice and NOD/SCID–IL-2R-γc-KO (NSG) mice, bred in the BC Cancer Research Centre ARC animal facility, were housed in sterile micro-isolator cages under specific pathogen-free conditions. Food and water were sterilized prior to use. Temperature (20-21°C) and humidity (50-60%) were controlled. Daily light cycles were 12h light and 12h dark. Cages were completely changed once or twice a week. Animals were handled under sterile conditions. Animal care and experiments were carried out in accordance with the guidelines of the Canadian Council on Animal Care.

4.2.10 LNCaP Xenograft Mouse Model and Treatment with Aneustat

LNCaP cells (in 1:1 HBSS:Matrigel) were grafted under the renal capsules of male athymic nude mice (Simonsen Laboratories; 2 groups; 5 mice/group; 4 grafts/mouse). Three weeks after engraftment, the mice were randomly distributed into 2 groups and treated with Aneustat (1652 mg/kg; orally; Q1d × 5/3) or vehicle control (Tween 80 in saline solution; orally; Q1d × 5/3). The health of the mice was monitored. After 3 weeks, the mice were euthanized and tissue sections prepared for histopathological analysis.

4.2.11 First-Generation Patient-derived Prostate Cancer Tissue Xenograft Model, Treatment with Aneustat

Fresh patient metastatic prostate cancer lymph node tissues (obtained from the Vancouver General Hospital with proper patients' consent; with approved biosafety certificates and animal protocol) were grafted under renal capsules of male NOD/SCID–IL-2R-γc-KO (NSG) mice supplemented with testosterone as previously described [269]. After 10 days, the mice were

randomly divided into two groups (3 mice/group; 4 grafts/mouse), and treated with Aneustat (1652 mg/kg; orally; Q1d × 5/3) or vehicle control (Tween 80 in saline solution; orally; Q1d × 5/3). The health of the mice was monitored. After 3 weeks, the mice were euthanized and tissue sections prepared for histopathological analysis.

4.2.12 Immunohistochemical Staining

Preparation of paraffin-embedded tissue sections and immunohistochemical analyses were performed as previously described [344]. Anti-mouse NK1.1 (CL8994AP, Cedarlane), anti-mouse Ly6G (127601, Biolegend), anti-human CD8 (ab93278, Abcam), anti-human Foxp3 (14-7979, eBioscience), anti-human CD33 (ab199432, Abcam) and anti-human NCR1 (ab14823, Abcam) antibodies were used for immunohistochemical staining. Three fields of each slide showing positively stained intratumoral lymphocytes were selected and images taken (×400 for LNCaP xenografts and ×200 for first-generation patient-derived tumor tissue xenografts) [406, 407], using an AxioCam HR CCD mounted on an Axioplan 2 microscope and ZEN 2.3 software (Carl Zeiss). Positively stained cells in each image were counted. Prior to use, antibodies were tested for target and species specificity.

4.2.13 Statistics

Statistical analysis was determined using GraphPad Prism 5 (GraphPad Software, Inc); otherwise the Student's t-test was used. Results are considered statistically significant when $p<0.05$ and are expressed as means ± SEM.

4.3 Results

4.3.1 Potential Biological Actions of Aneustat as Indicated by Oncomine Analysis of the Gene Expression Profile of Aneustat-treated Xenografts

Microarray data obtained in previous studies with LTL-313H patient-derived prostate cancer xenografts [288] were used for gene expression analysis. 218 genes showing ≥2-fold changes in expression in response to treatment of the xenografts with Aneustat compared to controls were uploaded onto Oncomine. The biological annotations of the data were used to estimate the potential actions of Aneustat. As shown in Table 4.2, the top five concepts of biological annotations were: immune response; metabolism; G-protein-coupled receptor activity; hormone receptor extracellular; and GPCR family 2, secretin-like.

Biological Annotations	***p* value**	**Odds Ratio**
Immune Response	0.002	3.1
Metabolism	0.003	2.9
G-protein coupled receptor activity	0.003	5.5
Hormone receptor, extracellular	0.003	11.4
GPCR, family 2, secretin-like	0.005	6.4

Table 4.2 Top 5 biological annotations obtained by Oncomine Analysis of the Gene Expression Profile of LTL-313H prostate cancer xenografts following treatment with Aneustat

4.3.2 Aneustat-induced Differentiation of RAW264.7 Macrophages to the M1 Phenotype

Mouse RAW264.7 macrophages have been shown to exhibit a differentiation ability toward two phenotypes, M1 or M2: (i) their treatment with antigens/cytokines, such as lipopolysaccharide (LPS), can induce the M1 phenotype (anticancer activity) associated with increased secretion of TNF-α [408] and (ii) treatment with IL-4 can lead to the M2 phenotype (pro-cancer activity), with increased secretion of TGF-β [409]. In this study, treatment with Aneustat did not inhibit the proliferation of the RAW264.7 cells (Fig. 4.1A). However, Aneustat markedly changed the morphology of the cells from round to dendritic-like (Fig. 4,1B) and increased the secretion by the cells of TNF-α, a marker of the M1 phenotype (Fig. 4.1C). Together, these changes indicate that Aneustat induced differentiation of the RAW264.7 macrophages to an M1 anticancer phenotype.

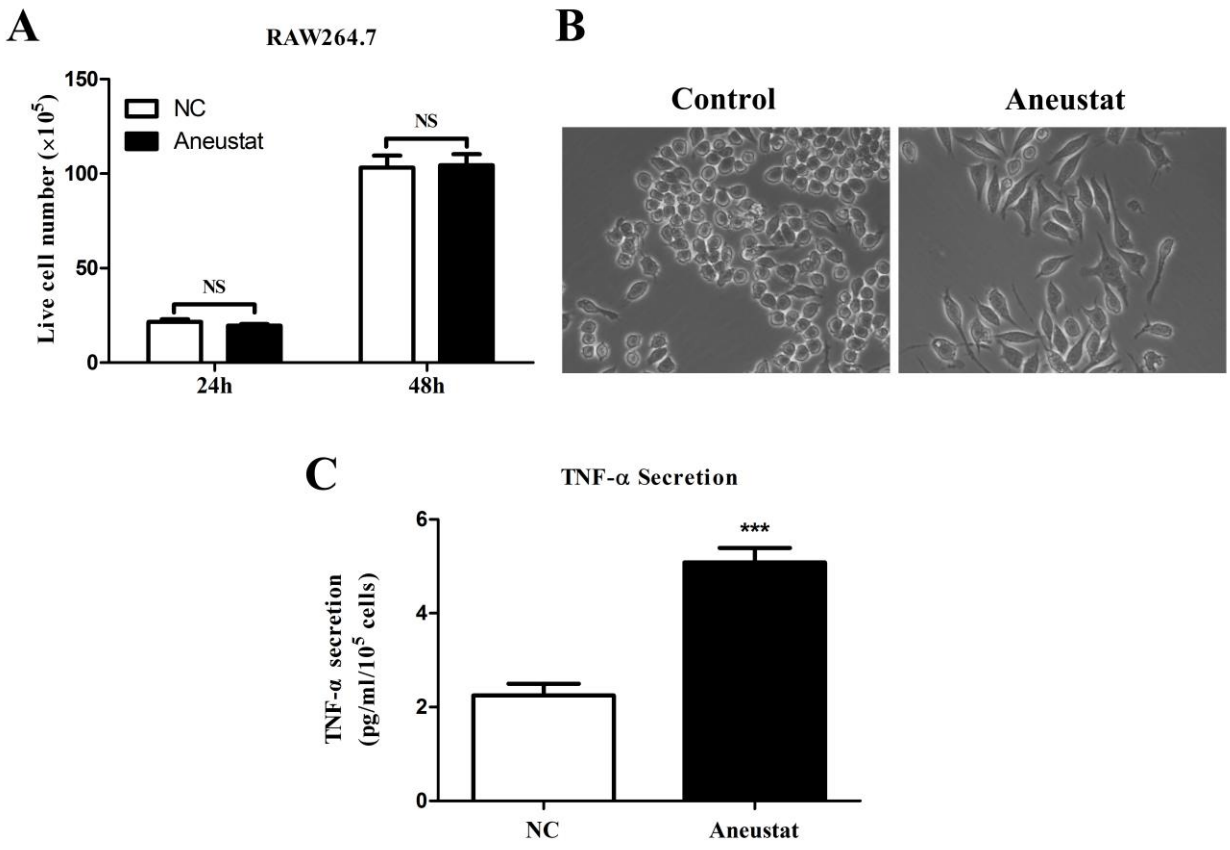

Figure 4.1 Effects of Aneustat on RAW264.7 macrophages.

Mouse RAW264.7 macrophages were treated with Aneustat (200 μg/ml). Effect of Aneustat on (A) cell numbers at 24h and 48h; (B) cell morphology; (C) TNF-α secretion. The experiment was performed in triplicate. *** indicates $p < 0.001$; NS indicates no statistical significance.

4.3.3 Inhibition by Aneustat of Proliferation and Metabolism of LNCaP Cells

LNCaP cells were incubated with Aneustat (200 μg/ml) or vehicle control; live cell numbers were counted at 24h and 48h. As shown in Figure 4.2A, the proliferation of LNCaP cells was markedly inhibited by Aneustat at 24h and 48h with inhibitions of 30% and 59%, respectively. An 82% decrease in glucose consumption was observed at 48h, while lactic acid secretion was reduced by 56% (Fig. 4.2B). Furthermore, the mRNA and protein expressions of key genes in the aerobic glycolysis pathway, i.e. *GLUT1* (glucose transporter), *LDHA* (enzyme to convert pyruvate to lactate) and *MCT4* (lactate transporter) were markedly down-regulated by Aneustat after 48h (Fig. 4.2C, D). Other genes in the aerobic glycolysis pathway (*ENO1*, *PDHA1*, *PDK1*, *PGAM1* and *PGK1*) were not affected by Aneustat (Fig. 4.2D). The treatment with Aneustat led to upregulation of genes of the glutaminolysis pathway (Fig. 4.3).

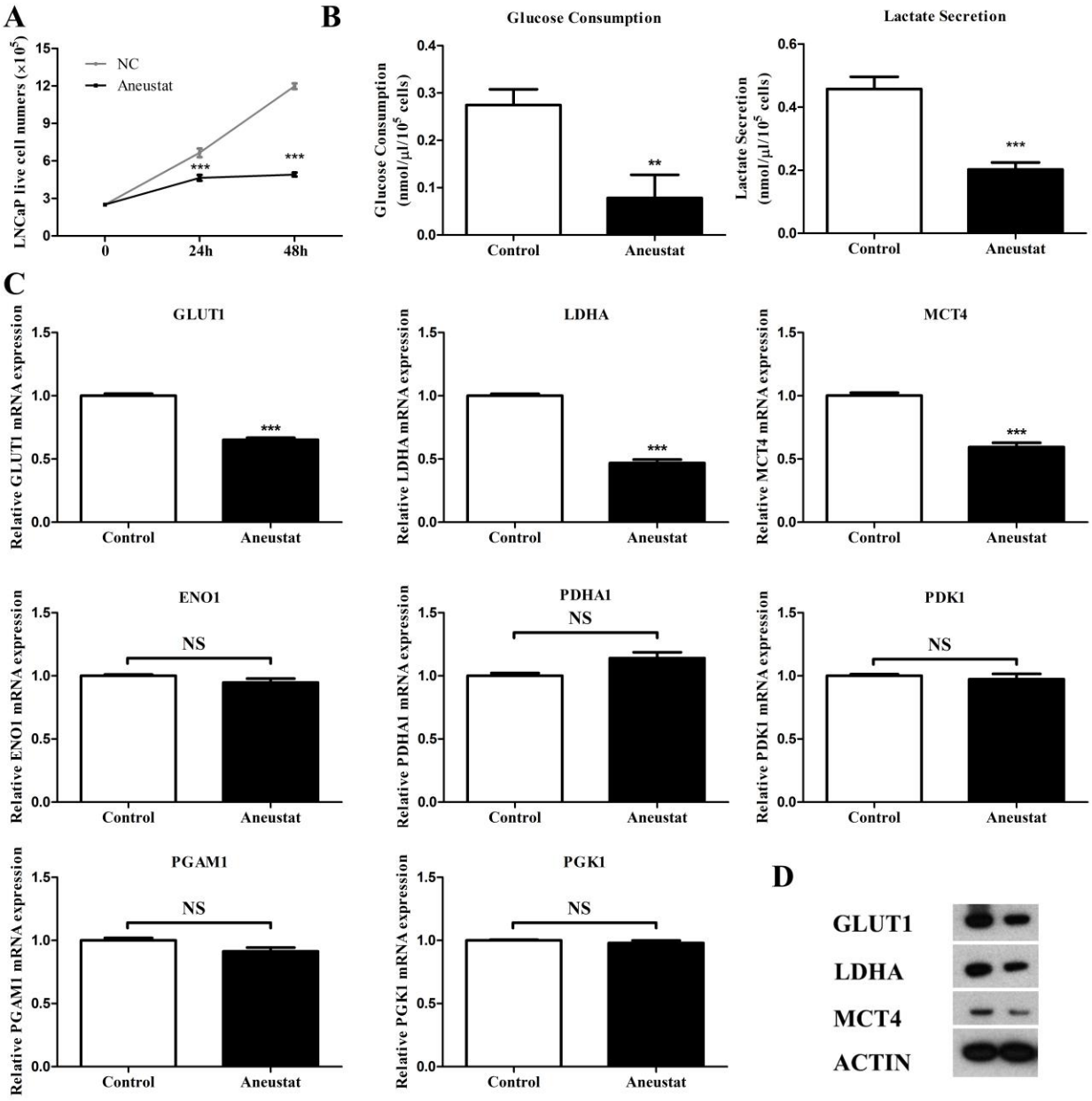

Figure 4.2 Effects of Aneustat on LNCaP Cells.

LNCaP prostate cancer cells were treated with Aneustat. Effect of Aneustat (200 μg/ml) on (A) cell numbers at 24h and 48h; (B) glucose consumption and lactate secretion at 48h; (C) mRNA expression of genes of the aerobic glycolysis pathway at 48h; (D) protein expression of *GLUT1*, *LDHA* and *MCT4* at 48h. The experiment was performed in triplicate. ** indicates $p < 0.01$; *** indicates $p < 0.001$; NS indicates no statistical significance.

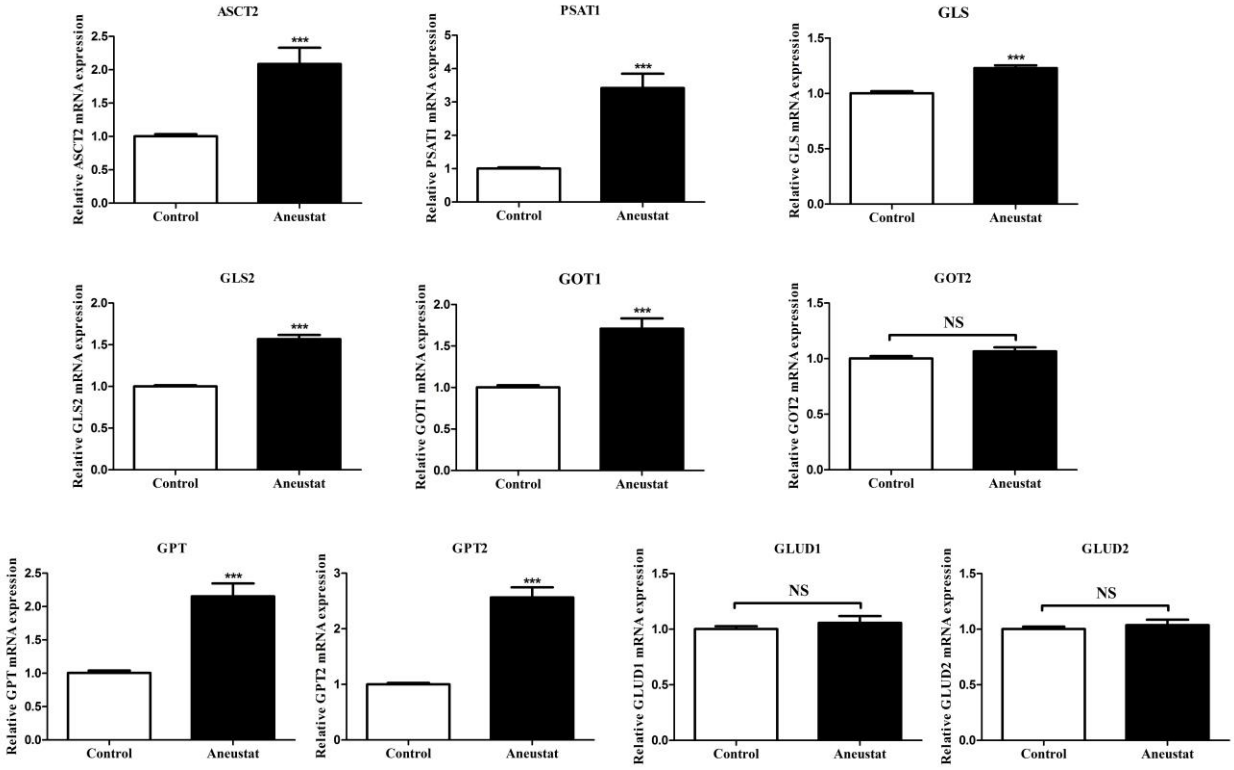

Figure 4.3 Up-regulation of glutaminolysis pathway genes by Aneustat.

LNCaP prostate cancer cells were treated with Aneustat (200 μg/ml) for 48h. The relative mRNA expressions of genes of the glutaminolysis pathway were determined by qPCR. The experiment was performed in triplicate. *** indicates $p < 0.001$; NS indicates no statistical significance.

4.3.4 Effects of Aneustat on Tumor Growth and Relative Levels of Mouse Host Immune Cells in LNCaP Xenografts

A 3-week treatment of male athymic nude mice bearing LNCaP xenografts with Aneustat (1652 mg/kg) markedly inhibited the growth of the xenografts (Fig. 4.4); there was no major host toxicity as assessed by animal body weights and behavior. Using tissue sections of the xenografts, the effect of Aneustat on the relative levels of host mouse NK cells and mouse myeloid-derived suppressor cells (MDSCs) were determined by IHC, using NK1.1 [410] and Ly6G [411] markers, respectively. As shown in Figure 4.5, the relative numbers of intratumoral $NK1.1^{+}$ NK cells, the major functional cytotoxic immune cell subtype in nude mice [412], were higher in the Aneustat-treated than in the control tissues; in contrast, the relative numbers of immunosuppressive MDSCs [210], were significantly lower in the Aneustat-treated tissues than in the control tissues.

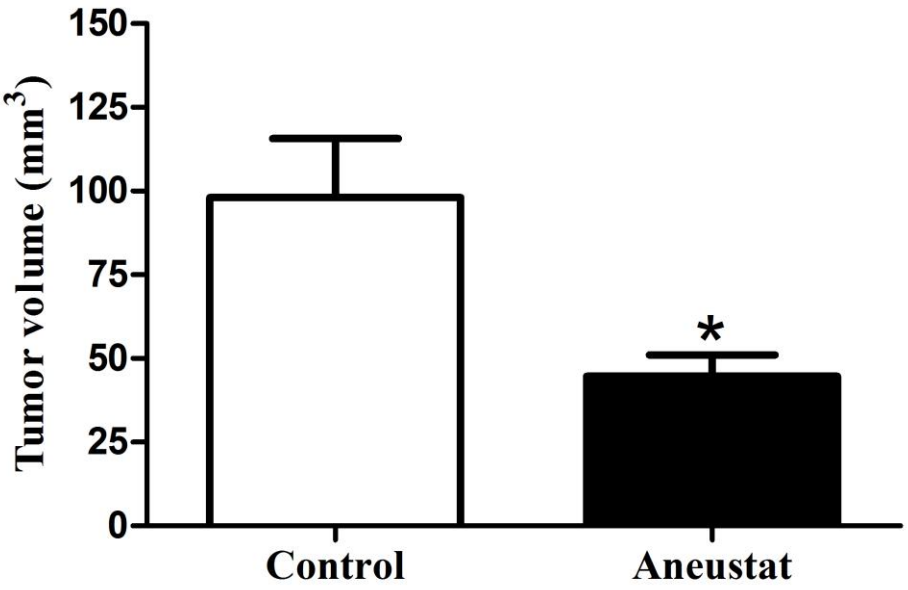

Figure 4.4 Effects of a 3-week treatment with Aneustat on the growth of LNCaP cell line xenografts.

Vehicle control; Aneustat (1652 mg/kg, Q1d×5/3). Treatment with Aneustat markedly inhibited the growth of LNCaP xenografts (n=20; mean ± SEM). No major host toxicity was observed. * indicates $p < 0.05$.

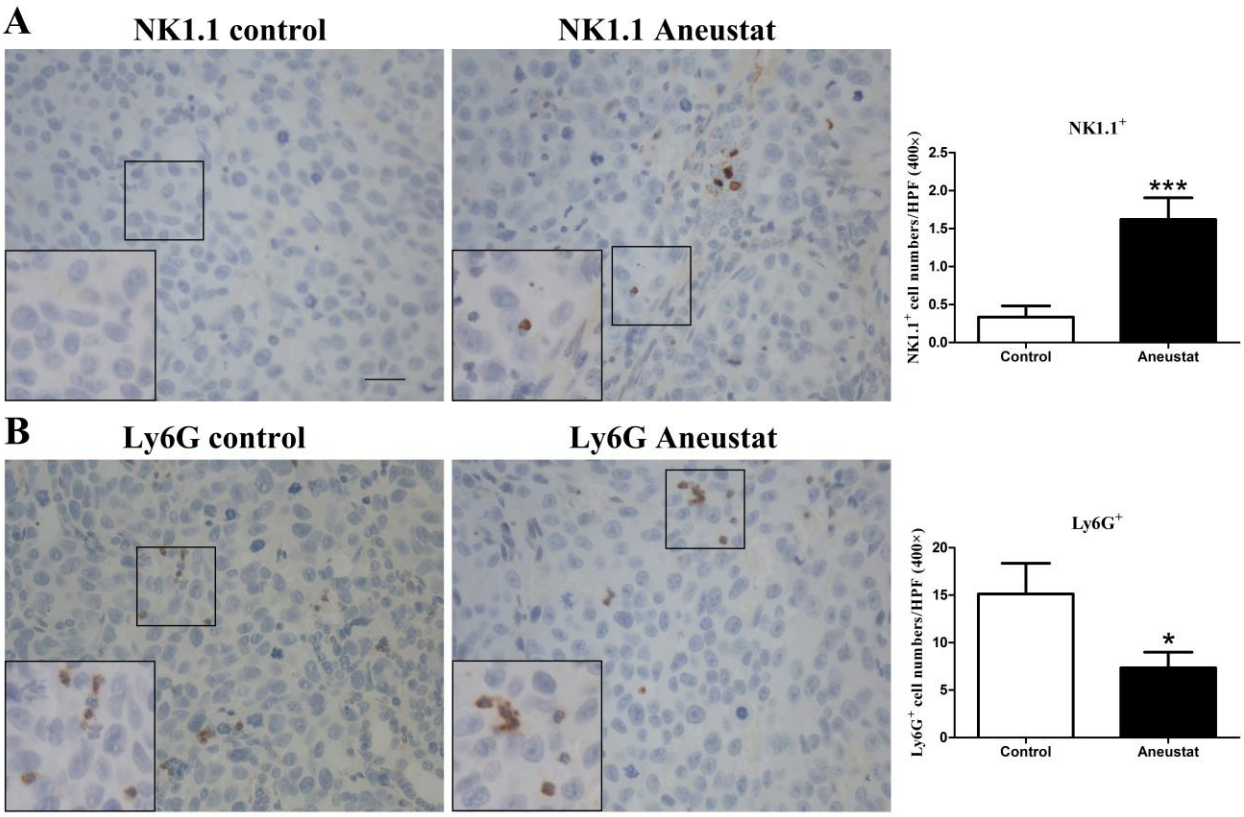

Figure 4.5 Effect of Aneustat on the relative levels of mouse NK1.1$^+$ cells and Ly6G$^+$ cells in LNCaP xenografts.

Athymic nude mice bearing LNCaP xenografts were treated for 3 weeks with Aneustat (1652 mg/kg) or vehicle control. The numbers of NK1.1$^+$ NK cells (A) and Ly6G$^+$ MDSCs (B) in the xenografts were counted using a 400× magnification. * indicates $p < 0.05$; *** indicates $p < 0.001$. Scale bar: 20 μm.

4.3.5 Effect of Aneustat on the Relative Levels of Patient Immune Cells in First-Generation Patient-derived Prostate Cancer Tissue Xenografts

To investigate whether Aneustat has an effect on the relative levels of intratumoral patient immune cells, a first-generation patient-derived xenograft model of metastatic prostate cancer lymph node tissue was used; later generations of xenografts would be deficient in human immune cells. To this end, the xenograft-bearing mice were treated, 10 days after grafting, for 3 weeks with Aneustat (1652 mg/kg) or vehicle control. No major host toxicity was observed. Quantification of patient immune cells in the xenograft tissues that positively stained for various human immune cell markers was used to assess the effect of Aneustat. As shown in Figure 4.6, the relative numbers of intratumoral patient $CD8^+$ cytotoxic T cells were similar in the Aneustat-treated and control tissues. In contrast, the numbers of $FOXP3^+$ Treg cells were markedly lower (by >90%) in the Aneustat-treated tissues than in the control tissues, reflecting a higher ratio of intratumoral patient cytotoxic T cells to regulatory T cells in the Aneustat-treated tissues. NK cells and MDSCs were identified by staining with NCR1 and CD33, respectively [413-415]. As shown in Figure 4.7, the Aneustat-treated tissues showed higher $NCR1^+$ NK cell numbers compared to controls, whereas the MDSCs in the Aneustat-treated tissues were lower in number than in the controls. Taken together, the data indicate that treatment of the metastatic prostate cancer lymph node xenografts with Aneustat was associated with higher numbers of host cytotoxic immune cells and lower numbers of host immunosuppressive cells.

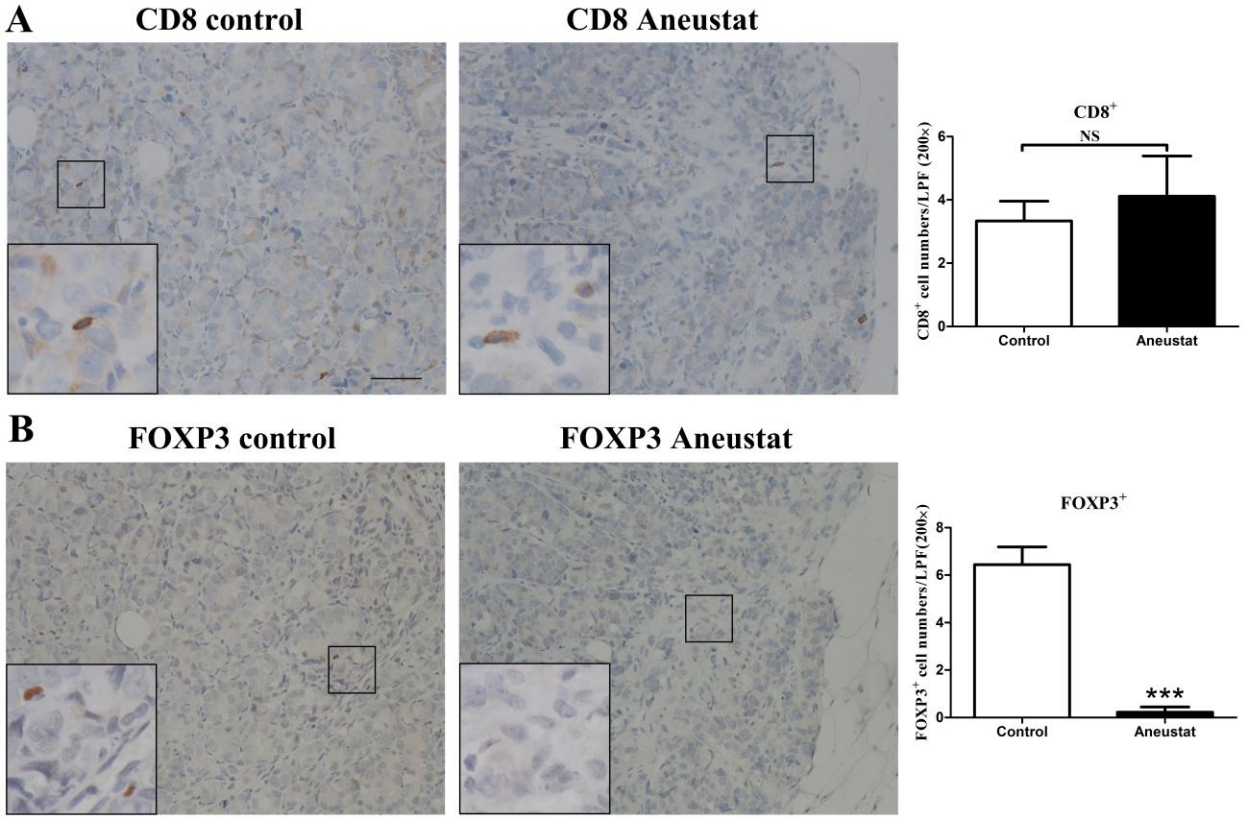

Figure 4.6 Effect of Aneustat on the relative levels of patient CD8$^+$ cells and FOXP3$^+$ cells in first-generation patient-derived prostate cancer xenografts.

NSG mice bearing first-generation prostate cancer xenografts were treated for 3 weeks with Aneustat (1652 mg/kg) or vehicle control. (A) The number of CD8$^+$ T cells and (B) the number of FOXP3$^+$ Treg cells in the xenografts were determined using a 200× magnification. *** indicates $p < 0.001$; NS indicates no significance. Scale bar: 50 μm.

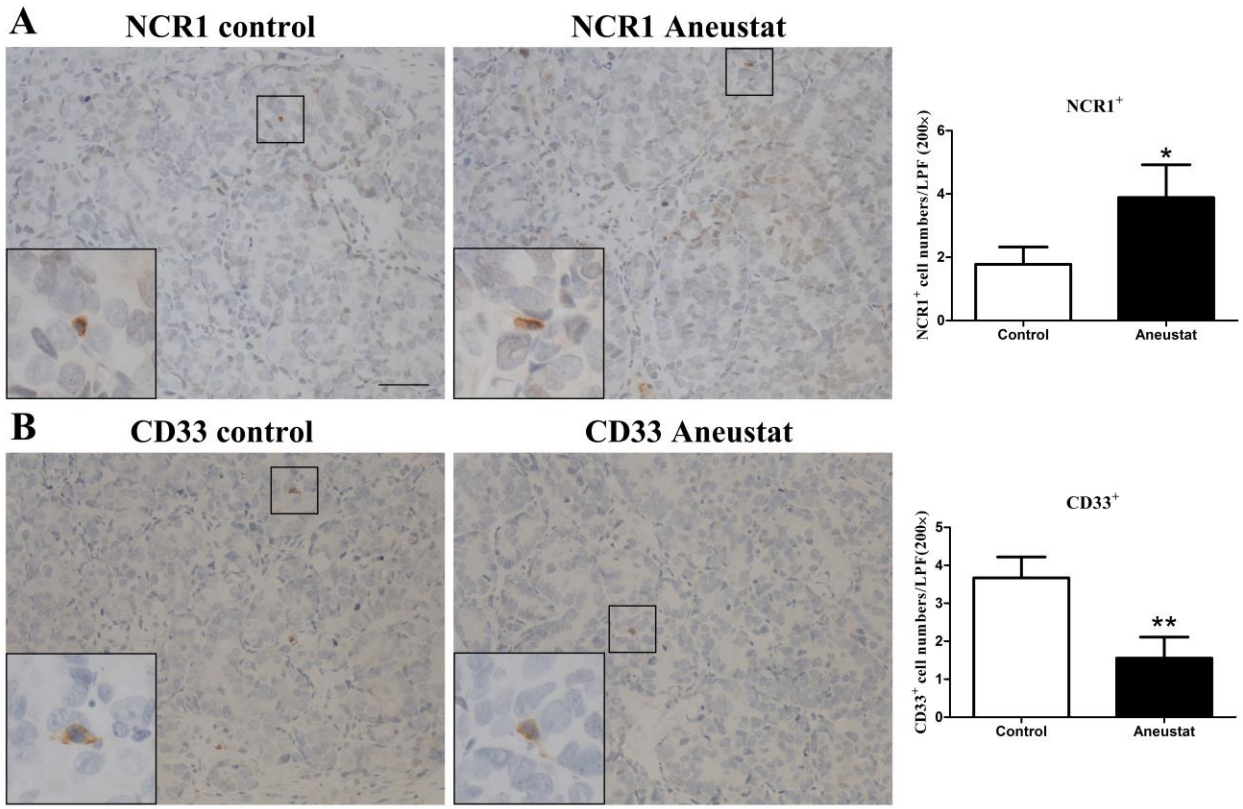

Figure 4.7 Effect of Aneustat on the relative levels of patient NCR1$^+$ cells and CD33$^+$ cells in first-generation patient-derived prostate cancer xenografts.

NSG mice bearing first-generation prostate cancer xenografts were treated for 3 weeks with Aneustat (1652 mg/kg) or vehicle control. (A) The numbers of NCR1$^+$ NK cells and (B) the number of CD33$^+$ MDSCs in the xenografts were counted using a 200× magnification. * indicates $p < 0.05$; ** indicates $p < 0.01$. Scale bar: 50 μm.

4.4 Discussion

The present study has demonstrated that Aneustat markedly inhibits LNCaP prostate cancer growth both *in vitro* and *in vivo*, consistent with previously reported findings [310]. The arrest of LNCaP cell proliferation by Aneustat is likely a result of its inhibition of aerobic glycolysis (Fig. 4.2). Thus, as shown in Figure 4.2, *in vitro* incubation of LNCaP cells with Aneustat led to a substantial decrease in their lactic acid secretion (~56%), which was associated with a substantial decrease in glucose consumption (~82%) and down regulation of the expression of major glycolysis-related genes, i.e. *GLUT1* (glucose transporter), *LDHA* (lactate dehydrogenase A) and *MCT4* (lactate transporter) (Fig. 4.2). The finding that Aneustat led to up-regulation of genes of the glutaminolysis pathway (Fig. 4.3), suggests that this pathway was used by the LNCaP cells as an alternative route to generate more lactate. However, as the amount of glutaminolysis-generated lactate in general is much smaller than the amount of lactate generated via aerobic glycolysis [416-418], it would not greatly affect the inhibition by Aneustat of lactic acid secretion (Fig. 4.2B). The finding that Aneustat inhibited the aerobic glycolysis of LNCaP prostate cancer cells confirms the predictions by Oncomine analysis that Aneustat plays an important role in energy metabolism as one of a number of important physiological processes (Table 4.2). As cancer growth greatly relies on aerobic glycolysis [352, 419], the inhibition of aerobic glycolysis by Aneustat could be a major mechanism by which it may inhibit the proliferation of LNCaP prostate cancer cells *in vitro* and *in vivo*.

Although Aneustat markedly inhibited the growth of LNCaP cell xenografts (Fig. 4.4), it did not significantly inhibit the growth of patient-derived LTL-313H prostate cancer xenografts (Fig. 2.2). This discrepancy may tentatively be explained by basic differences between the two mouse models. The LNCaP xenograft model is based on nude, immunocompromised mice that

still contain functional cytotoxic NK cells [412]. In contrast, the LTL-313H PDX model is based on immunodeficient mice totally lacking functional immune cells. In the present study, treatment with Aneustat was found to favor the host anticancer immune response. Consequently, the growth inhibition by Aneustat of the LNCaP xenografts may be based - to some extent - on Aneustat-induced stimulation of cytotoxic NK cells. Other differences that play a role may include: differences in responses to Aneustat between LTL-313H prostate cancer cells and LNCaP prostate cancer cells and greater cancer heterogeneity in the LTL-313H xenografts.

In the present study it was found that Aneustat has immunomodulatory activity. Thus treatment with Aneustat led to differentiation of RAW264.7 macrophages to the M1 anticancer phenotype (Fig. 4.1). Importantly, treatment with Aneustat of metastatic prostate cancer tissue xenografts and LNCaP xenografts led in both cases to marked changes in the levels of intratumoral host (patient/mouse) immune cells favoring the host anticancer immune response, i.e. a higher ratio of intratumoral cytotoxic $CD8^+$ T cells/Treg cells, higher numbers of intratumoral NK cells, and lower numbers of intratumoral MDSCs (Figs 4.5, 4.6 and 4.7). Similar changes in levels of host immune cells have been reported for mouse melanoma allografts in immunocompetent mice when their lactic acid secretion was reduced (via specific depletion of glycolysis-related LDHA the enzyme involved in the conversion of pyruvate to lactate) [236]. In view of this, it appears likely that the immunomodulatory activity of Aneustat is based on reduction of cancer-generated lactic acid secretion as obtained via aerobic glycolysis inhibition (Fig. 4.2). As such, this study shows, for the first time, that Aneustat has immunomodulatory properties based on (i) ability to induce macrophage differentiation, and (ii) inhibition of aerobic glycolysis leading to reduced secretion of cancer-generated lactic acid. The

data are consistent with the Oncomine analysis of the microarray data of Aneustat-treated LTL-313H xenografts indicating that Aneustat affected the immune response (Table 4.2).

Since treatment with Aneustat appears to favor the host anticancer immune response, as indicated by the present study, it may lead to reduction of cancer-induced immunosuppression in immunocompetent hosts. This suggestion is supported by the finding in the Aneustat Phase-I clinical trial that treatment with Aneustat led to a reduction in the levels of immune suppression markers in patients [326]. Further studies are needed to establish the mechanisms of action underlying the immunomodulatory activity of Aneustat. Restoration of the host anticancer immune response by Aneustat should be beneficial for potential clinical therapy of advanced prostate cancers using docetaxel combined with Aneustat.

Patient-derived xenograft (PDX) cancer models have become widely used in cancer research, in particular subrenal capsule xenografts which show very high fidelity to the original patient tumors with regard to histopathology, tumor heterogeneity, tissue architecture, gene expression profiles and tumor aggressiveness [272]. The main limitation of PDX models is the absence of a functional immune system, making them unsuitable for comprehensive immunological studies [420]. However, as shown by the present study, first-generation PDX models contain a variety of tumor-infiltrated patient immune cells, as distinct from later generation models that do not have this feature, since patient immune cells vanish on serial propagation of the xenografts. As such, first-generation PDX models may provide limited use for immunological studies such as investigations of the effect of candidate drugs on the levels of the patient immune cells. They may find application in screening drugs/compounds for immunomodulatory properties.

In conclusion, the present study has shown that Aneustat has immunomodulatory activity, as indicated, in particular, by its induction of a shift in the levels of intratumoral host immune cells which favor the host anticancer immune response. This immunomodulatory activity appears to be based on Aneustat-induced inhibition of aerobic glycolysis leading to a reduction in the secretion of cancer-generated lactic acid and hence reduced acidification of the tumor microenvironment. Furthermore, first-generation patient-derived cancer tissue xenograft models may be used for screening immunomodulatory activity of compounds.

Chapter 5: Conclusions

5.1 Summary of Study and Findings

Docetaxel, applied with or without prednisone, was the first chemotherapeutic drug whose application in advanced prostate cancer treatment led to a minor extension of patient survival. Nevertheless, docetaxel-based chemotherapy is currently the standard treatment for prostate cancers that no longer respond to hormone ablation therapy, i.e. CRPCs. Studies aimed at improving its efficacy against CRPCs have focused on combining docetaxel, as a pivot drug, with a wide variety of anticancer agents. Regrettably, none of such drug combinations in Phase III clinical trials has yet demonstrated an improvement in patient survival [192-194]. Prostate cancer is difficult to treat, as it is a heterogeneous disease and can consist of treatment-resistant subpopulations in addition to treatment-sensitive subpopulations; in addition it has an ability, based on plasticity, to evade therapy by switching from a targeted pathway to a non-targeted one. As such, it appeared useful to treat prostate cancer using multiple pathway targeting. For this purpose, the multivalent immuno-oncology drug candidate, Aneustat, was used in combination with docetaxel, as pre-clinical studies had indicated that it can target multiple independent pathways. Furthermore, a Phase I Clinical Trial had shown that Aneustat was well-tolerated by patients and that it had immunomodulatory properties that could promote the host anticancer immune response [326].

The main objectives of this doctoral study were (i) to determine whether docetaxel-based therapy of prostate cancer can be improved by combining docetaxel with Aneustat, and (ii) to confirm that Aneustat has immunomodulatory properties. My working hypotheses were: (i) As Aneustat has anti-prostate cancer and anti-metastatic activity, as well as multiple targeting ability, combined use of docetaxel and Aneustat can achieve more potent anticancer efficacy, and (ii)

Aneustat can enhance anticancer activity by immunomodulation leading to an increased host anticancer immune response.

In Chapter 2, I have examined the anticancer efficacies of docetaxel, Aneustat and docetaxel+Aneustat using the high fidelity, clinically relevant LTL-313H patient-derived prostate cancer xenograft model, as PDX models have recently been recommended by the NCI for determining efficacies of anticancer drugs. I found that the anticancer activity of docetaxel+Aneustat was much higher than the sum of the activities of docetaxel and Aneustat used as single drugs. In fact, docetaxel+Aneustat led to complete growth inhibition and shrinkage of prostate cancer xenografts without major host toxicity. Microarray analysis of gene expression profiles of the xenografts indicated that the combination of docetaxel and Aneustat led to expanded anticancer activities that were not obtained by the drugs on their own. The results are consistent with the notion that improved therapeutic efficacy in a heterogeneous prostate cancer could be achieved with drugs targeting multiple independent pathways and combination therapies. As such, the findings indicate, for the first time, that docetaxel-based therapy of advanced human prostate cancer may be improved by combining docetaxel with Aneustat.

In Chapter 3, I further investigated the biological effects of the combination of docetaxel and Aneustat on the LTL-313H prostate cancer xenograft model. Furthermore, I proposed a novel method for analyzing invasion by cancer cells of local kidney tissue, a unique phenomenon for subrenal capsule xenografts. I found that treatment with the combination of docetaxel and Aneustat can markedly inhibit LTL-313H prostate cancer xenograft lung micro-metastasis and local (kidney) tissue invasion *in vivo* and C4-2 cell migration *in vitro*. Analysis of gene expression microarray data using Oncomine software indicated that there was a high correlation

between the treatment with the drug combination and better patient outcome. The drug combination affected a variety of upstream regulators, in particular *FOXM1*, which was functionally validated as one of the cancer driver genes whose expression was suppressed by the combination. The data indicate that the combination of docetaxel and Aneustat may be exploited as a new regimen for metastatic prostate cancer treatment in the clinic.

In Chapter 4, I obtained evidence confirming that Aneustat has immunomodulatory activity. The data show that Aneustat induced the differentiation of RAW264.7 macrophages to the M1 phenotype and was not toxic. As well, Aneustat did not only inhibit prostate cancer growth both *in vitro* and *in vivo*, but it can also suppress cancer-generated lactic acid secretion by inhibiting the aerobic glycolysis pathway. This is of paramount importance as suppression of the host local anticancer immunity is thought to be mainly due to acidification of the tumor microenvironment caused by elevated secretion of cancer-generated lactic acid. Furthermore, it was found that treatment with Aneustat of a first-generation PDX prostate cancer model led to a relatively higher ratio of $CD8^+$ T cells to Treg cells, higher numbers of NK cells and relatively lower numbers of host Treg cells and MDSCs, i.e. changes favoring the host anticancer immune response. Similar changes have been reported for the levels of mouse host immune cells in mouse melanoma allografts following specific reduction of lactic acid production [236]. Accordingly, our study indicates, for the first time, that Aneustat may favor the host anticancer immune response by (i) inhibiting cancer-generated lactic acid secretion, and (ii) altering immune cell differentiation. Furthermore, first-generation PDX tumor models may be used for screening immunomodulatory activity of compounds and botanical products.

5.2 Conclusions Regarding the Study Hypotheses

In conclusion, this doctoral study has demonstrated that the anticancer activity of docetaxel+Aneustat was markedly higher than the sum of the anticancer activities of the single drugs, as the drug combination led to complete inhibition of tumor growth associated with some tumor shrinkage. Treatment with the drug combination also substantially inhibited prostate cancer lung micro-metastasis and local (kidney) tissue invasion. Functional validation of *FOXM1* demonstrated that it is one of the major cancer driver genes whose expression is suppressed by the drug combination. Analyses of gene expression microarray data indicated that treatment with docetaxel+Aneustat is associated with better prognosis, and that the drug combination showed expanded anticancer activity by targeting multiple pathways and hallmarks of cancer, particularly those not obtained by single drugs. The above findings support the hypothesis that the combination of Aneustat and docetaxel can lead to markedly higher anticancer activity than obtained with docetaxel alone. The Aneustat-induced shift in the levels of patient immune cells favoring the host anticancer immune response can be explained by Aneustat (i) acting as an inhibitor of aerobic glycolysis, thus reducing the secretion of lactic acid into the tumor microenvironment, which leads to lower local immunosuppression, and (ii) altering immune cell differentiation. These findings support the hypothesis that Aneustat may also enhance anticancer activity by boosting the local host immune response.

5.3 Strengths and Limitations

To obtain evidence that Aneustat could be used to improve docetaxel-based therapy of advanced prostate cancer patients, the anticancer efficacy of docetaxel+Aneustat, as distinct from the individual drugs, was determined using the high-fidelity LTL-313H patient-derived metastatic prostate cancer tissue xenograft model. The results obtained showed that the tumor growth-

inhibitory effect obtained with docetaxel+Aneustat markedly exceeded that obtained with docetaxel or Aneustat alone, and was associated with substantial inhibition of prostate cancer lung micro-metastasis and local (kidney) tissue invasion, not found for the individual drugs. Furthermore, the combination of docetaxel and Aneustat showed anticancer activities which were not exhibited by the drugs on their own, such as targeting (i) the master metastasis regulator FOXM1, (ii) multiple canonical pathways, in particular, aerobic glycolysis, and (iii) many cancer hallmarks. As the LTL-313H metastatic prostate cancer xenograft model has been demonstrated to have high clinical relevance, the data indicate that combining docetaxel with Aneustat may likely lead to improved clinical therapy of advanced prostate cancer.

Evidence strongly supporting the notion that treatment of cancers with Aneustat may lead to restoration (at least in part) of host local anticancer immunity was obtained by establishing that treatment with Aneustat can (i) inhibit aerobic glycolysis, thereby reducing cancer-generated secretion of lactic acid thought to underlie cancer-induced immunosuppression, and (ii) lead to a shift in the levels of intratumoral patient immune cells favoring the host anticancer immune response. The latter was demonstrated with first-generation patient-derived prostate cancer xenograft models, which I proposed, as a first, may be used for screening compounds and botanical preparations for immunomodulatory activity.

While the above studies of the anticancer efficacy of combined use of docetaxel and Aneustat are quite satisfying, only one patient-derived prostate cancer tissue xenograft model was used. Using a number of such models, more comprehensive information can be obtained with regard to, for example, tumor heterogeneity and identification of non-responsive subpopulations for future clinical trials.

With regard to the use of first-generation PDX models for immunological studies, there are a number of obvious limitations. Thus such first-generation xenografts do not contain a functional human immune system acting as a continuous source of human immune cells. Furthermore, increases and decreases in the number of patient immune cells, for example, can at present not be explained mechanistically. More studies are needed to establish the properties and potential applications of first-generation PDX models.

5.4 Overall Significance and Clinical Implications

The overall significance of this doctoral study is that it has made a number of observations, for the first time, which are potentially of high impact in the oncological field. First, although it is known that herbal medicine can have immunomodulatory activities, the mechanisms by which it can lead to changes in the levels/activities of immune cells are largely unknown. With today's increased understanding of the complexity of the tumor microenvironment, energy metabolism, immunology and the interaction of cancer cells and immune cells, it was possible to show that Aneustat, first-of-a-class of multivalent immuno-oncology drug candidates, is favoring the host anticancer immune response indirectly by inhibition of aerobic glycolysis leading to reduced production/secretion of cancer-generated lactic acid. This finding provides evidence and leads to a novel research direction in the field. Furthermore, this finding is of paramount importance in that it will likely expand the future clinical use of Aneustat, not only as anticancer drug, but also as immunomodulatory drug, for treatment of prostate cancer or other types of cancer.

Second, I have demonstrated that first-generation patient-derived xenograft models contain patients' immune cells, as distinct from well-established PDX models, and therefore may be used for limited immunological studies such as screening of compounds and botanical products for immunomodulatory activity. As such, first-generation PDX models will likely

provide fast and convenient tools with wide application in evaluating immunomodulatory activity of clinically useful drugs.

Third, the finding that docetaxel+Aneustat act synergistically with regard to arrest of tumor growth and inhibition of lung micro-metastasis and kidney invasion, is highly significant. As this was demonstrated with a clinically relevant PDX prostate cancer model, it indicates potential improvement of current clinical prostate cancer therapy: (i) the first-line docetaxel-based therapy of advanced human prostate cancer may be improved by using docetaxel in combination with Aneustat, and (ii) combined use of docetaxel and Aneustat could also be a regimen for treatment of early stage prostate cancer.

Gene expression analysis of prostate cancer xenografts treated with docetaxel, Aneustat and their combination, has indicated that the two drugs can synergistically target multiple pathways that are not targeted by the drugs on their own. Treatments based on single targets are considered to be less effective for heterogeneous malignancies such as prostate cancers. A combination of drugs such as docetaxel+Aneustat targeting multiple pathways would provide a potential solution to overcome therapy resistance due to tumor heterogeneity.

This study has shown that master transcription regulators of cancer progression, e.g., *FOXM1*, and multiple canonical pathways, such as aerobic glycolysis, are dramatically affected by docetaxel+Aneustat. This suggests that treatment with docetaxel+Aneustat may be particularly beneficial for prostate cancer patients exhibiting elevated FOXM1 expression or elevated aerobic glycolytic activity.

Overall survival and progression-free survival are widely used as endpoints in clinical trials of cancer therapeutics [421, 422]. In view of the above findings, it is very likely that

treatment of advanced prostate cancer patients with docetaxel+Aneustat will prolong their survival time and disease progression-free time.

The findings made in this doctoral study have promoted the registration and conduct of Aneustat in a Phase I clinical trial, and provided scientific evidence for Aneustat to enter a Phase II clinical trial.

5.5 Future Research Directions

Castration-resistant prostate cancer (CRPC), resulting from the development of treatment resistance in prostate cancers to androgen-deprivation therapy (ADT), is a major challenge in the clinical management of advanced prostate cancer. However, most CRPCs still rely on the androgen receptor (AR) for growth and survival. Consequently, Enzalutamide, a next generation AR-targeting therapeutic, was approved for treatment of CRPC patients as both post-docetaxel therapy in 2012 [145, 423] and pre-docetaxel therapy in 2014 [144, 423]. Unfortunately, treatment with Enzalutamide is not curative and treatment resistance is quickly developed in patients [424, 425]. When Enzalutamide was used as post-docetaxel therapy, about one-fourth of patients showed primary resistance to Enzalutamide and developed disease progression in 3 months, while other, initially responsive patients showed disease progression in 24 months [145, 426]. The mechanisms of Enzalutamide resistance development have been categorized as AR mutations; AR splicing variants, e.g., AR-V7; AR bypass pathways, e.g., glucocorticoid receptor activation; *de novo* androgen biosynthesis, such as adrenal or intratumoral androgen production; and complete AR independence, such as activation of the AKT pathway [424, 425].

The current project has shown that Aneustat, a herbal mixture, has multiple targeting capacities, including an ability to inhibit AR and p-AKT expression in C4-2 cells. As well, microarray analysis using IPA showed that treatment of LTL-313H xenografts with Aneustat

could activate the LXR/RXR pathway, which can reduce the levels of cholesterol, i.e. a precursor of *de novo* androgen biosynthesis [427]. As such, combined use of Enzalutamide and Aneustat could have synergistically increased anticancer activity, since Aneustat not only shares similar anti-prostate cancer mechanisms with Enzalutamide, such as inhibition of AR signaling, but also has complementary anticancer activity compared to Enzalutamide, as mentioned above.

In the present study, Aneustat has been demonstrated to have immunomodulatory activity favoring the host anticancer immune response. In addition, in view of its multiple targeting properties, it would be interesting to determine the anticancer efficacy of Aneustat against other types of cancer using immunocompetent models, used either as a single drug or in combination with other anticancer agents.

Bibliography

[1] R.L. Siegel, K.D. Miller, A. Jemal, Cancer statistics, 2016, CA Cancer J Clin, 66 (2016) 7-30.

[2] D.G. Bostwick, The pathology of early prostate cancer, CA Cancer J Clin, 39 (1989) 376-393.

[3] A. Prajapati, S. Gupta, B. Mistry, Prostate stem cells in the development of benign prostate hyperplasia and prostate cancer: emerging role and concepts, Biomed Res Int, 2013 (2013) 107954.

[4] F. Zustovich, D. Pastorelli, Therapeutic management of bone metastasis in prostate cancer: an update, Expert Rev Anticancer Ther, (2016) 1-13.

[5] E.J. Small, P.F. Schellhammer, C.S. Higano, C.H. Redfern, J.J. Nemunaitis, F.H. Valone, S.S. Verjee, L.A. Jones, R.M. Hershberg, Placebo-controlled phase III trial of immunologic therapy with sipuleucel-T (APC8015) in patients with metastatic, asymptomatic hormone refractory prostate cancer, J Clin Oncol, 24 (2006) 3089-3094.

[6] J.C. Thompson, J. Wood, D. Feuer, Prostate cancer: palliative care and pain relief, Br Med Bull, 83 (2007) 341-354.

[7] M. Kirby, C. Hirst, E.D. Crawford, Characterising the castration-resistant prostate cancer population: a systematic review, Int J Clin Pract, 65 (2011) 1180-1192.

[8] E.T. Ruijter, G.J. Miller, C.A. van de Kaa, A. van Bokhoven, M.J. Bussemakers, F.M. Debruyne, D.J. Ruiter, J.A. Schalken, Molecular analysis of multifocal prostate cancer lesions, J Pathol, 188 (1999) 271-277.

[9] W.A. Schulz, M. Burchardt, M.V. Cronauer, Molecular biology of prostate cancer, Mol Hum Reprod, 9 (2003) 437-448.

[10] B.J. Feldman, D. Feldman, The development of androgen-independent prostate cancer, Nat Rev Cancer, 1 (2001) 34-45.

[11] T. Karantanos, P.G. Corn, T.C. Thompson, Prostate cancer progression after androgen deprivation therapy: mechanisms of castrate resistance and novel therapeutic approaches, Oncogene, 32 (2013) 5501-5511.

[12] D. Lin, P.W. Gout, Y. Wang, Lessons from in-vivo models of castration-resistant prostate cancer, Curr Opin Urol, 23 (2013) 214-219.

[13] F. Crea, E. Venalainen, X. Ci, H. Cheng, L. Pikor, A. Parolia, H. Xue, N.R. Nur Saidy, D. Lin, W. Lam, C. Collins, Y. Wang, The role of epigenetics and long noncoding RNA MIAT in neuroendocrine prostate cancer, Epigenomics, 8 (2016) 721-731.

[14] K.H. Leissner, L.E. Tisell, The weight of the human prostate, Scand J Urol Nephrol, 13 (1979) 137-142.

[15] G.R. Cunha, A.A. Donjacour, P.S. Cooke, S. Mee, R.M. Bigsby, S.J. Higgins, Y. Sugimura, The endocrinology and developmental biology of the prostate, Endocr Rev, 8 (1987) 338-362.

[16] Y. Wang, S. Hayward, M. Cao, K. Thayer, G. Cunha, Cell differentiation lineage in the prostate, Differentiation, 68 (2001) 270-279.

[17] J.E. McNeal, Normal histology of the prostate, Am J Surg Pathol, 12 (1988) 619-633.

[18] A. Staack, A.A. Donjacour, J. Brody, G.R. Cunha, P. Carroll, Mouse urogenital development: a practical approach, Differentiation, 71 (2003) 402-413.

[19] S.W. Hayward, G.R. Cunha, The prostate: development and physiology, Radiol Clin North Am, 38 (2000) 1-14.

[20] G.R. Cunha, W. Ricke, A. Thomson, P.C. Marker, G. Risbridger, S.W. Hayward, Y.Z. Wang, A.A. Donjacour, T. Kurita, Hormonal, cellular, and molecular regulation of normal and neoplastic prostatic development, J Steroid Biochem Mol Biol, 92 (2004) 221-236.

[21] A.A. Thomson, G.R. Cunha, P.C. Marker, Prostate development and pathogenesis, Differentiation, 76 (2008) 559-564.

[22] G.R. Cunha, Y.K. Hom, Role of mesenchymal-epithelial interactions in mammary gland development, J Mammary Gland Biol Neoplasia, 1 (1996) 21-35.

[23] S.W. Hayward, R. Del Buono, N. Deshpande, P.A. Hall, A functional model of adult human prostate epithelium. The role of androgens and stroma in architectural organisation and the maintenance of differentiated secretory function, J Cell Sci, 102 (Pt 2) (1992) 361-372.

[24] A. Staack, A.P. Kassis, A. Olshen, Y. Wang, D. Wu, P.R. Carroll, G.D. Grossfeld, G.R. Cunha, S.W. Hayward, Quantitation of apoptotic activity following castration in human prostatic tissue in vivo, Prostate, 54 (2003) 212-219.

[25] P.H. Gann, Risk factors for prostate cancer, Rev Urol, 4 Suppl 5 (2002) S3-S10.

[26] M.M. Kgatle, A.A. Kalla, M.M. Islam, M. Sathekge, R. Moorad, Prostate Cancer: Epigenetic Alterations, Risk Factors, and Therapy, Prostate Cancer, 2016 (2016) 5653862.

[27] T. Kimura, East meets West: ethnic differences in prostate cancer epidemiology between East Asians and Caucasians, Chin J Cancer, 31 (2012) 421-429.

[28] C.F. Heyns, M. Fisher, A. Lecuona, A. van der Merwe, Prostate cancer among different racial groups in the Western Cape: presenting features and management, S Afr Med J, 101 (2011) 267-270.

[29] N.R. Perdana, C.A. Mochtar, R. Umbas, A.R. Hamid, The Risk Factors of Prostate Cancer and Its Prevention: A Literature Review, Acta Med Indones, 48 (2016) 228-238.

[30] J.F. Sauvé, J. Lavoué, M. Parent, Occupation, industry, and the risk of prostate cancer: a case-control study in Montréal, Canada, Environ Health, 15 (2016) 100.

[31] W.A. Sakr, D.J. Grignon, J.D. Crissman, L.K. Heilbrun, B.J. Cassin, J.J. Pontes, G.P. Haas, High grade prostatic intraepithelial neoplasia (HGPIN) and prostatic adenocarcinoma between the ages of 20-69: an autopsy study of 249 cases, In Vivo, 8 (1994) 439-443.

[32] J. Gordetsky, J. Epstein, Grading of prostatic adenocarcinoma: current state and prognostic implications, Diagn Pathol, 11 (2016) 25.

[33] P.A. Humphrey, Gleason grading and prognostic factors in carcinoma of the prostate, Mod Pathol, 17 (2004) 292-306.

[34] P.M. Pierorazio, P.C. Walsh, A.W. Partin, J.I. Epstein, Prognostic Gleason grade grouping: data based on the modified Gleason scoring system, BJU Int, 111 (2013) 753-760.

[35] J.R. Stark, S. Perner, M.J. Stampfer, J.A. Sinnott, S. Finn, A.S. Eisenstein, J. Ma, M. Fiorentino, T. Kurth, M. Loda, E.L. Giovannucci, M.A. Rubin, L.A. Mucci, Gleason score and lethal prostate cancer: does 3 + 4 = 4 + 3?, J Clin Oncol, 27 (2009) 3459-3464.

[36] L. Cheng, R. Montironi, D.G. Bostwick, A. Lopez-Beltran, D.M. Berney, Staging of prostate cancer, Histopathology, 60 (2012) 87-117.

[37] W.J. Catalona, J.P. Richie, F.R. Ahmann, M.A. Hudson, P.T. Scardino, R.C. Flanigan, J.B. deKernion, T.L. Ratliff, L.R. Kavoussi, B.L. Dalkin, Comparison of digital rectal examination and serum prostate specific antigen in the early detection of prostate cancer: results of a multicenter clinical trial of 6,630 men, J Urol, 151 (1994) 1283-1290.

[38] J.W. Moul, Comparison of DRE and PSA in the Detection of Prostate Cancer, J Urol, (2016).

[39] I. Romics, Ultrasound guided biopsy, a gold standard diagnostical test of the prostate cancer, Acta Chir Iugosl, 52 (2005) 23-26.

[40] T.A. Stamey, N. Yang, A.R. Hay, J.E. McNeal, F.S. Freiha, E. Redwine, Prostate-specific antigen as a serum marker for adenocarcinoma of the prostate, N Engl J Med, 317 (1987) 909-916.

[41] K. Lin, R. Lipsitz, T. Miller, S. Janakiraman, U.S.P.S.T. Force, Benefits and harms of prostate-specific antigen screening for prostate cancer: an evidence update for the U.S. Preventive Services Task Force, Ann Intern Med, 149 (2008) 192-199.

[42] F.C. Hamdy, J.L. Donovan, J.A. Lane, M. Mason, C. Metcalfe, P. Holding, M. Davis, T.J. Peters, E.L. Turner, R.M. Martin, J. Oxley, M. Robinson, J. Staffurth, E. Walsh, P. Bollina, J. Catto, A. Doble, A. Doherty, D. Gillatt, R. Kockelbergh, H. Kynaston, A. Paul, P. Powell, S. Prescott, D.J. Rosario, E. Rowe, D.E. Neal, P.S. Group, 10-Year Outcomes after Monitoring, Surgery, or Radiotherapy for Localized Prostate Cancer, N Engl J Med, 375 (2016) 1415-1424.

[43] D.E. Neal, J.L. Donovan, R.M. Martin, F.C. Hamdy, Screening for prostate cancer remains controversial, Lancet, 374 (2009) 1482-1483.

[44] S.A. Strope, G.L. Andriole, Prostate cancer screening: current status and future perspectives, Nat Rev Urol, 7 (2010) 487-493.

[45] M.J. Bussemakers, A. van Bokhoven, G.W. Verhaegh, F.P. Smit, H.F. Karthaus, J.A. Schalken, F.M. Debruyne, N. Ru, W.B. Isaacs, DD3: a new prostate-specific gene, highly overexpressed in prostate cancer, Cancer Res, 59 (1999) 5975-5979.

[46] J. Romero Otero, B. Garcia Gomez, F. Campos Juanatey, K.A. Touijer, Prostate cancer biomarkers: an update, Urol Oncol, 32 (2014) 252-260.

[47] M. Salagierski, J.A. Schalken, Molecular diagnosis of prostate cancer: PCA3 and TMPRSS2:ERG gene fusion, J Urol, 187 (2012) 795-801.

[48] D.A. Sartori, D.W. Chan, Biomarkers in prostate cancer: what's new?, Curr Opin Oncol, 26 (2014) 259-264.

[49] J.J. Tu, S. Rohan, J. Kao, N. Kitabayashi, S. Mathew, Y.T. Chen, Gene fusions between TMPRSS2 and ETS family genes in prostate cancer: frequency and transcript variant analysis by RT-PCR and FISH on paraffin-embedded tissues, Mod Pathol, 20 (2007) 921-928.

[50] B. Han, R. Mehra, R.J. Lonigro, L. Wang, K. Suleman, A. Menon, N. Palanisamy, S.A. Tomlins, A.M. Chinnaiyan, R.B. Shah, Fluorescence in situ hybridization study shows association of PTEN deletion with ERG rearrangement during prostate cancer progression, Mod Pathol, 22 (2009) 1083-1093.

[51] C. Kumar-Sinha, S.A. Tomlins, A.M. Chinnaiyan, Recurrent gene fusions in prostate cancer, Nat Rev Cancer, 8 (2008) 497-511.

[52] J.R. Prensner, A.M. Chinnaiyan, Oncogenic gene fusions in epithelial carcinomas, Curr Opin Genet Dev, 19 (2009) 82-91.

[53] S. Perner, F. Demichelis, R. Beroukhim, F.H. Schmidt, J.M. Mosquera, S. Setlur, J. Tchinda, S.A. Tomlins, M.D. Hofer, K.G. Pienta, R. Kuefer, R. Vessella, X.W. Sun, M. Meyerson, C. Lee, W.R. Sellers, A.M. Chinnaiyan, M.A. Rubin, TMPRSS2:ERG fusion-associated deletions provide insight into the heterogeneity of prostate cancer, Cancer Res, 66 (2006) 8337-8341.

[54] R. Mehra, S.A. Tomlins, J. Yu, X. Cao, L. Wang, A. Menon, M.A. Rubin, K.J. Pienta, R.B. Shah, A.M. Chinnaiyan, Characterization of TMPRSS2-ETS gene aberrations in androgen-independent metastatic prostate cancer, Cancer Res, 68 (2008) 3584-3590.

[55] C. Cai, H. Wang, Y. Xu, S. Chen, S.P. Balk, Reactivation of androgen receptor-regulated TMPRSS2:ERG gene expression in castration-resistant prostate cancer, Cancer Res, 69 (2009) 6027-6032.

[56] X. Qu, G. Randhawa, C. Friedman, B.F. Kurland, L. Glaskova, I. Coleman, E. Mostaghel, C.S. Higano, C. Porter, R. Vessella, P.S. Nelson, M. Fang, A three-marker FISH panel detects more genetic aberrations of AR, PTEN and TMPRSS2/ERG in castration-resistant or metastatic prostate cancers than in primary prostate tumors, PLoS One, 8 (2013) e74671.

[57] K.M. Koo, E.J. Wee, M. Trau, Colorimetric TMPRSS2-ERG Gene Fusion Detection in Prostate Cancer Urinary Samples via Recombinase Polymerase Amplification, Theranostics, 6 (2016) 1415-1424.

[58] D. Gasi Tandefelt, J. Boormans, K. Hermans, J. Trapman, ETS fusion genes in prostate cancer, Endocr Relat Cancer, 21 (2014) R143-152.

[59] C. Alix-Panabières, K. Pantel, Clinical Applications of Circulating Tumor Cells and Circulating Tumor DNA as Liquid Biopsy, Cancer Discov, 6 (2016) 479-491.

[60] J.C. Wan, C. Massie, J. Garcia-Corbacho, F. Mouliere, J.D. Brenton, C. Caldas, S. Pacey, R. Baird, N. Rosenfeld, Liquid biopsies come of age: towards implementation of circulating tumour DNA, Nat Rev Cancer, 17 (2017) 223-238.

[61] G. Siravegna, S. Marsoni, S. Siena, A. Bardelli, Integrating liquid biopsies into the management of cancer, Nat Rev Clin Oncol, (2017).

[62] J.M. Millholland, S. Li, C.A. Fernandez, A.P. Shuber, Detection of low frequency FGFR3 mutations in the urine of bladder cancer patients using next-generation deep sequencing, Res Rep Urol, 4 (2012) 33-40.

[63] Y. Wang, S. Springer, C.L. Mulvey, N. Silliman, J. Schaefer, M. Sausen, N. James, E.M. Rettig, T. Guo, C.R. Pickering, J.A. Bishop, C.H. Chung, J.A. Califano, D.W. Eisele, C. Fakhry, C.G. Gourin, P.K. Ha, H. Kang, A. Kiess, W.M. Koch, J.N. Myers, H. Quon, J.D. Richmon, D. Sidransky, R.P. Tufano, W.H. Westra, C. Bettegowda, L.A. Diaz, N. Papadopoulos, K.W. Kinzler, B. Vogelstein, N. Agrawal, Detection of somatic mutations and HPV in the saliva and plasma of patients with head and neck squamous cell carcinomas, Sci Transl Med, 7 (2015) 293ra104.

[64] Y. Li, X. Zhou, M.A. St John, D.T. Wong, RNA profiling of cell-free saliva using microarray technology, J Dent Res, 83 (2004) 199-203.

[65] W. Pan, W. Gu, S. Nagpal, M.H. Gephart, S.R. Quake, Brain tumor mutations detected in cerebral spinal fluid, Clin Chem, 61 (2015) 514-522.

[66] L. De Mattos-Arruda, B. Weigelt, J. Cortes, H.H. Won, C.K. Ng, P. Nuciforo, F.C. Bidard, C. Aura, C. Saura, V. Peg, S. Piscuoglio, M. Oliveira, Y. Smolders, P. Patel, L. Norton, J. Tabernero, M.F. Berger, J. Seoane, J.S. Reis-Filho, Capturing intra-tumor genetic heterogeneity by de novo mutation profiling of circulating cell-free tumor DNA: a proof-of-principle, Ann Oncol, 25 (2014) 1729-1735.

[67] J.W. Davis, H. Nakanishi, V.S. Kumar, V.A. Bhadkamkar, R. McCormack, H.A. Fritsche, B. Handy, T. Gornet, R.J. Babaian, Circulating tumor cells in peripheral blood samples from patients with increased serum prostate specific antigen: initial results in early prostate cancer, J Urol, 179 (2008) 2187-2191; discussion 2191.

[68] H.I. Scher, X. Jia, J.S. de Bono, M. Fleisher, K.J. Pienta, D. Raghavan, G. Heller, Circulating tumour cells as prognostic markers in progressive, castration-resistant prostate cancer: a reanalysis of IMMC38 trial data, Lancet Oncol, 10 (2009) 233-239.

[69] M.C. Miller, G.V. Doyle, L.W. Terstappen, Significance of Circulating Tumor Cells Detected by the CellSearch System in Patients with Metastatic Breast Colorectal and Prostate Cancer, J Oncol, 2010 (2010) 617421.

[70] S. Volik, M. Alcaide, R.D. Morin, C. Collins, Cell-free DNA (cfDNA): Clinical Significance and Utility in Cancer Shaped By Emerging Technologies, Mol Cancer Res, 14 (2016) 898-908.

[71] L. Legisi, E. DeSa, M.N. Qureshi, Use of the Prostate Core Mitomic Test in Repeated Biopsy Decision-Making: Real-World Assessment of Clinical Utility in a Multicenter Patient Population, Am Health Drug Benefits, 9 (2016) 497-502.

[72] H.Q. Ontario, Prolaris Cell Cycle Progression Test for Localized Prostate Cancer: A Health Technology Assessment, Ont Health Technol Assess Ser, 17 (2017) 1-75.

[73] K.J. Luzzi, I.C. MacDonald, E.E. Schmidt, N. Kerkvliet, V.L. Morris, A.F. Chambers, A.C. Groom, Multistep nature of metastatic inefficiency: dormancy of solitary cells after successful extravasation and limited survival of early micrometastases, Am J Pathol, 153 (1998) 865-873.

[74] R.D. Loberg, D.A. Bradley, S.A. Tomlins, A.M. Chinnaiyan, K.J. Pienta, The lethal phenotype of cancer: the molecular basis of death due to malignancy, CA Cancer J Clin, 57 (2007) 225-241.

[75] P. Mehlen, A. Puisieux, Metastasis: a question of life or death, Nat Rev Cancer, 6 (2006) 449-458.

[76] C.L. Chaffer, R.A. Weinberg, A perspective on cancer cell metastasis, Science, 331 (2011) 1559-1564.

[77] D. Hanahan, R.A. Weinberg, Hallmarks of cancer: the next generation, Cell, 144 (2011) 646-674.

[78] S.Y. Wong, R.O. Hynes, Lymphatic or hematogenous dissemination: how does a metastatic tumor cell decide?, Cell Cycle, 5 (2006) 812-817.

[79] R. Paduch, The role of lymphangiogenesis and angiogenesis in tumor metastasis, Cell Oncol (Dordr), 39 (2016) 397-410.

[80] I.J. Fidler, The organ microenvironment and cancer metastasis, Differentiation, 70 (2002) 498-505.

[81] G. Poste, I.J. Fidler, The pathogenesis of cancer metastasis, Nature, 283 (1980) 139-146.

[82] I.J. Fidler, The pathogenesis of cancer metastasis: the 'seed and soil' hypothesis revisited, Nat Rev Cancer, 3 (2003) 453-458.

[83] P.S. Steeg, Tumor metastasis: mechanistic insights and clinical challenges, Nat Med, 12 (2006) 895-904.

[84] T.D. Duong, C.A. Erickson, MMP-2 plays an essential role in producing epithelial-mesenchymal transformations in the avian embryo, Dev Dyn, 229 (2004) 42-53.

[85] S.A. Illman, K. Lehti, J. Keski-Oja, J. Lohi, Epilysin (MMP-28) induces TGF-beta mediated epithelial to mesenchymal transition in lung carcinoma cells, J Cell Sci, 119 (2006) 3856-3865.

[86] H. Son, A. Moon, Epithelial-mesenchymal Transition and Cell Invasion, Toxicol Res, 26 (2010) 245-252.

[87] L. Larue, A. Bellacosa, Epithelial-mesenchymal transition in development and cancer: role of phosphatidylinositol 3' kinase/AKT pathways, Oncogene, 24 (2005) 7443-7454.

[88] S.J. Serrano-Gomez, M. Maziveyi, S.K. Alahari, Regulation of epithelial-mesenchymal transition through epigenetic and post-translational modifications, Mol Cancer, 15 (2016) 18.

[89] S. Valastyan, R.A. Weinberg, Tumor metastasis: molecular insights and evolving paradigms, Cell, 147 (2011) 275-292.

[90] L.J. Gay, B. Felding-Habermann, Contribution of platelets to tumour metastasis, Nat Rev Cancer, 11 (2011) 123-134.

[91] P. Jurasz, D. Alonso-Escolano, M.W. Radomski, Platelet--cancer interactions: mechanisms and pharmacology of tumour cell-induced platelet aggregation, Br J Pharmacol, 143 (2004) 819-826.

[92] L. Amo, E. Tamayo-Orbegozo, N. Maruri, C. Eguizabal, O. Zenarruzabeitia, M. Riñón, A. Arrieta, S. Santos, J. Monge, M.A. Vesga, F. Borrego, S. Larrucea, Involvement of platelet-tumor cell interaction in immune evasion. Potential role of podocalyxin-like protein 1, Front Oncol, 4 (2014) 245.

[93] N.M. Bambace, C.E. Holmes, The platelet contribution to cancer progression, J Thromb Haemost, 9 (2011) 237-249.

[94] S.Y. Choi, P.W. Gout, C.C. Collins, Y. Wang, Epithelial immune cell-like transition (EIT): a proposed transdifferentiation process underlying immune-suppressive activity of epithelial cancers, Differentiation, 83 (2012) 293-298.

[95] A.F. Chambers, A.C. Groom, I.C. MacDonald, Dissemination and growth of cancer cells in metastatic sites, Nat Rev Cancer, 2 (2002) 563-572.

[96] J. Massagué, A.C. Obenauf, Metastatic colonization by circulating tumour cells, Nature, 529 (2016) 298-306.

[97] B. Psaila, D. Lyden, The metastatic niche: adapting the foreign soil, Nat Rev Cancer, 9 (2009) 285-293.

[98] R.R. Langley, I.J. Fidler, Tumor cell-organ microenvironment interactions in the pathogenesis of cancer metastasis, Endocr Rev, 28 (2007) 297-321.

[99] E. Fokas, R. Engenhart-Cabillic, K. Daniilidis, F. Rose, H.X. An, Metastasis: the seed and soil theory gains identity, Cancer Metastasis Rev, 26 (2007) 705-715.

[100] L.A. Liotta, An attractive force in metastasis, Nature, 410 (2001) 24-25.

[101] J. Sturge, M.P. Caley, J. Waxman, Bone metastasis in prostate cancer: emerging therapeutic strategies, Nat Rev Clin Oncol, 8 (2011) 357-368.

[102] P.I. Croucher, M.M. McDonald, T.J. Martin, Bone metastasis: the importance of the neighbourhood, Nat Rev Cancer, 16 (2016) 373-386.

[103] A. So, J. Chin, N. Fleshner, F. Saad, Management of skeletal-related events in patients with advanced prostate cancer and bone metastases: Incorporating new agents into clinical practice, Can Urol Assoc J, 6 (2012) 465-470.

[104] A. Jensen, J.B. Jacobsen, M. Nørgaard, M. Yong, J.P. Fryzek, H.T. Sørensen, Incidence of bone metastases and skeletal-related events in breast cancer patients: a population-based cohort study in Denmark, BMC Cancer, 11 (2011) 29.

[105] W.P. Witjes, A. Patel, M. Wirth, Reply from authors re: Bertrand Tombal. Zometa European Study (ZEUS): another failed crusade for the holy grail of prostate cancer bone metastases prevention? Eur Urol 2015;67:492-4: ZEUS: the quest for the holy grail of prostate cancer bone metastases prevention continues, Eur Urol, 67 (2015) 494-495.

[106] C.J. Logothetis, S.H. Lin, Osteoblasts in prostate cancer metastasis to bone, Nat Rev Cancer, 5 (2005) 21-28.

[107] E.T. Keller, J. Brown, Prostate cancer bone metastases promote both osteolytic and osteoblastic activity, J Cell Biochem, 91 (2004) 718-729.

[108] L.J. Suva, C. Washam, R.W. Nicholas, R.J. Griffin, Bone metastasis: mechanisms and therapeutic opportunities, Nat Rev Endocrinol, 7 (2011) 208-218.

[109] A.C. Obenauf, J. Massagué, Surviving at a distance: organ specific metastasis, Trends Cancer, 1 (2015) 76-91.

[110] J.J. Yin, C.B. Pollock, K. Kelly, Mechanisms of cancer metastasis to the bone, Cell Res, 15 (2005) 57-62.

[111] R.S. Taichman, C. Cooper, E.T. Keller, K.J. Pienta, N.S. Taichman, L.K. McCauley, Use of the stromal cell-derived factor-1/CXCR4 pathway in prostate cancer metastasis to bone, Cancer Res, 62 (2002) 1832-1837.

[112] A.C. Hirbe, E.A. Morgan, K.N. Weilbaecher, The CXCR4/SDF-1 chemokine axis: a potential therapeutic target for bone metastases?, Curr Pharm Des, 16 (2010) 1284-1290.

[113] Y.X. Sun, A. Schneider, Y. Jung, J. Wang, J. Dai, K. Cook, N.I. Osman, A.J. Koh-Paige, H. Shim, K.J. Pienta, E.T. Keller, L.K. McCauley, R.S. Taichman, Skeletal localization and neutralization of the SDF-1(CXCL12)/CXCR4 axis blocks prostate cancer metastasis and growth in osseous sites in vivo, J Bone Miner Res, 20 (2005) 318-329.

[114] L. Ye, H.G. Kynaston, W.G. Jiang, Bone metastasis in prostate cancer: molecular and cellular mechanisms (Review), Int J Mol Med, 20 (2007) 103-111.

[115] J.J. Body, S. Casimiro, L. Costa, Targeting bone metastases in prostate cancer: improving clinical outcome, Nat Rev Urol, 12 (2015) 340-356.

[116] D.H. Jones, T. Nakashima, O.H. Sanchez, I. Kozieradzki, S.V. Komarova, I. Sarosi, S. Morony, E. Rubin, R. Sarao, C.V. Hojilla, V. Komnenovic, Y.Y. Kong, M. Schreiber, S.J. Dixon, S.M. Sims, R. Khokha, T. Wada, J.M. Penninger, Regulation of cancer cell migration and bone metastasis by RANKL, Nature, 440 (2006) 692-696.

[117] G. Chen, K. Sircar, A. Aprikian, A. Potti, D. Goltzman, S.A. Rabbani, Expression of RANKL/RANK/OPG in primary and metastatic human prostate cancer as markers of disease stage and functional regulation, Cancer, 107 (2006) 289-298.

[118] J.M. Brown, E. Corey, Z.D. Lee, L.D. True, T.J. Yun, M. Tondravi, R.L. Vessella, Osteoprotegerin and rank ligand expression in prostate cancer, Urology, 57 (2001) 611-616.

[119] R.M. Kypta, J. Waxman, Wnt/β-catenin signalling in prostate cancer, Nat Rev Urol, 9 (2012) 418-428.

[120] J. Heuberger, W. Birchmeier, Interplay of cadherin-mediated cell adhesion and canonical Wnt signaling, Cold Spring Harb Perspect Biol, 2 (2010) a002915.

[121] P. Raychaudhuri, H.J. Park, FoxM1: a master regulator of tumor metastasis, Cancer Res, 71 (2011) 4329-4333.

[122] Y. Cai, D. Balli, V. Ustiyan, L. Fulford, A. Hiller, V. Misetic, Y. Zhang, A.M. Paluch, S.E. Waltz, S. Kasper, T.V. Kalin, Foxm1 expression in prostate epithelial cells is essential for prostate carcinogenesis, J Biol Chem, 288 (2013) 22527-22541.

[123] A. Aytes, A. Mitrofanova, C. Lefebvre, M.J. Alvarez, M. Castillo-Martin, T. Zheng, J.A. Eastham, A. Gopalan, K.J. Pienta, M.M. Shen, A. Califano, C. Abate-Shen, Cross-species regulatory network analysis identifies a synergistic interaction between FOXM1 and CENPF that drives prostate cancer malignancy, Cancer Cell, 25 (2014) 638-651.

[124] S.C. Lin, C.Y. Kao, H.J. Lee, C.J. Creighton, M.M. Ittmann, S.J. Tsai, S.Y. Tsai, M.J. Tsai, Dysregulation of miRNAs-COUP-TFII-FOXM1-CENPF axis contributes to the metastasis of prostate cancer, Nat Commun, 7 (2016) 11418.

[125] M. Keyes, J. Crook, G. Morton, E. Vigneault, N. Usmani, W.J. Morris, Treatment options for localized prostate cancer, Can Fam Physician, 59 (2013) 1269-1274.

[126] J.H. Hayes, D.A. Ollendorf, S.D. Pearson, M.J. Barry, P.W. Kantoff, S.T. Stewart, V. Bhatnagar, C.J. Sweeney, J.E. Stahl, P.M. McMahon, Active surveillance compared with initial treatment for men with low-risk prostate cancer: a decision analysis, JAMA, 304 (2010) 2373-2380.

[127] S.M. Bruinsma, C.H. Bangma, P.R. Carroll, M.S. Leapman, A. Rannikko, N. Petrides, M. Weerakoon, L.P. Bokhorst, M.J. Roobol, M.G. consortium, Active surveillance for prostate cancer: a narrative review of clinical guidelines, Nat Rev Urol, 13 (2016) 151-167.

[128] B. Akduman, E.D. Crawford, Treatment of localized prostate cancer, Rev Urol, 8 Suppl 2 (2006) S15-21.

[129] N. Fleshner, Defining high-risk prostate cancer: current status, Can J Urol, 12 Suppl 1 (2005) 14-17; discussion 94-16.

[130] L.G. Gomella, Effective testosterone suppression for prostate cancer: is there a best castration therapy?, Rev Urol, 11 (2009) 52-60.

[131] T. Nishiyama, Serum testosterone levels after medical or surgical androgen deprivation: a comprehensive review of the literature, Urol Oncol, 32 (2014) 38.e17-28.

[132] S.J. Hotte, F. Saad, Current management of castrate-resistant prostate cancer, Curr Oncol, 17 Suppl 2 (2010) S72-79.

[133] J.H. Hong, I.Y. Kim, Nonmetastatic castration-resistant prostate cancer, Korean J Urol, 55 (2014) 153-160.

[134] L. Jia, J. Kim, H. Shen, P.E. Clark, W.D. Tilley, G.A. Coetzee, Androgen receptor activity at the prostate specific antigen locus: steroidal and non-steroidal mechanisms, Mol Cancer Res, 1 (2003) 385-392.

[135] C.D. Chen, D.S. Welsbie, C. Tran, S.H. Baek, R. Chen, R. Vessella, M.G. Rosenfeld, C.L. Sawyers, Molecular determinants of resistance to antiandrogen therapy, Nat Med, 10 (2004) 33-39.

[136] J.L. Mohler, C.W. Gregory, O.H. Ford, D. Kim, C.M. Weaver, P. Petrusz, E.M. Wilson, F.S. French, The androgen axis in recurrent prostate cancer, Clin Cancer Res, 10 (2004) 440-448.

[137] K. McKeage, Docetaxel: a review of its use for the first-line treatment of advanced castration-resistant prostate cancer, Drugs, 72 (2012) 1559-1577.

[138] J.S. de Bono, C.J. Logothetis, A. Molina, K. Fizazi, S. North, L. Chu, K.N. Chi, R.J. Jones, O.B. Goodman, F. Saad, J.N. Staffurth, P. Mainwaring, S. Harland, T.W. Flaig, T.E. Hutson, T. Cheng, H. Patterson, J.D. Hainsworth, C.J. Ryan, C.N. Sternberg, S.L. Ellard, A. Fléchon, M. Saleh, M. Scholz, E. Efstathiou, A. Zivi, D. Bianchini, Y. Loriot, N. Chieffo, T. Kheoh, C.M. Haqq, H.I. Scher, C.-A.-. Investigators, Abiraterone and increased survival in metastatic prostate cancer, N Engl J Med, 364 (2011) 1995-2005.

[139] F. Saad, K.N. Chi, A. Finelli, S.J. Hotte, J. Izawa, A. Kapoor, W. Kassouf, A. Loblaw, S. North, R. Rendon, A. So, N. Usmani, E. Vigneault, N.E. Fleshner, The 2015 CUA-CUOG Guidelines for the management of castration-resistant prostate cancer (CRPC), Can Urol Assoc J, 9 (2015) 90-96.

[140] D.E. Rathkopf, M.R. Smith, J.S. de Bono, C.J. Logothetis, N.D. Shore, P. de Souza, K. Fizazi, P.F. Mulders, P. Mainwaring, J.D. Hainsworth, T.M. Beer, S. North, Y. Fradet, H. Van Poppel, J. Carles, T.W. Flaig, E. Efstathiou, E.Y. Yu, C.S. Higano, M.E. Taplin, T.W. Griffin, M.B. Todd, M.K. Yu, Y.C. Park, T. Kheoh, E.J. Small, H.I. Scher, A. Molina, C.J. Ryan, F. Saad, Updated interim efficacy analysis and long-term safety of abiraterone acetate in metastatic

castration-resistant prostate cancer patients without prior chemotherapy (COU-AA-302), Eur Urol, 66 (2014) 815-825.

[141] C.N. Sternberg, D. Castellano, G. Daugaard, L. Géczi, S.J. Hotte, P.N. Mainwaring, F. Saad, C. Souza, M.H. Tay, J.M. Garrido, L. Galli, A. Londhe, P. De Porre, B. Goon, E. Lee, T. McGowan, V. Naini, M.B. Todd, A. Molina, D.J. George, A.G.E. Investigators, Abiraterone acetate for patients with metastatic castration-resistant prostate cancer progressing after chemotherapy: final analysis of a multicentre, open-label, early-access protocol trial, Lancet Oncol, 15 (2014) 1263-1268.

[142] N. Agarwal, G. Sonpavde, C.N. Sternberg, Novel molecular targets for the therapy of castration-resistant prostate cancer, Eur Urol, 61 (2012) 950-960.

[143] C. Tran, S. Ouk, N.J. Clegg, Y. Chen, P.A. Watson, V. Arora, J. Wongvipat, P.M. Smith-Jones, D. Yoo, A. Kwon, T. Wasielewska, D. Welsbie, C.D. Chen, C.S. Higano, T.M. Beer, D.T. Hung, H.I. Scher, M.E. Jung, C.L. Sawyers, Development of a second-generation antiandrogen for treatment of advanced prostate cancer, Science, 324 (2009) 787-790.

[144] T.M. Beer, A.J. Armstrong, D.E. Rathkopf, Y. Loriot, C.N. Sternberg, C.S. Higano, P. Iversen, S. Bhattacharya, J. Carles, S. Chowdhury, I.D. Davis, J.S. de Bono, C.P. Evans, K. Fizazi, A.M. Joshua, C.S. Kim, G. Kimura, P. Mainwaring, H. Mansbach, K. Miller, S.B. Noonberg, F. Perabo, D. Phung, F. Saad, H.I. Scher, M.E. Taplin, P.M. Venner, B. Tombal, P. Investigators, Enzalutamide in metastatic prostate cancer before chemotherapy, N Engl J Med, 371 (2014) 424-433.

[145] H.I. Scher, K. Fizazi, F. Saad, M.E. Taplin, C.N. Sternberg, K. Miller, R. de Wit, P. Mulders, K.N. Chi, N.D. Shore, A.J. Armstrong, T.W. Flaig, A. Fléchon, P. Mainwaring, M. Fleming, J.D. Hainsworth, M. Hirmand, B. Selby, L. Seely, J.S. de Bono, A. Investigators,

Increased survival with enzalutamide in prostate cancer after chemotherapy, N Engl J Med, 367 (2012) 1187-1197.

[146] K.L. Noonan, S. North, R.L. Bitting, A.J. Armstrong, S.L. Ellard, K.N. Chi, Clinical activity of abiraterone acetate in patients with metastatic castration-resistant prostate cancer progressing after enzalutamide, Ann Oncol, 24 (2013) 1802-1807.

[147] A.J. Schrader, M. Boegemann, C.H. Ohlmann, T.J. Schnoeller, L.M. Krabbe, T. Hajili, F. Jentzmik, M. Stoeckle, M. Schrader, E. Herrmann, M.V. Cronauer, Enzalutamide in castration-resistant prostate cancer patients progressing after docetaxel and abiraterone, Eur Urol, 65 (2014) 30-36.

[148] M.D. Galsky, A. Dritselis, P. Kirkpatrick, W.K. Oh, Cabazitaxel, Nat Rev Drug Discov, 9 (2010) 677-678.

[149] S. Oudard, TROPIC: Phase III trial of cabazitaxel for the treatment of metastatic castration-resistant prostate cancer, Future Oncol, 7 (2011) 497-506.

[150] J.S. de Bono, S. Oudard, M. Ozguroglu, S. Hansen, J.P. Machiels, I. Kocak, G. Gravis, I. Bodrogi, M.J. Mackenzie, L. Shen, M. Roessner, S. Gupta, A.O. Sartor, T. Investigators, Prednisone plus cabazitaxel or mitoxantrone for metastatic castration-resistant prostate cancer progressing after docetaxel treatment: a randomised open-label trial, Lancet, 376 (2010) 1147-1154.

[151] C.J. Pezaro, A.G. Omlin, A. Altavilla, D. Lorente, R. Ferraldeschi, D. Bianchini, D. Dearnaley, C. Parker, J.S. de Bono, G. Attard, Activity of cabazitaxel in castration-resistant prostate cancer progressing after docetaxel and next-generation endocrine agents, Eur Urol, 66 (2014) 459-465.

[152] C.S. Higano, P.F. Schellhammer, E.J. Small, P.A. Burch, J. Nemunaitis, L. Yuh, N. Provost, M.W. Frohlich, Integrated data from 2 randomized, double-blind, placebo-controlled, phase 3 trials of active cellular immunotherapy with sipuleucel-T in advanced prostate cancer, Cancer, 115 (2009) 3670-3679.

[153] P.W. Kantoff, C.S. Higano, N.D. Shore, E.R. Berger, E.J. Small, D.F. Penson, C.H. Redfern, A.C. Ferrari, R. Dreicer, R.B. Sims, Y. Xu, M.W. Frohlich, P.F. Schellhammer, I.S. Investigators, Sipuleucel-T immunotherapy for castration-resistant prostate cancer, N Engl J Med, 363 (2010) 411-422.

[154] J.N. Graff, E.D. Chamberlain, Sipuleucel-T in the treatment of prostate cancer: an evidence-based review of its place in therapy, Core Evid, 10 (2015) 1-10.

[155] V.B. Shahinian, Y.F. Kuo, J.L. Freeman, J.S. Goodwin, Risk of fracture after androgen deprivation for prostate cancer, N Engl J Med, 352 (2005) 154-164.

[156] T.J. Polascik, V. Mouraviev, Zoledronic acid in the management of metastatic bone disease, Ther Clin Risk Manag, 4 (2008) 261-268.

[157] S. Boissier, M. Ferreras, O. Peyruchaud, S. Magnetto, F.H. Ebetino, M. Colombel, P. Delmas, J.M. Delaissé, P. Clézardin, Bisphosphonates inhibit breast and prostate carcinoma cell invasion, an early event in the formation of bone metastases, Cancer Res, 60 (2000) 2949-2954.

[158] M. Wirth, T. Tammela, V. Cicalese, F. Gomez Veiga, K. Delaere, K. Miller, A. Tubaro, M. Schulze, F. Debruyne, H. Huland, A. Patel, F. Lecouvet, C. Caris, W. Witjes, Prevention of bone metastases in patients with high-risk nonmetastatic prostate cancer treated with zoledronic acid: efficacy and safety results of the Zometa European Study (ZEUS), Eur Urol, 67 (2015) 482-491.

[159] W.C. Dougall, I. Holen, E. González Suárez, Targeting RANKL in metastasis, Bonekey Rep, 3 (2014) 519.

[160] P. Narayanan, Denosumab: A comprehensive review, South Asian J Cancer, 2 (2013) 272-277.

[161] M.R. Smith, F. Saad, R. Coleman, N. Shore, K. Fizazi, B. Tombal, K. Miller, P. Sieber, L. Karsh, R. Damião, T.L. Tammela, B. Egerdie, H. Van Poppel, J. Chin, J. Morote, F. Gómez-Veiga, T. Borkowski, Z. Ye, A. Kupic, R. Dansey, C. Goessl, Denosumab and bone-metastasis-free survival in men with castration-resistant prostate cancer: results of a phase 3, randomised, placebo-controlled trial, Lancet, 379 (2012) 39-46.

[162] N.D. Shore, Radium-223 dichloride for metastatic castration-resistant prostate cancer: the urologist's perspective, Urology, 85 (2015) 717-724.

[163] F.E. Buroni, M.G. Persico, F. Pasi, L. Lodola, R. Nano, C. Aprile, Radium-223: Insight and Perspectives in Bone-metastatic Castration-resistant Prostate Cancer, Anticancer Res, 36 (2016) 5719-5730.

[164] P.J. Cheetham, D.P. Petrylak, Alpha particles as radiopharmaceuticals in the treatment of bone metastases: mechanism of action of radium-223 chloride (Alpharadin) and radiation protection, Oncology (Williston Park), 26 (2012) 330-337, 341.

[165] L. Mangatal, M. Adeline, D. Guénard, F. Guéritte-Voegelein, P. Potier, Application of the vicinal oxyamination reaction with asymmetric induction to the hemisynthesis of taxol and analogues, Tetrahedron, 45 (1989) 4177–4190.

[166] B.A. Teply, B. Luber, S.R. Denmeade, E.S. Antonarakis, The influence of prednisone on the efficacy of docetaxel in men with metastatic castration-resistant prostate cancer, Prostate Cancer Prostatic Dis, 19 (2016) 72-78.

[167] M. Fakih, C.S. Johnson, D.L. Trump, Glucocorticoids and treatment of prostate cancer: a preclinical and clinical review, Urology, 60 (2002) 553-561.

[168] A. Ramos-Esquivel, C. Fernández, Z. Zeledón, Androgen-deprivation therapy plus chemotherapy in metastatic hormone-sensitive prostate cancer. A systematic review and meta-analysis of randomized clinical trials, Urol Oncol, 34 (2016) 335.e339-335.e319.

[169] M. Tucci, V. Bertaglia, F. Vignani, C. Buttigliero, C. Fiori, F. Porpiglia, G.V. Scagliotti, M. Di Maio, Addition of Docetaxel to Androgen Deprivation Therapy for Patients with Hormone-sensitive Metastatic Prostate Cancer: A Systematic Review and Meta-analysis, Eur Urol, 69 (2016) 563-573.

[170] K.J. Pienta, Preclinical mechanisms of action of docetaxel and docetaxel combinations in prostate cancer, Semin Oncol, 28 (2001) 3-7.

[171] K. Kuroda, H. Liu, S. Kim, M. Guo, V. Navarro, N.H. Bander, Docetaxel down-regulates the expression of androgen receptor and prostate-specific antigen but not prostate-specific membrane antigen in prostate cancer cell lines: implications for PSA surrogacy, Prostate, 69 (2009) 1579-1585.

[172] L. Gan, S. Chen, Y. Wang, A. Watahiki, L. Bohrer, Z. Sun, H. Huang, Inhibition of the androgen receptor as a novel mechanism of taxol chemotherapy in prostate cancer, Cancer Res, 69 (2009) 8386-8394.

[173] M. Thadani-Mulero, D.M. Nanus, P. Giannakakou, Androgen receptor on the move: boarding the microtubule expressway to the nucleus, Cancer Res, 72 (2012) 4611-4615.

[174] I.F. Tannock, R. de Wit, W.R. Berry, J. Horti, A. Pluzanska, K.N. Chi, S. Oudard, C. Théodore, N.D. James, I. Turesson, M.A. Rosenthal, M.A. Eisenberger, T. Investigators,

Docetaxel plus prednisone or mitoxantrone plus prednisone for advanced prostate cancer, N Engl J Med, 351 (2004) 1502-1512.

[175] D.P. Petrylak, C.M. Tangen, M.H. Hussain, P.N. Lara, J.A. Jones, M.E. Taplin, P.A. Burch, D. Berry, C. Moinpour, M. Kohli, M.C. Benson, E.J. Small, D. Raghavan, E.D. Crawford, Docetaxel and estramustine compared with mitoxantrone and prednisone for advanced refractory prostate cancer, N Engl J Med, 351 (2004) 1513-1520.

[176] W.K. Kelly, S. Halabi, M. Carducci, D. George, J.F. Mahoney, W.M. Stadler, M. Morris, P. Kantoff, J.P. Monk, E. Kaplan, N.J. Vogelzang, E.J. Small, Randomized, double-blind, placebo-controlled phase III trial comparing docetaxel and prednisone with or without bevacizumab in men with metastatic castration-resistant prostate cancer: CALGB 90401, J Clin Oncol, 30 (2012) 1534-1540.

[177] P.L. Kellokumpu-Lehtinen, U. Harmenberg, T. Joensuu, R. McDermott, P. Hervonen, C. Ginman, M. Luukkaa, P. Nyandoto, A. Hemminki, S. Nilsson, J. McCaffrey, R. Asola, T. Turpeenniemi-Hujanen, F. Laestadius, T. Tasmuth, K. Sandberg, M. Keane, I. Lehtinen, T. Luukkaala, H. Joensuu, P.s. group, 2-Weekly versus 3-weekly docetaxel to treat castration-resistant advanced prostate cancer: a randomised, phase 3 trial, Lancet Oncol, 14 (2013) 117-124.

[178] G. Colloca, A. Venturino, F. Checcaglini, Second-line chemotherapy in metastatic docetaxel-resistant prostate cancer: a review, Med Oncol, 29 (2012) 776-785.

[179] E.S. Antonarakis, A.J. Armstrong, Evolving standards in the treatment of docetaxel-refractory castration-resistant prostate cancer, Prostate Cancer Prostatic Dis, 14 (2011) 192-205.

[180] O. Trédan, C.M. Galmarini, K. Patel, I.F. Tannock, Drug resistance and the solid tumor microenvironment, J Natl Cancer Inst, 99 (2007) 1441-1454.

[181] J.M. Brown, W.R. Wilson, Exploiting tumour hypoxia in cancer treatment, Nat Rev Cancer, 4 (2004) 437-447.

[182] C.H. Heldin, K. Rubin, K. Pietras, A. Ostman, High interstitial fluid pressure - an obstacle in cancer therapy, Nat Rev Cancer, 4 (2004) 806-813.

[183] D.M. Bradshaw, R.J. Arceci, Clinical relevance of transmembrane drug efflux as a mechanism of multidrug resistance, J Clin Oncol, 16 (1998) 3674-3690.

[184] M.M. Gottesman, T. Fojo, S.E. Bates, Multidrug resistance in cancer: role of ATP-dependent transporters, Nat Rev Cancer, 2 (2002) 48-58.

[185] R. van Amerongen, A. Berns, TXR1-mediated thrombospondin repression: a novel mechanism of resistance to taxanes?, Genes Dev, 20 (2006) 1975-1981.

[186] K. Yamanaka, P. Rocchi, H. Miyake, L. Fazli, A. So, U. Zangemeister-Wittke, M.E. Gleave, Induction of apoptosis and enhancement of chemosensitivity in human prostate cancer LNCaP cells using bispecific antisense oligonucleotide targeting Bcl-2 and Bcl-xL genes, BJU Int, 97 (2006) 1300-1308.

[187] J.C. Araujo, G.C. Trudel, F. Saad, A.J. Armstrong, E.Y. Yu, J. Bellmunt, G. Wilding, J. McCaffrey, S.V. Serrano, V.B. Matveev, E. Efstathiou, S. Oudard, M.J. Morris, B. Sizer, P.J. Goebell, A. Heidenreich, J.S. de Bono, S. Begbie, J.H. Hong, E. Richardet, E. Gallardo, P. Paliwal, S. Durham, S. Cheng, C.J. Logothetis, Docetaxel and dasatinib or placebo in men with metastatic castration-resistant prostate cancer (READY): a randomised, double-blind phase 3 trial, Lancet Oncol, 14 (2013) 1307-1316.

[188] N.D. James, M.R. Sydes, N.W. Clarke, M.D. Mason, D.P. Dearnaley, M.R. Spears, A.W. Ritchie, C.C. Parker, J.M. Russell, G. Attard, J. de Bono, W. Cross, R.J. Jones, G. Thalmann, C. Amos, D. Matheson, R. Millman, M. Alzouebi, S. Beesley, A.J. Birtle, S. Brock, R. Cathomas,

P. Chakraborti, S. Chowdhury, A. Cook, T. Elliott, J. Gale, S. Gibbs, J.D. Graham, J. Hetherington, R. Hughes, R. Laing, F. McKinna, D.B. McLaren, J.M. O'Sullivan, O. Parikh, C. Peedell, A. Protheroe, A.J. Robinson, N. Srihari, R. Srinivasan, J. Staffurth, S. Sundar, S. Tolan, D. Tsang, J. Wagstaff, M.K. Parmar, S. investigators, Addition of docetaxel, zoledronic acid, or both to first-line long-term hormone therapy in prostate cancer (STAMPEDE): survival results from an adaptive, multiarm, multistage, platform randomised controlled trial, Lancet, 387 (2016) 1163-1177.

[189] D.I. Quinn, C.M. Tangen, M. Hussain, P.N. Lara, A. Goldkorn, C.M. Moinpour, M.G. Garzotto, P.C. Mack, M.A. Carducci, J.P. Monk, P.W. Twardowski, P.J. Van Veldhuizen, N. Agarwal, C.S. Higano, N.J. Vogelzang, I.M. Thompson, Docetaxel and atrasentan versus docetaxel and placebo for men with advanced castration-resistant prostate cancer (SWOG S0421): a randomised phase 3 trial, Lancet Oncol, 14 (2013) 893-900.

[190] K.N. Chi, C.S. Higano, B. Blumenstein, J.M. Ferrero, J. Reeves, S. Feyerabend, G. Gravis, A.S. Merseburger, A. Stenzl, A.M. Bergman, S.D. Mukherjee, P. Zalewski, F. Saad, C. Jacobs, M. Gleave, J.S. de Bono, Custirsen in combination with docetaxel and prednisone for patients with metastatic castration-resistant prostate cancer (SYNERGY trial): a phase 3, multicentre, open-label, randomised trial, Lancet Oncol, 18 (2017) 473-485.

[191] H.I. Scher, X. Jia, K. Chi, R. de Wit, W.R. Berry, P. Albers, B. Henick, D. Waterhouse, D.J. Ruether, P.J. Rosen, A.A. Meluch, L.T. Nordquist, P.M. Venner, A. Heidenreich, L. Chu, G. Heller, Randomized, open-label phase III trial of docetaxel plus high-dose calcitriol versus docetaxel plus prednisone for patients with castration-resistant prostate cancer, J Clin Oncol, 29 (2011) 2191-2198.

[192] W.X. Qi, S. Fu, Q. Zhang, X.M. Guo, Efficacy and toxicity of molecular targeted therapies in combination with docetaxel for metastatic castration-resistant prostate cancer: a meta-analysis of phase III randomized controlled trials, J Chemother, 27 (2015) 181-187.

[193] E.S. Antonarakis, M.A. Eisenberger, Phase III trials with docetaxel-based combinations for metastatic castration-resistant prostate cancer: time to learn from past experiences, J Clin Oncol, 31 (2013) 1709-1712.

[194] M.D. Galsky, N.J. Vogelzang, Docetaxel-based combination therapy for castration-resistant prostate cancer, Ann Oncol, 21 (2010) 2135-2144.

[195] Y. Liu, X. Cao, Immunosuppressive cells in tumor immune escape and metastasis, J Mol Med (Berl), 94 (2016) 509-522.

[196] R.D. Schreiber, L.J. Old, M.J. Smyth, Cancer immunoediting: integrating immunity's roles in cancer suppression and promotion, Science, 331 (2011) 1565-1570.

[197] B.F. Zamarron, W. Chen, Dual roles of immune cells and their factors in cancer development and progression, Int J Biol Sci, 7 (2011) 651-658.

[198] K.E. de Visser, A. Eichten, L.M. Coussens, Paradoxical roles of the immune system during cancer development, Nat Rev Cancer, 6 (2006) 24-37.

[199] D. Mittal, M.M. Gubin, R.D. Schreiber, M.J. Smyth, New insights into cancer immunoediting and its three component phases--elimination, equilibrium and escape, Curr Opin Immunol, 27 (2014) 16-25.

[200] V. Shankaran, H. Ikeda, A.T. Bruce, J.M. White, P.E. Swanson, L.J. Old, R.D. Schreiber, IFNgamma and lymphocytes prevent primary tumour development and shape tumour immunogenicity, Nature, 410 (2001) 1107-1111.

[201] G.P. Dunn, C.M. Koebel, R.D. Schreiber, Interferons, immunity and cancer immunoediting, Nat Rev Immunol, 6 (2006) 836-848.

[202] G.P. Dunn, L.J. Old, R.D. Schreiber, The three Es of cancer immunoediting, Annu Rev Immunol, 22 (2004) 329-360.

[203] C.M. Koebel, W. Vermi, J.B. Swann, N. Zerafa, S.J. Rodig, L.J. Old, M.J. Smyth, R.D. Schreiber, Adaptive immunity maintains occult cancer in an equilibrium state, Nature, 450 (2007) 903-907.

[204] T.J. Stewart, S.I. Abrams, How tumours escape mass destruction, Oncogene, 27 (2008) 5894-5903.

[205] T.F. Gajewski, H. Schreiber, Y.X. Fu, Innate and adaptive immune cells in the tumor microenvironment, Nat Immunol, 14 (2013) 1014-1022.

[206] T. Kitamura, B.Z. Qian, J.W. Pollard, Immune cell promotion of metastasis, Nat Rev Immunol, 15 (2015) 73-86.

[207] S.S. McAllister, R.A. Weinberg, The tumour-induced systemic environment as a critical regulator of cancer progression and metastasis, Nat Cell Biol, 16 (2014) 717-727.

[208] D.F. Quail, J.A. Joyce, Microenvironmental regulation of tumor progression and metastasis, Nat Med, 19 (2013) 1423-1437.

[209] M.D. Vesely, M.H. Kershaw, R.D. Schreiber, M.J. Smyth, Natural innate and adaptive immunity to cancer, Annu Rev Immunol, 29 (2011) 235-271.

[210] D.I. Gabrilovich, S. Ostrand-Rosenberg, V. Bronte, Coordinated regulation of myeloid cells by tumours, Nat Rev Immunol, 12 (2012) 253-268.

[211] S.J. Galli, N. Borregaard, T.A. Wynn, Phenotypic and functional plasticity of cells of innate immunity: macrophages, mast cells and neutrophils, Nat Immunol, 12 (2011) 1035-1044.

[212] K. Sato, Helper T cell diversity and plasticity, Circ J, 78 (2014) 2843-2844.

[213] P.P. Hsu, D.M. Sabatini, Cancer cell metabolism: Warburg and beyond, Cell, 134 (2008) 703-707.

[214] D. Daye, K.E. Wellen, Metabolic reprogramming in cancer: unraveling the role of glutamine in tumorigenesis, Semin Cell Dev Biol, 23 (2012) 362-369.

[215] S. WEINHOUSE, On respiratory impairment in cancer cells, Science, 124 (1956) 267-269.

[216] O. Feron, Pyruvate into lactate and back: from the Warburg effect to symbiotic energy fuel exchange in cancer cells, Radiother Oncol, 92 (2009) 329-333.

[217] S. Ben-Haim, P. Ell, 18F-FDG PET and PET/CT in the evaluation of cancer treatment response, J Nucl Med, 50 (2009) 88-99.

[218] D. Lin, S.L. Ettinger, S. Qu, H. Xue, N. Nabavi, S.Y.C. Choi, R.H. Bell, F. Mo, A.M. Haegert, P.W. Gout, N. Fleshner, M.E. Gleave, M. Pollak, C.C. Collins, Y. Wang, Metabolic heterogeneity signature of primary treatment-naïve prostate cancer, Oncotarget, 8 (2017) 25928-25941.

[219] J.B. Tennakoon, Y. Shi, J.J. Han, E. Tsouko, M.A. White, A.R. Burns, A. Zhang, X. Xia, O.R. Ilkayeva, L. Xin, M.M. Ittmann, F.G. Rick, A.V. Schally, D.E. Frigo, Androgens regulate prostate cancer cell growth via an AMPK-PGC-1α-mediated metabolic switch, Oncogene, 33 (2014) 5251-5261.

[220] F. Cutruzzolà, G. Giardina, M. Marani, A. Macone, A. Paiardini, S. Rinaldo, A. Paone, Glucose Metabolism in the Progression of Prostate Cancer, Front Physiol, 8 (2017) 97.

[221] R.J. DeBerardinis, T. Cheng, Q's next: the diverse functions of glutamine in metabolism, cell biology and cancer, Oncogene, 29 (2010) 313-324.

[222] R.J. Deberardinis, N. Sayed, D. Ditsworth, C.B. Thompson, Brick by brick: metabolism and tumor cell growth, Curr Opin Genet Dev, 18 (2008) 54-61.

[223] B.A. Webb, M. Chimenti, M.P. Jacobson, D.L. Barber, Dysregulated pH: a perfect storm for cancer progression, Nat Rev Cancer, 11 (2011) 671-677.

[224] A. Calcinotto, P. Filipazzi, M. Grioni, M. Iero, A. De Milito, A. Ricupito, A. Cova, R. Canese, E. Jachetti, M. Rossetti, V. Huber, G. Parmiani, L. Generoso, M. Santinami, M. Borghi, S. Fais, M. Bellone, L. Rivoltini, Modulation of microenvironment acidity reverses anergy in human and murine tumor-infiltrating T lymphocytes, Cancer Res, 72 (2012) 2746-2756.

[225] A. De Milito, R. Canese, M.L. Marino, M. Borghi, M. Iero, A. Villa, G. Venturi, F. Lozupone, E. Iessi, M. Logozzi, P. Della Mina, M. Santinami, M. Rodolfo, F. Podo, L. Rivoltini, S. Fais, pH-dependent antitumor activity of proton pump inhibitors against human melanoma is mediated by inhibition of tumor acidity, Int J Cancer, 127 (2010) 207-219.

[226] H. Xie, J. Hanai, J.G. Ren, L. Kats, K. Burgess, P. Bhargava, S. Signoretti, J. Billiard, K.J. Duffy, A. Grant, X. Wang, P.K. Lorkiewicz, S. Schatzman, M. Bousamra, A.N. Lane, R.M. Higashi, T.W. Fan, P.P. Pandolfi, V.P. Sukhatme, P. Seth, Targeting lactate dehydrogenase--a inhibits tumorigenesis and tumor progression in mouse models of lung cancer and impacts tumor-initiating cells, Cell Metab, 19 (2014) 795-809.

[227] S.Y. Choi, C.C. Collins, P.W. Gout, Y. Wang, Cancer-generated lactic acid: a regulatory, immunosuppressive metabolite?, J Pathol, 230 (2013) 350-355.

[228] E.A. Mazzio, N. Boukli, N. Rivera, K.F. Soliman, Pericellular pH homeostasis is a primary function of the Warburg effect: inversion of metabolic systems to control lactate steady state in tumor cells, Cancer Sci, 103 (2012) 422-432.

[229] K. Fischer, P. Hoffmann, S. Voelkl, N. Meidenbauer, J. Ammer, M. Edinger, E. Gottfried, S. Schwarz, G. Rothe, S. Hoves, K. Renner, B. Timischl, A. Mackensen, L. Kunz-Schughart, R. Andreesen, S.W. Krause, M. Kreutz, Inhibitory effect of tumor cell-derived lactic acid on human T cells, Blood, 109 (2007) 3812-3819.

[230] Z. Husain, Y. Huang, P. Seth, V.P. Sukhatme, Tumor-derived lactate modifies antitumor immune response: effect on myeloid-derived suppressor cells and NK cells, J Immunol, 191 (2013) 1486-1495.

[231] E. Gottfried, L.A. Kunz-Schughart, S. Ebner, W. Mueller-Klieser, S. Hoves, R. Andreesen, A. Mackensen, M. Kreutz, Tumor-derived lactic acid modulates dendritic cell activation and antigen expression, Blood, 107 (2006) 2013-2021.

[232] S.K. Biswas, Metabolic Reprogramming of Immune Cells in Cancer Progression, Immunity, 43 (2015) 435-449.

[233] T. Wang, G. Liu, R. Wang, The Intercellular Metabolic Interplay between Tumor and Immune Cells, Front Immunol, 5 (2014) 358.

[234] Z. Husain, P. Seth, V.P. Sukhatme, Tumor-derived lactate and myeloid-derived suppressor cells: Linking metabolism to cancer immunology, Oncoimmunology, 2 (2013) e26383.

[235] S.Y. Choi, H. Xue, R. Wu, L. Fazli, D. Lin, C.C. Collins, M.E. Gleave, P.W. Gout, Y. Wang, The MCT4 Gene: A Novel, Potential Target for Therapy of Advanced Prostate Cancer, Clin Cancer Res, 22 (2016) 2721-2733.

[236] A. Brand, K. Singer, G.E. Koehl, M. Kolitzus, G. Schoenhammer, A. Thiel, C. Matos, C. Bruss, S. Klobuch, K. Peter, M. Kastenberger, C. Bogdan, U. Schleicher, A. Mackensen, E. Ullrich, S. Fichtner-Feigl, R. Kesselring, M. Mack, U. Ritter, M. Schmid, C. Blank, K. Dettmer, P.J. Oefner, P. Hoffmann, S. Walenta, E.K. Geissler, J. Pouyssegur, A. Villunger, A. Steven, B.

Seliger, S. Schreml, S. Haferkamp, E. Kohl, S. Karrer, M. Berneburg, W. Herr, W. Mueller-Klieser, K. Renner, M. Kreutz, LDHA-Associated Lactic Acid Production Blunts Tumor Immunosurveillance by T and NK Cells, Cell Metab, 24 (2016) 657-671.

[237] H. Ledford, Translational research: 4 ways to fix the clinical trial, Nature, 477 (2011) 526-528.

[238] S. Kummar, R. Kinders, L. Rubinstein, R.E. Parchment, A.J. Murgo, J. Collins, O. Pickeral, J. Low, S.M. Steinberg, M. Gutierrez, S. Yang, L. Helman, R. Wiltrout, J.E. Tomaszewski, J.H. Doroshow, Compressing drug development timelines in oncology using phase '0' trials, Nat Rev Cancer, 7 (2007) 131-139.

[239] N.E. Sharpless, R.A. Depinho, The mighty mouse: genetically engineered mouse models in cancer drug development, Nat Rev Drug Discov, 5 (2006) 741-754.

[240] H. Ledford, US cancer institute to overhaul tumour cell lines, Nature, 530 (2016) 391.

[241] J.R. Gingrich, R.J. Barrios, M.W. Kattan, H.S. Nahm, M.J. Finegold, N.M. Greenberg, Androgen-independent prostate cancer progression in the TRAMP model, Cancer Res, 57 (1997) 4687-4691.

[242] J.R. Gingrich, R.J. Barrios, R.A. Morton, B.F. Boyce, F.J. DeMayo, M.J. Finegold, R. Angelopoulou, J.M. Rosen, N.M. Greenberg, Metastatic prostate cancer in a transgenic mouse, Cancer Res, 56 (1996) 4096-4102.

[243] S.F. Winter, A.B. Cooper, N.M. Greenberg, Models of metastatic prostate cancer: a transgenic perspective, Prostate Cancer Prostatic Dis, 6 (2003) 204-211.

[244] T. Chiaverotti, S.S. Couto, A. Donjacour, J.H. Mao, H. Nagase, R.D. Cardiff, G.R. Cunha, A. Balmain, Dissociation of epithelial and neuroendocrine carcinoma lineages in the transgenic adenocarcinoma of mouse prostate model of prostate cancer, Am J Pathol, 172 (2008) 236-246.

[245] R.D. Klein, The use of genetically engineered mouse models of prostate cancer for nutrition and cancer chemoprevention research, Mutat Res, 576 (2005) 111-119.

[246] S. Kasper, P.C. Sheppard, Y. Yan, N. Pettigrew, A.D. Borowsky, G.S. Prins, J.G. Dodd, M.L. Duckworth, R.J. Matusik, Development, progression, and androgen-dependence of prostate tumors in probasin-large T antigen transgenic mice: a model for prostate cancer, Lab Invest, 78 (1998) 319-333.

[247] S. Kasper, P.C. Sheppard, Y. Yan, N. Pettigrew, A.D. Borowsky, G.S. Prins, J.G. Dodd, M.L. Duckworth, R.J. Matusik, Development, progression, and androgen-dependence of prostate tumors in probasin-large T antigen transgenic mice: a model for prostate cancer, Lab Invest, 78 (1998) i-xv.

[248] K. Ishii, S.B. Shappell, R.J. Matusik, S.W. Hayward, Use of tissue recombination to predict phenotypes of transgenic mouse models of prostate carcinoma, Lab Invest, 85 (2005) 1086-1103.

[249] V. Jeet, P.J. Russell, A. Khatri, Modeling prostate cancer: a perspective on transgenic mouse models, Cancer Metastasis Rev, 29 (2010) 123-142.

[250] N. Masumori, T.Z. Thomas, P. Chaurand, T. Case, M. Paul, S. Kasper, R.M. Caprioli, T. Tsukamoto, S.B. Shappell, R.J. Matusik, A probasin-large T antigen transgenic mouse line develops prostate adenocarcinoma and neuroendocrine carcinoma with metastatic potential, Cancer Res, 61 (2001) 2239-2249.

[251] S. Wang, J. Gao, Q. Lei, N. Rozengurt, C. Pritchard, J. Jiao, G.V. Thomas, G. Li, P. Roy-Burman, P.S. Nelson, X. Liu, H. Wu, Prostate-specific deletion of the murine Pten tumor suppressor gene leads to metastatic prostate cancer, Cancer Cell, 4 (2003) 209-221.

[252] M.M. Georgescu, PTEN Tumor Suppressor Network in PI3K-Akt Pathway Control, Genes Cancer, 1 (2010) 1170-1177.

[253] L. Cordero-Espinoza, T. Hagen, Increased concentrations of fructose 2,6-bisphosphate contribute to the Warburg effect in phosphatase and tensin homolog (PTEN)-deficient cells, J Biol Chem, 288 (2013) 36020-36028.

[254] A. Toso, A. Revandkar, D. Di Mitri, I. Guccini, M. Proietti, M. Sarti, S. Pinton, J. Zhang, M. Kalathur, G. Civenni, D. Jarrossay, E. Montani, C. Marini, R. Garcia-Escudero, E. Scanziani, F. Grassi, P.P. Pandolfi, C.V. Catapano, A. Alimonti, Enhancing chemotherapy efficacy in Pten-deficient prostate tumors by activating the senescence-associated antitumor immunity, Cell Rep, 9 (2014) 75-89.

[255] E.S. Antonarakis, D. Keizman, Z. Zhang, B. Gurel, T.L. Lotan, J.L. Hicks, H.L. Fedor, M.A. Carducci, A.M. De Marzo, M.A. Eisenberger, An immunohistochemical signature comprising PTEN, MYC, and Ki67 predicts progression in prostate cancer patients receiving adjuvant docetaxel after prostatectomy, Cancer, 118 (2012) 6063-6071.

[256] M.M. Grabowska, D.J. DeGraff, X. Yu, R.J. Jin, Z. Chen, A.D. Borowsky, R.J. Matusik, Mouse models of prostate cancer: picking the best model for the question, Cancer Metastasis Rev, 33 (2014) 377-397.

[257] D. Lin, H. Xue, Y. Wang, R. Wu, A. Watahiki, X. Dong, H. Cheng, A.W. Wyatt, C.C. Collins, P.W. Gout, Next generation patient-derived prostate cancer xenograft models, Asian J Androl, 16 (2014) 407-412.

[258] W.M. van Weerden, C.M. de Ridder, C.L. Verdaasdonk, J.C. Romijn, T.H. van der Kwast, F.H. Schröder, G.J. van Steenbrugge, Development of seven new human prostate tumor

xenograft models and their histopathological characterization, Am J Pathol, 149 (1996) 1055-1062.

[259] B.M. Holzapfel, F. Wagner, L. Thibaudeau, J.P. Levesque, D.W. Hutmacher, Concise review: humanized models of tumor immunology in the 21st century: convergence of cancer research and tissue engineering, Stem Cells, 33 (2015) 1696-1704.

[260] G.C. Koo, A. Hasan, R.J. O'Reilly, Use of humanized severe combined immunodeficient mice for human vaccine development, Expert Rev Vaccines, 8 (2009) 113-120.

[261] M. Werner-Klein, J. Proske, C. Werno, K. Schneider, H.S. Hofmann, B. Rack, S. Buchholz, R. Ganzer, A. Blana, B. Seelbach-Göbel, U. Nitsche, D.N. Männel, C.A. Klein, Immune humanization of immunodeficient mice using diagnostic bone marrow aspirates from carcinoma patients, PLoS One, 9 (2014) e97860.

[262] N. Legrand, K. Weijer, H. Spits, Experimental models to study development and function of the human immune system in vivo, J Immunol, 176 (2006) 2053-2058.

[263] K. Kikuchi, M. Kondo, Developmental switch of mouse hematopoietic stem cells from fetal to adult type occurs in bone marrow after birth, Proc Natl Acad Sci U S A, 103 (2006) 17852-17857.

[264] G.R. Cunha, L.W. Chung, J.M. Shannon, O. Taguchi, H. Fujii, Hormone-induced morphogenesis and growth: role of mesenchymal-epithelial interactions, Recent Prog Horm Res, 39 (1983) 559-598.

[265] G.R. Cunha, B. Lung, K. Kato, Role of the epithelial-stromal interaction during the development and expression of ovary-independent vaginal hyperplasia, Dev Biol, 56 (1977) 52-67.

[266] A.E. Bogden, P.M. Haskell, D.J. LePage, D.E. Kelton, W.R. Cobb, H.J. Esber, Growth of human tumor xenografts implanted under the renal capsule of normal immunocompetent mice, Exp Cell Biol, 47 (1979) 281-293.

[267] A.E. Bogden, The subrenal capsule assay (SRCA) and its predictive value in oncology, Ann Chir Gynaecol Suppl, 199 (1985) 12-27.

[268] N.J. Robertson, P.J. Fairchild, H. Waldmann, Ectopic transplantation of tissues under the kidney capsule, Methods Mol Biol, 380 (2007) 347-353.

[269] Y. Wang, M.P. Revelo, D. Sudilovsky, M. Cao, W.G. Chen, L. Goetz, H. Xue, M. Sadar, S.B. Shappell, G.R. Cunha, S.W. Hayward, Development and characterization of efficient xenograft models for benign and malignant human prostate tissue, Prostate, 64 (2005) 149-159.

[270] C. Priolo, M. Agostini, N. Vena, A.H. Ligon, M. Fiorentino, E. Shin, A. Farsetti, A. Pontecorvi, E. Sicinska, M. Loda, Establishment and genomic characterization of mouse xenografts of human primary prostate tumors, Am J Pathol, 176 (2010) 1901-1913.

[271] H. Zhao, R. Nolley, Z. Chen, D.M. Peehl, Tissue slice grafts: an in vivo model of human prostate androgen signaling, Am J Pathol, 177 (2010) 229-239.

[272] D. Lin, A.W. Wyatt, H. Xue, Y. Wang, X. Dong, A. Haegert, R. Wu, S. Brahmbhatt, F. Mo, L. Jong, R.H. Bell, S. Anderson, A. Hurtado-Coll, L. Fazli, M. Sharma, H. Beltran, M. Rubin, M. Cox, P.W. Gout, J. Morris, L. Goldenberg, S.V. Volik, M.E. Gleave, C.C. Collins, High fidelity patient-derived xenografts for accelerating prostate cancer discovery and drug development, Cancer Res, 74 (2014) 1272-1283.

[273] Y. Wang, J.X. Wang, H. Xue, D. Lin, X. Dong, P.W. Gout, X. Gao, J. Pang, Subrenal capsule grafting technology in human cancer modeling and translational cancer research, Differentiation, 91 (2016) 15-19.

[274] S.Y. Choi, D. Lin, P.W. Gout, C.C. Collins, Y. Xu, Y. Wang, Lessons from patient-derived xenografts for better in vitro modeling of human cancer, Adv Drug Deliv Rev, 79-80 (2014) 222-237.

[275] F. Mo, D. Lin, M. Takhar, V.R. Ramnarine, X. Dong, R.H. Bell, S.V. Volik, K. Wang, H. Xue, Y. Wang, A. Haegert, S. Anderson, S. Brahmbhatt, N. Erho, X. Wang, P.W. Gout, J. Morris, R.J. Karnes, R.B. Den, E.A. Klein, E.M. Schaeffer, A. Ross, S. Ren, S.C. Sahinalp, Y. Li, X. Xu, J. Wang, M.E. Gleave, E. Davicioni, Y. Sun, C.C. Collins, Stromal Gene Expression is Predictive for Metastatic Primary Prostate Cancer, Eur Urol, (2017).

[276] C.I. Gill, A. Boyd, E. McDermott, M. McCann, M. Servili, R. Selvaggini, A. Taticchi, S. Esposto, G. Montedoro, H. McGlynn, I. Rowland, Potential anti-cancer effects of virgin olive oil phenols on colorectal carcinogenesis models in vitro, Int J Cancer, 117 (2005) 1-7.

[277] S. Rockwell, Y. Liu, S.A. Higgins, Alteration of the effects of cancer therapy agents on breast cancer cells by the herbal medicine black cohosh, Breast Cancer Res Treat, 90 (2005) 233-239.

[278] A. Shen, J. Lin, Y. Chen, W. Lin, L. Liu, Z. Hong, T.J. Sferra, J. Peng, Pien Tze Huang inhibits tumor angiogenesis in a mouse model of colorectal cancer via suppression of multiple cellular pathways, Oncol Rep, 30 (2013) 1701-1706.

[279] K. Hedigan, Cancer: Herbal medicine reduces chemotherapy toxicity, Nat Rev Drug Discov, 9 (2010) 765.

[280] D. Xiao, A. Herman-Antosiewicz, J. Antosiewicz, H. Xiao, M. Brisson, J.S. Lazo, S.V. Singh, Diallyl trisulfide-induced G(2)-M phase cell cycle arrest in human prostate cancer cells is caused by reactive oxygen species-dependent destruction and hyperphosphorylation of Cdc 25 C, Oncogene, 24 (2005) 6256-6268.

[281] Z. Lian, K. Niwa, J. Gao, K. Tagami, H. Mori, T. Tamaya, Association of cellular apoptosis with anti-tumor effects of the Chinese herbal complex in endocrine-resistant cancer cell line, Cancer Detect Prev, 27 (2003) 147-154.

[282] S. Pei, X. Yang, H. Wang, H. Zhang, B. Zhou, D. Zhang, D. Lin, Plantamajoside, a potential anti-tumor herbal medicine inhibits breast cancer growth and pulmonary metastasis by decreasing the activity of matrix metalloproteinase-9 and -2, BMC Cancer, 15 (2015) 965.

[283] X. Chen, Z.P. Hu, X.X. Yang, M. Huang, Y. Gao, W. Tang, S.Y. Chan, X. Dai, J. Ye, P.C. Ho, W. Duan, H.Y. Yang, Y.Z. Zhu, S.F. Zhou, Monitoring of immune responses to a herbal immuno-modulator in patients with advanced colorectal cancer, Int Immunopharmacol, 6 (2006) 499-508.

[284] M. Gordaliza, Natural products as leads to anticancer drugs, Clin Transl Oncol, 9 (2007) 767-776.

[285] P.W. Gout, L.L. Wijcik, C.T. Beer, Differences between vinblastine and vincristine in distribution in the blood of rats and binding by platelets and malignant cells, Eur J Cancer, 14 (1978) 1167-1178.

[286] P.G. Gobbi, C. Broglia, F. Merli, M. Dell'Olio, C. Stelitano, E. Iannitto, M. Federico, R. Bertè, D. Luisi, S. Molica, C. Cavalli, L. Dezza, E. Ascari, Vinblastine, bleomycin, and methotrexate chemotherapy plus irradiation for patients with early-stage, favorable Hodgkin lymphoma: the experience of the Gruppo Italiano Studio Linfomi, Cancer, 98 (2003) 2393-2401.

[287] E. Groninger, T. Meeuwsen-de Boar, P. Koopmans, D. Uges, W. Sluiter, A. Veerman, W. Kamps, S. de Graaf, Pharmacokinetics of vincristine monotherapy in childhood acute lymphoblastic leukemia, Pediatr Res, 52 (2002) 113-118.

[288] S. Qu, K. Wang, H. Xue, Y. Wang, R. Wu, C. Liu, A.C. Gao, P.W. Gout, C.C. Collins, Y. Wang, Enhanced anticancer activity of a combination of docetaxel and Aneustat (OMN54) in a patient-derived, advanced prostate cancer tissue xenograft model, Mol Oncol, 8 (2014) 311-322.

[289] A. Montero, F. Fossella, G. Hortobagyi, V. Valero, Docetaxel for treatment of solid tumours: a systematic review of clinical data, Lancet Oncol, 6 (2005) 229-239.

[290] S. Cheng, D. Sliva, Ganoderma lucidum for cancer treatment: we are close but still not there, Integr Cancer Ther, 14 (2015) 249-257.

[291] P. Batra, A.K. Sharma, R. Khajuria, Probing Lingzhi or Reishi medicinal mushroom Ganoderma lucidum (higher Basidiomycetes): a bitter mushroom with amazing health benefits, Int J Med Mushrooms, 15 (2013) 127-143.

[292] J. Jiang, V. Slivova, K. Harvey, T. Valachovicova, D. Sliva, Ganoderma lucidum suppresses growth of breast cancer cells through the inhibition of Akt/NF-kappaB signaling, Nutr Cancer, 49 (2004) 209-216.

[293] G. Stanley, K. Harvey, V. Slivova, J. Jiang, D. Sliva, Ganoderma lucidum suppresses angiogenesis through the inhibition of secretion of VEGF and TGF-beta1 from prostate cancer cells, Biochem Biophys Res Commun, 330 (2005) 46-52.

[294] S.Y. Wang, M.L. Hsu, H.C. Hsu, C.H. Tzeng, S.S. Lee, M.S. Shiao, C.K. Ho, The anti-tumor effect of Ganoderma lucidum is mediated by cytokines released from activated macrophages and T lymphocytes, Int J Cancer, 70 (1997) 699-705.

[295] X. Jin, J. Ruiz Beguerie, D.M. Sze, G.C. Chan, Ganoderma lucidum (Reishi mushroom) for cancer treatment, Cochrane Database Syst Rev, 4 (2016) CD007731.

[296] L. Zhou, Z. Zuo, M.S. Chow, Danshen: an overview of its chemistry, pharmacology, pharmacokinetics, and clinical use, J Clin Pharmacol, 45 (2005) 1345-1359.

[297] H. Gao, W. Sun, J. Zhao, X. Wu, J.J. Lu, X. Chen, Q.M. Xu, I.A. Khan, S. Yang, Tanshinones and diethyl blechnics with anti-inflammatory and anti-cancer activities from Salvia miltiorrhiza Bunge (Danshen), Sci Rep, 6 (2016) 33720.

[298] T. Hu, K.K. To, L. Wang, L. Zhang, L. Lu, J. Shen, R.L. Chan, M. Li, J.H. Yeung, C.H. Cho, Reversal of P-glycoprotein (P-gp) mediated multidrug resistance in colon cancer cells by cryptotanshinone and dihydrotanshinone of Salvia miltiorrhiza, Phytomedicine, 21 (2014) 1264-1272.

[299] X. Yin, J. Zhou, C. Jie, D. Xing, Y. Zhang, Anticancer activity and mechanism of Scutellaria barbata extract on human lung cancer cell line A549, Life Sci, 75 (2004) 2233-2244.

[300] Z.J. Dai, W.F. Lu, J. Gao, H.F. Kang, Y.G. Ma, S.Q. Zhang, Y. Diao, S. Lin, X.J. Wang, W.Y. Wu, Anti-angiogenic effect of the total flavonoids in Scutellaria barbata D. Don, BMC Complement Altern Med, 13 (2013) 150.

[301] J. Lin, Y. Chen, Q. Cai, L. Wei, Y. Zhan, A. Shen, T.J. Sferra, J. Peng, Scutellaria Barbata D Don Inhibits Colorectal Cancer Growth via Suppression of Multiple Signaling Pathways, Integr Cancer Ther, 13 (2013) 240-248.

[302] B.Y. Wong, D.L. Nguyen, T. Lin, H.H. Wong, A. Cavalcante, N.M. Greenberg, R.P. Hausted, J. Zheng, Chinese medicinal herb Scutellaria barbata modulates apoptosis and cell survival in murine and human prostate cancer cells and tumor development in TRAMP mice, Eur J Cancer Prev, 18 (2009) 331-341.

[303] A.L. Shiau, Y.T. Shen, J.L. Hsieh, C.L. Wu, C.H. Lee, Scutellaria barbata inhibits angiogenesis through downregulation of HIF-1 α in lung tumor, Environ Toxicol, 29 (2014) 363-370.

[304] C.L. Ye, Q. Huang, Extraction of polysaccharides from herbal Scutellaria barbata D. Don (Ban-Zhi-Lian) and their antioxidant activity, Carbohydr Polym, 89 (2012) 1131-1137.

[305] X. Kan, W. Zhang, R. You, Y. Niu, J. Guo, J. Xue, Scutellaria barbata D. Don extract inhibits the tumor growth through down-regulating of Treg cells and manipulating Th1/Th17 immune response in hepatoma H22-bearing mice, BMC Complement Altern Med, 17 (2017) 41.

[306] H. Rugo, E. Shtivelman, A. Perez, C. Vogel, S. Franco, E. Tan Chiu, M. Melisko, M. Tagliaferri, I. Cohen, M. Shoemaker, Z. Tran, D. Tripathy, Phase I trial and antitumor effects of BZL101 for patients with advanced breast cancer, Breast Cancer Res Treat, 105 (2007) 17-28.

[307] A.T. Perez, B. Arun, D. Tripathy, M.A. Tagliaferri, H.S. Shaw, G.G. Kimmick, I. Cohen, E. Shtivelman, K.A. Caygill, D. Grady, M. Schactman, C.L. Shapiro, A phase 1B dose escalation trial of Scutellaria barbata (BZL101) for patients with metastatic breast cancer, Breast Cancer Res Treat, 120 (2010) 111-118.

[308] S. Fong, M. Shoemaker, J. Cadaoas, A. Lo, W. Liao, M. Tagliaferri, I. Cohen, E. Shtivelman, Molecular mechanisms underlying selective cytotoxic activity of BZL101, an extract of Scutellaria barbata, towards breast cancer cells, Cancer Biol Ther, 7 (2008) 577-586.

[309] V. Chen, R.E. Staub, S. Fong, M. Tagliaferri, I. Cohen, E. Shtivelman, Bezielle selectively targets mitochondria of cancer cells to inhibit glycolysis and OXPHOS, PLoS One, 7 (2012) e30300.

[310] J.A. Mikovits, L. Gerwick, E. Oroudjev, T. Okouneva, L. Xiang, L. Wilson, M.A. Jordan, Y.Z. Wang, W.H. Gerwick, Preclinical development of Aneustat (OMN54): A multifunctional multi-targeted natural product derivative with anti-tumor, anti-inflammatory and immuno-modulatory activity, Molecular Cancer Therapeutics, 6 (2007) 3548s-3548s.

[311] F.F. Radwan, A. Hossain, J.M. God, N. Leaphart, M. Elvington, M. Nagarkatti, S. Tomlinson, A. Haque, Reduction of myeloid-derived suppressor cells and lymphoma growth by a natural triterpenoid, J Cell Biochem, 116 (2015) 102-114.

[312] A. Das, R. Miller, P. Lee, C.A. Holden, S.M. Lindhorst, J. Jaboin, W.A. Vandergrift, N.L. Banik, P. Giglio, A.K. Varma, J.J. Raizer, S.J. Patel, A novel component from citrus, ginger, and mushroom family exhibits antitumor activity on human meningioma cells through suppressing the Wnt/β-catenin signaling pathway, Tumour Biol, 36 (2015) 7027-7034.

[313] J. Jiang, B. Grieb, A. Thyagarajan, D. Sliva, Ganoderic acids suppress growth and invasive behavior of breast cancer cells by modulating AP-1 and NF-kappaB signaling, Int J Mol Med, 21 (2008) 577-584.

[314] B.S. Gill, S. Kumar, Navgeet, Evaluating anti-oxidant potential of ganoderic acid A in STAT 3 pathway in prostate cancer, Mol Biol Rep, 43 (2016) 1411-1422.

[315] J. Liu, K. Kurashiki, K. Shimizu, R. Kondo, Structure-activity relationship for inhibition of 5alpha-reductase by triterpenoids isolated from Ganoderma lucidum, Bioorg Med Chem, 14 (2006) 8654-8660.

[316] S.H. Won, H.J. Lee, S.J. Jeong, E.O. Lee, D.B. Jung, J.M. Shin, T.R. Kwon, S.M. Yun, M.H. Lee, S.H. Choi, J. Lü, S.H. Kim, Tanshinone IIA induces mitochondria dependent apoptosis in prostate cancer cells in association with an inhibition of phosphoinositide 3-kinase/AKT pathway, Biol Pharm Bull, 33 (2010) 1828-1834.

[317] K. Ketola, M. Viitala, P. Kohonen, V. Fey, Z. Culig, O. Kallioniemi, K. Iljin, High-throughput cell-based compound screen identifies pinosylvin methyl ether and tanshinone IIA as inhibitors of castration-resistant prostate cancer, J Mol Biochem, 5 (2016) 12-22.

[318] D.S. Ouyang, W.H. Huang, D. Chen, W. Zhang, Z.R. Tan, J.B. Peng, Y.C. Wang, Y. Guo, D.L. Hu, J. Xiao, Y. Chen, Kinetics of cytochrome P450 enzymes for metabolism of sodium tanshinone IIA sulfonate in vitro, Chin Med, 11 (2016) 11.

[319] D. Chen, X.X. Lin, W.H. Huang, W. Zhang, Z.R. Tan, J.B. Peng, Y.C. Wang, Y. Guo, D.L. Hu, Y. Chen, Sodium tanshinone IIA sulfonate and its interactions with human CYP450s, Xenobiotica, 46 (2016) 1085-1092.

[320] J. Hirth, P.B. Watkins, M. Strawderman, A. Schott, R. Bruno, L.H. Baker, The effect of an individual's cytochrome CYP3A4 activity on docetaxel clearance, Clin Cancer Res, 6 (2000) 1255-1258.

[321] V. Chen, R.E. Staub, S. Baggett, R. Chimmani, M. Tagliaferri, I. Cohen, E. Shtivelman, Identification and analysis of the active phytochemicals from the anti-cancer botanical extract Bezielle, PLoS One, 7 (2012) e30107.

[322] X. Shi, G. Chen, X. Liu, Y. Qiu, S. Yang, Y. Zhang, X. Fang, C. Zhang, Scutellarein inhibits cancer cell metastasis in vitro and attenuates the development of fibrosarcoma in vivo, Int J Mol Med, 35 (2015) 31-38.

[323] S. Erdogan, O. Doganlar, Z.B. Doganlar, R. Serttas, K. Turkekul, I. Dibirdik, A. Bilir, The flavonoid apigenin reduces prostate cancer CD44(+) stem cell survival and migration through PI3K/Akt/NF-κB signaling, Life Sci, 162 (2016) 77-86.

[324] J.C. King, Q.Y. Lu, G. Li, A. Moro, H. Takahashi, M. Chen, V.L. Go, H.A. Reber, G. Eibl, O.J. Hines, Evidence for activation of mutated p53 by apigenin in human pancreatic cancer, Biochim Biophys Acta, 1823 (2012) 593-604.

[325] L.G. Melstrom, M.R. Salabat, X.Z. Ding, B.M. Milam, M. Strouch, J.C. Pelling, D.J. Bentrem, Apigenin inhibits the GLUT-1 glucose transporter and the phosphoinositide 3-kinase/Akt pathway in human pancreatic cancer cells, Pancreas, 37 (2008) 426-431.

[326] D. Renouf, C. Kollmannsberger, K. Chi, S. Chia, A. Tinker, T. Mitchell, S. Lam, T. Joshi, D. Kwok, J. Ostrem, S. Sutcliffe, K. Gelmon, Abstract C41: A phase 1 study of OMN54 in patients with advanced malignancies, Molecular Cancer Therapeutics, 14 (2015) C41-C41.

[327] J. Luo, N.L. Solimini, S.J. Elledge, Principles of cancer therapy: oncogene and non-oncogene addiction, Cell, 136 (2009) 823-837.

[328] W.K. Oh, P.W. Kantoff, Management of hormone refractory prostate cancer: current standards and future prospects, J Urol, 160 (1998) 1220-1229.

[329] M. Gao, R. Patel, I. Ahmad, J. Fleming, J. Edwards, S. McCracken, K. Sahadevan, M. Seywright, J. Norman, O. Sansom, H.Y. Leung, SPRY2 loss enhances ErbB trafficking and PI3K/AKT signalling to drive human and mouse prostate carcinogenesis, EMBO Mol Med, 4 (2012) 776-790.

[330] L. Li, M.M. Ittmann, G. Ayala, M.J. Tsai, R.J. Amato, T.M. Wheeler, B.J. Miles, D. Kadmon, T.C. Thompson, The emerging role of the PI3-K-Akt pathway in prostate cancer progression, Prostate Cancer Prostatic Dis, 8 (2005) 108-118.

[331] T. Tian, K.J. Nan, H. Guo, W.J. Wang, Z.P. Ruan, S.H. Wang, X. Liang, C.X. Lu, PTEN inhibits the migration and invasion of HepG2 cells by coordinately decreasing MMP expression via the PI3K/Akt pathway, Oncol Rep, 23 (2010) 1593-1600.

[332] E. Tokunaga, A. Kataoka, Y. Kimura, E. Oki, K. Mashino, K. Nishida, T. Koga, M. Morita, Y. Kakeji, H. Baba, S. Ohno, Y. Maehara, The association between Akt activation and resistance to hormone therapy in metastatic breast cancer, Eur J Cancer, 42 (2006) 629-635.

[333] S. Tabaczar, A. Koceva-Chyła, K. Matczak, K. Gwoździński, [Molecular mechanisms of antitumor activity of taxanes. I. Interaction of docetaxel with microtubules], Postepy Hig Med Dosw (Online), 64 (2010) 568-581.

[334] P. Garcia, D. Braguer, G. Carles, S. el Khyari, Y. Barra, C. de Ines, I. Barasoain, C. Briand, Comparative effects of taxol and Taxotere on two different human carcinoma cell lines, Cancer Chemother Pharmacol, 34 (1994) 335-343.

[335] F. Lavelle, M.C. Bissery, C. Combeau, J.F. Riou, P. Vrignaud, S. André, Preclinical evaluation of docetaxel (Taxotere), Semin Oncol, 22 (1995) 3-16.

[336] C.A. Stein, Mechanisms of action of taxanes in prostate cancer, Semin Oncol, 26 (1999) 3-7.

[337] B. Lewis, E. Chalhoub, C. Chalouhy, O. Sartor, Radium-223 in Bone-Metastatic Prostate Cancer: Current Data and Future Prospects, Oncology (Williston Park), 29 (2015) 483-488.

[338] J.B. Aragon-Ching, Enzalutamide (formerly MDV3100) as a new therapeutic option for men with metastatic castration-resistant prostate cancer, Asian J Androl, 14 (2012) 805-806.

[339] C.J. Logothetis, E. Efstathiou, F. Manuguid, P. Kirkpatrick, Abiraterone acetate, Nat Rev Drug Discov, 10 (2011) 573-574.

[340] A.G. Musende, A. Eberding, W. Jia, E. Ramsay, M.B. Bally, E.T. Guns, Rh2 or its aglycone aPPD in combination with docetaxel for treatment of prostate cancer, Prostate, 70 (2010) 1437-1447.

[341] T.C. Chou, Drug combination studies and their synergy quantification using the Chou-Talalay method, Cancer Res, 70 (2010) 440-446.

[342] T.C. Chou, Theoretical basis, experimental design, and computerized simulation of synergism and antagonism in drug combination studies, Pharmacol Rev, 58 (2006) 621-681.

[343] A. Watahiki, Y. Wang, J. Morris, K. Dennis, H.M. O'Dwyer, M. Gleave, P.W. Gout, MicroRNAs associated with metastatic prostate cancer, PLoS One, 6 (2011) e24950.

[344] Y. Wang, H. Xue, J.C. Cutz, J. Bayani, N.R. Mawji, W.G. Chen, L.J. Goetz, S.W. Hayward, M.D. Sadar, C.B. Gilks, P.W. Gout, J.A. Squire, G.R. Cunha, Y.Z. Wang, An orthotopic metastatic prostate cancer model in SCID mice via grafting of a transplantable human prostate tumor line, Lab Invest, 85 (2005) 1392-1404.

[345] N. Nadiminty, J.Y. Chun, W. Lou, X. Lin, A.C. Gao, NF-kappaB2/p52 enhances androgen-independent growth of human LNCaP cells via protection from apoptotic cell death and cell cycle arrest induced by androgen-deprivation, Prostate, 68 (2008) 1725-1733.

[346] H. Nakamura, Y. Wang, T. Kurita, H. Adomat, G.R. Cunha, Genistein increases epidermal growth factor receptor signaling and promotes tumor progression in advanced human prostate cancer, PLoS One, 6 (2011) e20034.

[347] H. Savli, A. Szendröi, I. Romics, B. Nagy, Gene network and canonical pathway analysis in prostate cancer: a microarray study, Exp Mol Med, 40 (2008) 176-185.

[348] M. Juríková, Ľ. Danihel, Š. Polák, I. Varga, Ki67, PCNA, and MCM proteins: Markers of proliferation in the diagnosis of breast cancer, Acta Histochem, 118 (2016) 544-552.

[349] C.A. Heinlein, C. Chang, Androgen receptor in prostate cancer, Endocr Rev, 25 (2004) 276-308.

[350] D. Sarker, A.H. Reid, T.A. Yap, J.S. de Bono, Targeting the PI3K/AKT pathway for the treatment of prostate cancer, Clin Cancer Res, 15 (2009) 4799-4805.

[351] Y. Li, X. Li, M. Hussain, F.H. Sarkar, Regulation of microtubule, apoptosis, and cell cycle-related genes by taxotere in prostate cancer cells analyzed by microarray, Neoplasia, 6 (2004) 158-167.

[352] M.G. Vander Heiden, L.C. Cantley, C.B. Thompson, Understanding the Warburg effect: the metabolic requirements of cell proliferation, Science, 324 (2009) 1029-1033.

[353] J.I. Johnson, S. Decker, D. Zaharevitz, L.V. Rubinstein, J.M. Venditti, S. Schepartz, S. Kalyandrug, M. Christian, S. Arbuck, M. Hollingshead, E.A. Sausville, Relationships between drug activity in NCI preclinical in vitro and in vivo models and early clinical trials, Br J Cancer, 84 (2001) 1424-1431.

[354] A. Kamb, What's wrong with our cancer models?, Nat Rev Drug Discov, 4 (2005) 161-165.

[355] C. Leaf, Why we're losing the war on cancer (and how to win it), Fortune, 149 (2004) 76-82, 84-76, 88 passim.

[356] C.C. Collins, S.V. Volik, A.V. Lapuk, Y. Wang, P.W. Gout, C. Wu, H. Xue, H. Cheng, A. Haegert, R.H. Bell, S. Brahmbhatt, S. Anderson, L. Fazli, A. Hurtado-Coll, M.A. Rubin, F. Demichelis, H. Beltran, M. Hirst, M. Marra, C.A. Maher, A.M. Chinnaiyan, M. Gleave, J.R. Bertino, M. Lubin, Next generation sequencing of prostate cancer from a patient identifies a deficiency of methylthioadenosine phosphorylase, an exploitable tumor target, Mol Cancer Ther, 11 (2012) 775-783.

[357] W.L. Tung, Y. Wang, P.W. Gout, D.M. Liu, M. Gleave, Use of irinotecan for treatment of small cell carcinoma of the prostate, Prostate, 71 (2011) 675-681.

[358] C. Liu, Y. Zhu, W. Lou, N. Nadiminty, X. Chen, Q. Zhou, X.B. Shi, R.W. deVere White, A.C. Gao, Functional p53 determines docetaxel sensitivity in prostate cancer cells, Prostate, 73 (2013) 418-427.

[359] C. Guyader, J. Céraline, E. Gravier, A. Morin, S. Michel, E. Erdmann, G. de Pinieux, F. Cabon, J.P. Bergerat, M.F. Poupon, S. Oudard, Risk of hormone escape in a human prostate

cancer model depends on therapy modalities and can be reduced by tyrosine kinase inhibitors, PLoS One, 7 (2012) e42252.

[360] D.J. Mulholland, S. Dedhar, H. Wu, C.C. Nelson, PTEN and GSK3beta: key regulators of progression to androgen-independent prostate cancer, Oncogene, 25 (2006) 329-337.

[361] L. Xin, M.A. Teitell, D.A. Lawson, A. Kwon, I.K. Mellinghoff, O.N. Witte, Progression of prostate cancer by synergy of AKT with genotropic and nongenotropic actions of the androgen receptor, Proc Natl Acad Sci U S A, 103 (2006) 7789-7794.

[362] A.J. Pommier, G. Alves, E. Viennois, S. Bernard, Y. Communal, B. Sion, G. Marceau, C. Damon, K. Mouzat, F. Caira, S. Baron, J.M. Lobaccaro, Liver X Receptor activation downregulates AKT survival signaling in lipid rafts and induces apoptosis of prostate cancer cells, Oncogene, 29 (2010) 2712-2723.

[363] N. Dizeyi, P. Hedlund, A. Bjartell, M. Tinzl, K. Austild-Taskén, P.A. Abrahamsson, Serotonin activates MAP kinase and PI3K/Akt signaling pathways in prostate cancer cell lines, Urol Oncol, 29 (2011) 436-445.

[364] T. Shinka, D. Onodera, T. Tanaka, N. Shoji, T. Miyazaki, T. Moriuchi, T. Fukumoto, Serotonin synthesis and metabolism-related molecules in a human prostate cancer cell line, Oncol Lett, 2 (2011) 211-215.

[365] B.H. Lee, M.G. Taylor, P. Robinet, J.D. Smith, J. Schweitzer, E. Sehayek, S.M. Falzarano, C. Magi-Galluzzi, E.A. Klein, A.H. Ting, Dysregulation of cholesterol homeostasis in human prostate cancer through loss of ABCA1, Cancer Res, 73 (2013) 1211-1218.

[366] K. Pelton, M.R. Freeman, K.R. Solomon, Cholesterol and prostate cancer, Curr Opin Pharmacol, 12 (2012) 751-759.

[367] D. Hanahan, L.M. Coussens, Accessories to the crime: functions of cells recruited to the tumor microenvironment, Cancer Cell, 21 (2012) 309-322.

[368] B.S. Carver, C. Chapinski, J. Wongvipat, H. Hieronymus, Y. Chen, S. Chandarlapaty, V.K. Arora, C. Le, J. Koutcher, H. Scher, P.T. Scardino, N. Rosen, C.L. Sawyers, Reciprocal feedback regulation of PI3K and androgen receptor signaling in PTEN-deficient prostate cancer, Cancer Cell, 19 (2011) 575-586.

[369] S.J. Oh, H.H. Erb, A. Hobisch, F.R. Santer, Z. Culig, Sorafenib decreases proliferation and induces apoptosis of prostate cancer cells by inhibition of the androgen receptor and Akt signaling pathways, Endocr Relat Cancer, 19 (2012) 305-319.

[370] C. Wu, A.W. Wyatt, A. McPherson, D. Lin, B.J. McConeghy, F. Mo, R. Shukin, A.V. Lapuk, S.J. M Jones, Y. Zhao, M.A. Marra, M.E. Gleave, S.V. Volik, Y. Wang, S.C. Sahinalp, C.C. Collins, Poly-gene fusion transcripts and chromothripsis in prostate cancer, Genes Chromosomes Cancer, 51 (2012) 1144-1153.

[371] G. Attard, C. Parker, R.A. Eeles, F. Schröder, S.A. Tomlins, I. Tannock, C.G. Drake, J.S. de Bono, Prostate cancer, Lancet, 387 (2016) 70-82.

[372] G. Gravis, F. Audenet, J. Irani, M.O. Timsit, P. Barthelemy, P. Beuzeboc, A. Fléchon, C. Linassier, S. Oudard, X. Rebillard, P. Richaud, M. Rouprêt, A. Thiery Vuillemin, S. Vincendeau, L. Albiges, F. Rozet, Chemotherapy in hormone-sensitive metastatic prostate cancer: Evidences and uncertainties from the literature, Cancer Treat Rev, (2016).

[373] Y.T. Chiang, K. Wang, L. Fazli, R.Z. Qi, M.E. Gleave, C.C. Collins, P.W. Gout, Y. Wang, GATA2 as a potential metastasis-driving gene in prostate cancer, Oncotarget, 5 (2014) 451-461.

[374] D.R. Rhodes, S. Kalyana-Sundaram, V. Mahavisno, R. Varambally, J. Yu, B.B. Briggs, T.R. Barrette, M.J. Anstet, C. Kincead-Beal, P. Kulkarni, S. Varambally, D. Ghosh, A.M.

Chinnaiyan, Oncomine 3.0: genes, pathways, and networks in a collection of 18,000 cancer gene expression profiles, Neoplasia, 9 (2007) 166-180.

[375] A. Krämer, J. Green, J. Pollard, S. Tugendreich, Causal analysis approaches in Ingenuity Pathway Analysis, Bioinformatics, 30 (2014) 523-530.

[376] C.Y. Koo, K.W. Muir, E.W. Lam, FOXM1: From cancer initiation to progression and treatment, Biochim Biophys Acta, 1819 (2012) 28-37.

[377] Y.H. Kim, M.H. Choi, J.H. Kim, I.K. Lim, T.J. Park, C-terminus-deleted FoxM1 is expressed in cancer cell lines and induces chromosome instability, Carcinogenesis, 34 (2013) 1907-1917.

[378] X. Ci, C. Xing, B. Zhang, Z. Zhang, J.J. Ni, W. Zhou, J.T. Dong, KLF5 inhibits angiogenesis in PTEN-deficient prostate cancer by attenuating AKT activation and subsequent HIF1α accumulation, Mol Cancer, 14 (2015) 91.

[379] C.J. Barger, W. Zhang, J. Hillman, A.B. Stablewski, M.J. Higgins, B.C. Vanderhyden, K. Odunsi, A.R. Karpf, Genetic determinants of FOXM1 overexpression in epithelial ovarian cancer and functional contribution to cell cycle progression, Oncotarget, 6 (2015) 27613-27627.

[380] I.C. Wang, Y.J. Chen, D. Hughes, V. Petrovic, M.L. Major, H.J. Park, Y. Tan, T. Ackerson, R.H. Costa, Forkhead box M1 regulates the transcriptional network of genes essential for mitotic progression and genes encoding the SCF (Skp2-Cks1) ubiquitin ligase, Mol Cell Biol, 25 (2005) 10875-10894.

[381] J. Laoukili, M.R. Kooistra, A. Brás, J. Kauw, R.M. Kerkhoven, A. Morrison, H. Clevers, R.H. Medema, FoxM1 is required for execution of the mitotic programme and chromosome stability, Nat Cell Biol, 7 (2005) 126-136.

[382] G.D. Grant, L. Brooks, X. Zhang, J.M. Mahoney, V. Martyanov, T.A. Wood, G. Sherlock, C. Cheng, M.L. Whitfield, Identification of cell cycle-regulated genes periodically expressed in U2OS cells and their regulation by FOXM1 and E2F transcription factors, Mol Biol Cell, 24 (2013) 3634-3650.

[383] J. Zhou, C. Wang, Z. Wang, W. Dampier, K. Wu, M.C. Casimiro, I. Chepelev, V.M. Popov, A. Quong, A. Tozeren, K. Zhao, M.P. Lisanti, R.G. Pestell, Attenuation of Forkhead signaling by the retinal determination factor DACH1, Proc Natl Acad Sci U S A, 107 (2010) 6864-6869.

[384] X. Sun, P.L. Clermont, W. Jiao, C.D. Helgason, P.W. Gout, Y. Wang, S. Qu, Elevated expression of the centromere protein-A(CENP-A)-encoding gene as a prognostic and predictive biomarker in human cancers, Int J Cancer, 139 (2016) 899-907.

[385] X. Chen, G.A. Müller, M. Quaas, M. Fischer, N. Han, B. Stutchbury, A.D. Sharrocks, K. Engeland, The forkhead transcription factor FOXM1 controls cell cycle-dependent gene expression through an atypical chromatin binding mechanism, Mol Cell Biol, 33 (2013) 227-236.

[386] Y. Zheng, J. Guo, J. Zhou, J. Lu, Q. Chen, C. Zhang, C. Qing, H.P. Koeffler, Y. Tong, FoxM1 transactivates PTTG1 and promotes colorectal cancer cell migration and invasion, BMC Med Genomics, 8 (2015) 49.

[387] J.R. Carr, H.J. Park, Z. Wang, M.M. Kiefer, P. Raychaudhuri, FoxM1 mediates resistance to herceptin and paclitaxel, Cancer Res, 70 (2010) 5054-5063.

[388] X. Li, R. Yao, L. Yue, W. Qiu, W. Qi, S. Liu, Y. Yao, J. Liang, FOXM1 mediates resistance to docetaxel in gastric cancer via up-regulating Stathmin, J Cell Mol Med, 18 (2014) 811-823.

[389] X.Y. Kuang, H.S. Jiang, K. Li, Y.Z. Zheng, Y.R. Liu, F. Qiao, S. Li, X. Hu, Z.M. Shao, The phosphorylation-specific association of STMN1 with GRP78 promotes breast cancer metastasis, Cancer Lett, 377 (2016) 87-96.

[390] I. Lokody, Signalling: FOXM1 and CENPF: co-pilots driving prostate cancer, Nat Rev Cancer, 14 (2014) 450-451.

[391] M.M. Donaldson, A.A. Tavares, I.M. Hagan, E.A. Nigg, D.M. Glover, The mitotic roles of Polo-like kinase, J Cell Sci, 114 (2001) 2357-2358.

[392] J. Cui, M. Shi, D. Xie, D. Wei, Z. Jia, S. Zheng, Y. Gao, S. Huang, K. Xie, FOXM1 promotes the warburg effect and pancreatic cancer progression via transactivation of LDHA expression, Clin Cancer Res, 20 (2014) 2595-2606.

[393] K. Ketola, R.S.N. Munuganti, A. Davies, K.M. Nip, J.L. Bishop, A. Zoubeidi, Targeting Prostate Cancer Subtype 1 by Forkhead Box M1 Pathway Inhibition, Clin Cancer Res, (2017).

[394] M. Niu, W. Cai, H. Liu, Y. Chong, W. Hu, S. Gao, Q. Shi, X. Zhou, X. Liu, R. Yu, Plumbagin inhibits growth of gliomas in vivo via suppression of FOXM1 expression, J Pharmacol Sci, 128 (2015) 131-136.

[395] L.P. Smith, G.R. Thomas, Animal models for the study of squamous cell carcinoma of the upper aerodigestive tract: a historical perspective with review of their utility and limitations. Part A. Chemically-induced de novo cancer, syngeneic animal models of HNSCC, animal models of transplanted xenogeneic human tumors, Int J Cancer, 118 (2006) 2111-2122.

[396] R. Kim, M. Emi, K. Tanabe, Cancer immunoediting from immune surveillance to immune escape, Immunology, 121 (2007) 1-14.

[397] S. Ostrand-Rosenberg, Immune surveillance: a balance between protumor and antitumor immunity, Curr Opin Genet Dev, 18 (2008) 11-18.

[398] T.L. Whiteside, Inhibiting the inhibitors: evaluating agents targeting cancer immunosuppression, Expert Opin Biol Ther, 10 (2010) 1019-1035.

[399] T.J. Stewart, M.J. Smyth, Improving cancer immunotherapy by targeting tumor-induced immune suppression, Cancer Metastasis Rev, 30 (2011) 125-140.

[400] C. Liu, C.J. Workman, D.A. Vignali, Targeting regulatory T cells in tumors, FEBS J, 283 (2016) 2731-2748.

[401] C. Pasero, G. Gravis, S. Granjeaud, M. Guerin, J. Thomassin-Piana, P. Rocchi, N. Salem, J. Walz, A. Moretta, D. Olive, Highly effective NK cells are associated with good prognosis in patients with metastatic prostate cancer, Oncotarget, 6 (2015) 14360-14373.

[402] E. Sato, S.H. Olson, J. Ahn, B. Bundy, H. Nishikawa, F. Qian, A.A. Jungbluth, D. Frosina, S. Gnjatic, C. Ambrosone, J. Kepner, T. Odunsi, G. Ritter, S. Lele, Y.T. Chen, H. Ohtani, L.J. Old, K. Odunsi, Intraepithelial CD8+ tumor-infiltrating lymphocytes and a high CD8+/regulatory T cell ratio are associated with favorable prognosis in ovarian cancer, Proc Natl Acad Sci U S A, 102 (2005) 18538-18543.

[403] Q. Gao, S.J. Qiu, J. Fan, J. Zhou, X.Y. Wang, Y.S. Xiao, Y. Xu, Y.W. Li, Z.Y. Tang, Intratumoral balance of regulatory and cytotoxic T cells is associated with prognosis of hepatocellular carcinoma after resection, J Clin Oncol, 25 (2007) 2586-2593.

[404] E.A. Vasievich, L. Huang, The suppressive tumor microenvironment: a challenge in cancer immunotherapy, Mol Pharm, 8 (2011) 635-641.

[405] D.R. Rhodes, J. Yu, K. Shanker, N. Deshpande, R. Varambally, D. Ghosh, T. Barrette, A. Pandey, A.M. Chinnaiyan, ONCOMINE: a cancer microarray database and integrated data-mining platform, Neoplasia, 6 (2004) 1-6.

[406] R. Salgado, C. Denkert, S. Demaria, N. Sirtaine, F. Klauschen, G. Pruneri, S. Wienert, G. Van den Eynden, F.L. Baehner, F. Penault-Llorca, E.A. Perez, E.A. Thompson, W.F. Symmans, A.L. Richardson, J. Brock, C. Criscitiello, H. Bailey, M. Ignatiadis, G. Floris, J. Sparano, Z. Kos, T. Nielsen, D.L. Rimm, K.H. Allison, J.S. Reis-Filho, S. Loibl, C. Sotiriou, G. Viale, S. Badve, S. Adams, K. Willard-Gallo, S. Loi, I.T.W.G. 2014, The evaluation of tumor-infiltrating lymphocytes (TILs) in breast cancer: recommendations by an International TILs Working Group 2014, Ann Oncol, 26 (2015) 259-271.

[407] K. Garg, R.A. Soslow, Lynch syndrome (hereditary non-polyposis colorectal cancer) and endometrial carcinoma, J Clin Pathol, 62 (2009) 679-684.

[408] B.P. Huang, C.H. Lin, Y.C. Chen, S.H. Kao, Anti-inflammatory effects of Perilla frutescens leaf extract on lipopolysaccharide-stimulated RAW264.7 cells, Mol Med Rep, 10 (2014) 1077-1083.

[409] P. Mandal, B.T. Pratt, M. Barnes, M.R. McMullen, L.E. Nagy, Molecular mechanism for adiponectin-dependent M2 macrophage polarization: link between the metabolic and innate immune activity of full-length adiponectin, J Biol Chem, 286 (2011) 13460-13469.

[410] M.T. Orr, J.N. Beilke, I. Proekt, L.L. Lanier, Natural killer cells in NOD.NK1.1 mice acquire cytolytic function during viral infection and provide protection against cytomegalovirus, Proc Natl Acad Sci U S A, 107 (2010) 15844-15849.

[411] V. Bronte, S. Brandau, S.H. Chen, M.P. Colombo, A.B. Frey, T.F. Greten, S. Mandruzzato, P.J. Murray, A. Ochoa, S. Ostrand-Rosenberg, P.C. Rodriguez, A. Sica, V. Umansky, R.H. Vonderheide, D.I. Gabrilovich, Recommendations for myeloid-derived suppressor cell nomenclature and characterization standards, Nat Commun, 7 (2016) 12150.

[412] L.D. Shultz, F. Ishikawa, D.L. Greiner, Humanized mice in translational biomedical research, Nat Rev Immunol, 7 (2007) 118-130.

[413] U. Hadad, T.J. Thauland, O.M. Martinez, M.J. Butte, A. Porgador, S.M. Krams, NKp46 Clusters at the Immune Synapse and Regulates NK Cell Polarization, Front Immunol, 6 (2015) 495.

[414] S. Sivori, D. Pende, C. Bottino, E. Marcenaro, A. Pessino, R. Biassoni, L. Moretta, A. Moretta, NKp46 is the major triggering receptor involved in the natural cytotoxicity of fresh or cultured human NK cells. Correlation between surface density of NKp46 and natural cytotoxicity against autologous, allogeneic or xenogeneic target cells, Eur J Immunol, 29 (1999) 1656-1666.

[415] P.R. Gielen, B.M. Schulte, E.D. Kers-Rebel, K. Verrijp, H.M. Petersen-Baltussen, M. ter Laan, P. Wesseling, G.J. Adema, Increase in both CD14-positive and CD15-positive myeloid-derived suppressor cell subpopulations in the blood of patients with glioma but predominance of CD15-positive myeloid-derived suppressor cells in glioma tissue, J Neuropathol Exp Neurol, 74 (2015) 390-400.

[416] W.J. Israelsen, T.L. Dayton, S.M. Davidson, B.P. Fiske, A.M. Hosios, G. Bellinger, J. Li, Y. Yu, M. Sasaki, J.W. Horner, L.N. Burga, J. Xie, M.J. Jurczak, R.A. DePinho, C.B. Clish, T. Jacks, R.G. Kibbey, G.M. Wulf, D. Di Vizio, G.B. Mills, L.C. Cantley, M.G. Vander Heiden, PKM2 isoform-specific deletion reveals a differential requirement for pyruvate kinase in tumor cells, Cell, 155 (2013) 397-409.

[417] D.A. Scott, A.D. Richardson, F.V. Filipp, C.A. Knutzen, G.G. Chiang, Z.A. Ronai, A.L. Osterman, J.W. Smith, Comparative metabolic flux profiling of melanoma cell lines: beyond the Warburg effect, J Biol Chem, 286 (2011) 42626-42634.

[418] E.D. Montal, R. Dewi, K. Bhalla, L. Ou, B.J. Hwang, A.E. Ropell, C. Gordon, W.J. Liu, R.J. DeBerardinis, J. Sudderth, W. Twaddel, L.G. Boros, K.R. Shroyer, S. Duraisamy, R. Drapkin, R.S. Powers, J.M. Rohde, M.B. Boxer, K.K. Wong, G.D. Girnun, PEPCK Coordinates the Regulation of Central Carbon Metabolism to Promote Cancer Cell Growth, Mol Cell, 60 (2015) 571-583.

[419] P.S. Ward, C.B. Thompson, Metabolic reprogramming: a cancer hallmark even warburg did not anticipate, Cancer Cell, 21 (2012) 297-308.

[420] S. Aparicio, M. Hidalgo, A.L. Kung, Examining the utility of patient-derived xenograft mouse models, Nat Rev Cancer, 15 (2015) 311-316.

[421] H. Imai, K. Kaira, K. Minato, Clinical significance of post-progression survival in lung cancer, Thorac Cancer, 8 (2017) 379-386.

[422] R.L. Korn, J.J. Crowley, Overview: progression-free survival as an endpoint in clinical trials with solid tumors, Clin Cancer Res, 19 (2013) 2607-2612.

[423] A.S. Merseburger, G.P. Haas, C.A. von Klot, An update on enzalutamide in the treatment of prostate cancer, Ther Adv Urol, 7 (2015) 9-21.

[424] F. Claessens, C. Helsen, S. Prekovic, T. Van den Broeck, L. Spans, H. Van Poppel, S. Joniau, Emerging mechanisms of enzalutamide resistance in prostate cancer, Nat Rev Urol, 11 (2014) 712-716.

[425] P.A. Watson, V.K. Arora, C.L. Sawyers, Emerging mechanisms of resistance to androgen receptor inhibitors in prostate cancer, Nat Rev Cancer, 15 (2015) 701-711.

[426] T. Chandrasekar, J.C. Yang, A.C. Gao, C.P. Evans, Targeting molecular resistance in castration-resistant prostate cancer, BMC Med, 13 (2015) 206.

[427] H. de Boussac, A.J. Pommier, J. Dufour, A. Trousson, F. Caira, D.H. Volle, S. Baron, J.M. Lobaccaro, LXR, prostate cancer and cholesterol: the Good, the Bad and the Ugly, Am J Cancer Res, 3 (2013) 58-69.